# In Vivo and in Vitro Characterization of the Tumor Suppressive Function of INPP4B

# *In vivo* and *in vitro* characterization of the tumor suppressive function of INPP4B

A dissertation presented

by

**Chen Li Chew**

to

**The Division of Medical Sciences**

in partial fulfillment of the requirements

for the degree of

Doctor of Philosophy

in the subject of

Biological and Biomedical Sciences

Harvard University

Cambridge, Massachusetts

May, 2015

Dissertation adviser: Dr. Pier Paolo Pandolfi Chen Li Chew

# *In vivo* and *in vitro* characterization of the tumor suppressive function of INPP4B

**Abstract**

The phosphatases PTEN and INPP4B are frequently deregulated in human cancer and have been proposed to act as tumor suppressor genes by coordinately antagonizing PI3K/AKT signaling. While the function of PTEN has been extensively studied, little is known about the underlying molecular mechanisms by which INPP4B exerts its tumor suppressive function. Additionally, its role in tumorigenesis *in vivo* has not been studied.

Here, we show that a partial or complete loss of the phosphatase function of *Inpp4b* morphs benign thyroid adenoma lesions observed in *Pten* heterozygous mice into lethal and metastatic follicular-like thyroid cancer (FTC) (Chapter 2). Importantly, analysis of human thyroid cancer cell lines and specimens reveals that INPP4B expression is downregulated in FTC. Mechanistically, we have found that INPP4B, but not PTEN, is enriched in the early endosomes of thyroid cancer cells, where it blocks PI3K-C2α mediated AKT2 activation and in turn tumor proliferation and anchorage-independent cell growth. Taken together, these data identify INPP4B as a novel tumor suppressor in FTC oncogenesis and metastasis through localized regulation of PI3K/AKT pathway at the endosomes.

Further, we present evidence that INPP4B downregulation cooperates with PTEN loss in prostate cancer progression and metastasis (Chapter 3). *In vivo*, a partial loss of Inpp4b

cooperates with *Pten* haploinsufficiency to promote prostate tumorigenesis. *In vitro*, we have found that knockdown of INPP4B in cell lines increased their migratory and invasive properties. Overall, our studies have greatly increased our understanding of the molecular mechanisms of the tumor suppressive functions of INPP4B and provided *in vivo* evidence for the cooperation of *Inpp4b* with *Pten* haploinsufficiency in both thyroid and prostate tumorigenesis.

**Table of contents**

**Acknowledgements**

First and foremost, I'd like to thank my adviser, Pier Paolo Pandolfi for his support and mentorship. He gave me the opportunity to pursue my interests and ideas, while still ensuring that I was given guidance and direction and offered invaluable advice. This has been a remarkably transformative time, and Pier Paolo's motivation, optimism and passion working towards a cure for cancer will undoubtedly continue to inspire me in whatever I do in future.

I would like to thank my Dissertation Advisory Committee members Lewis Cantley, Marcia Haigis and Alex Toker for making time for me, for all their help and for providing useful suggestions and encouragement through the years. I am grateful for their scientific and professional guidance. In addition, I would like to thank Antonio Di Cristofano, Thomas Roberts and Jean Zhao for serving on my defense committee.

Next, I would like to thank all of the Pandolfi Lab members, past and present. I am thankful for their support, the kindness they have shown me, and for the friendships that have formed. In particular, I would like to thank Leonardo Salmena, Yvonne Tay, Andrea Lunardi, Daniel Ruan and Ming Chen for being such wonderful mentors through the years. They have taught me so much, way more than I can list here – from techniques, critical interpretation of the results, experimental design, troubleshooting, to pushing past the lowest points in the project. I am thankful for their scientific and professional inspiration throughout. I would also like to thank Antonella Papa, Min Sup Song and Su Jung Song for their advice and kindness. Also, I would like to thank Lauren Fawls, Viktoriya Marusyk, Kaitlyn Doherty and Thomas Garvey for administrative support. I am also grateful to Letizia Longo for her sweetness, support and encouragement. Lastly, I would like to thank Ming Chen, Andrea Lunardi, Antonella Papa, Federico Gulluni, Lauren Fawls and Kaitlyn Doherty for insightful editing of this thesis.

Throughout this time, I am truly grateful for the love and support that my friends, family and in-laws have given me. All these would not be possible without their faith in me and their constant encouragement. I am thankful for friendships that lasted through graduate school, and also for ones that I formed here. I want to express my heartfelt thanks to my father and my mother, for their unconditional love, support and encouragement throughout the entire time I have been away from home, and for always believing in me no matter what. Thank you also to my brother and my sister for your love and undying support.

Finally, I want to thank my husband, Khian Hong Pua. It has been a privilege and huge blessing to be able to share the same graduate school experience with my closest friend, confidante and partner. I am thankful for his unwavering support through the many ups and downs along the way, for always providing a listening ear and putting things into perspective. Last but not least, I want to thank our daughter, Hannah Pua, for being a part of our lives, and for the immeasurable joy and happiness she brings.

# CHAPTER 1

## Introduction

## Introduction

### 1.1 Phosphoinositide 3-kinase biology and its role in cancer

Phosphoinositide 3-kinase (PI3K), AKT and mammalian target of rapamycin (mTOR) define a signaling network that regulates important biological processes such as cell cycle, survival, metabolism and motility, all of which are often disrupted in cancer (1). PI3Ks phosphorylate the 3-OH group of phosphatidylinositols, generating intracellular lipids that modulate biological processes and signaling. The eight mammalian PI3K isoforms have been divided into three classes (class I, class II and class III) based on their lipid substrate preferences and structure (2) (Figures 1.1A and B). There are four Class I PI3K isoforms that produce phosphatidylinositol (3,4,5)-trisphosphate ($PI(3,4,5)P_3$) (Figure 1.1A). These isoforms, PIK3CA (p110α), PIK3CB (p110β), PIK3CD (p110δ) and PIK3CG (p110γ), differ on their 110kDa catalytic subunit. Class II PI3Ks are comprised of PI3K-C2α (PIK3C2A), PI3K-C2β (PIK3C2B) and PI3K-C2γ (PIK3C2G), and they produce $PI(3,4)P_2$ and PI(3)P (Figures 1.1A and B). Class III is comprised of a single PI3K isoform, VPS34 (PIK3C3) and it produces PI(3)P (Figures 1.1A and B) (2).

Class I PI3Ks, in particular *PIK3CA*, are perhaps the most relevant to human cancer. Cancer genetics studies reveal the high frequency of *PIK3CA* amplifications and mutations in glioblastomas, gastric cancers, hepatocellular carcinomas and breast cancers (3). In addition, 80% of *PIK3CA* mutations cluster in two hotspots, the helical and catalytic domains (3). Helical domain mutations of glutamic acid (E) to lysine (K) (e.g. E542K or E545K) relieve N-terminal p85 inhibition of p110α (4). Kinase domain mutations (e.g. H1047R) result in an allosteric change of p110α, allowing easier access of substrates to the catalytic site (4). These mutations result in the constitutive activation of PI3K signaling, thus initiating cancer-relevant pathways.

**A**

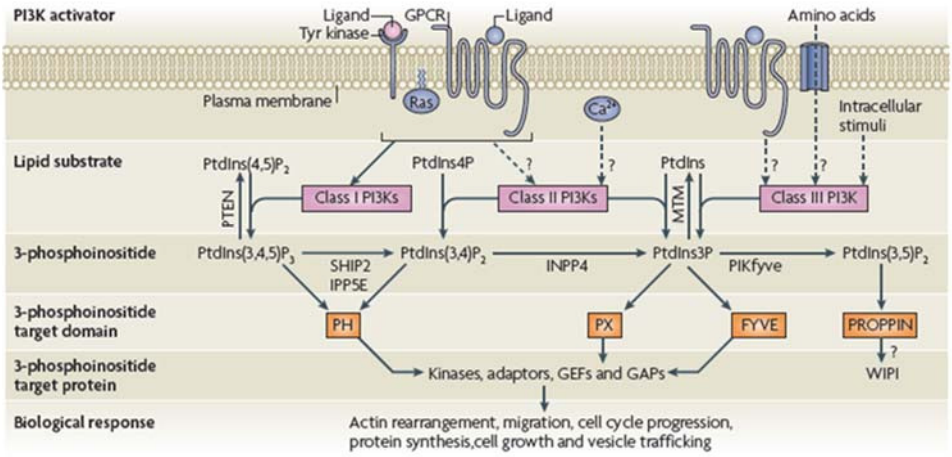


**B**

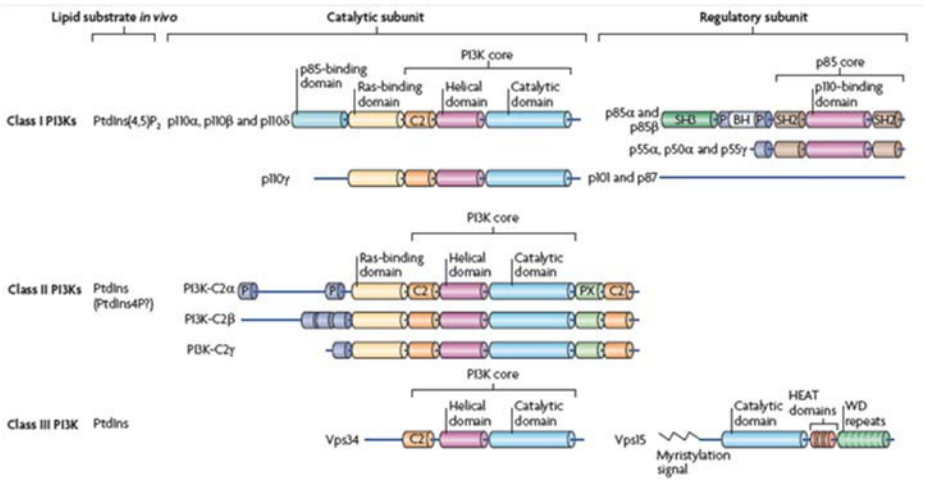


**Figure 1.1 The PI3K signaling network, substrate specificity and structure**

(A) Activation, substrate specificity and downstream effectors of PI3K isoforms. (B) Classification and domain architecture of PI3K isoforms. BH: BCR homology domain; P: proline-rich region; SH3: Src-homology 3 domain. Figure adapted from Vanhaesebroeck, 2010.

Genetically engineered mouse models (GEMMs) with tissue-specific mutations of *Pik3ca* have been used to study the oncogenic function of PIK3CA hyperactivation. Knock-in of the H1047R mutation in mammary tissue using *MMTV-Cre* results in adenosquamous carcinoma or adenomyoepithelioma of the mammary gland (5). Crossing these mice with *Trp53* knockout mice accelerates mammary tumor progression, indicating possible cooperation between the two genetic events (5). Because loss of p110α and p110β is embryonically lethal (6), studies on PI3K deficiency utilize knock-ins of catalytically dead alleles of the p110 gene. Homozygosity for $p110\alpha^{D933A}$ is embryonically lethal; however, mice that are heterozygous for $p110\alpha^{D933A}$ are viable and fertile, but have impaired insulin signaling (7). This indicates the importance of p110α in growth and metabolism. Loss of p110α activity in the mammary tissue impairs development of normal mammary glands. On the contrary, p110β ablation increases ductal branching and tumor formation (8), suggesting the importance of p110α signaling in regulating growth and development in mammary tissue, and that p110α activity could be regulated by p110β, through competition for receptor binding sites (8). *In-vitro* studies utilizing *PIK3CA*-knockout mouse embryonic fibroblasts (MEFs) further reveal the oncogenic role of p110α in growth factor signaling and oncogenic transformation (9).

A role for class II and class III PI3Ks in cancer has not yet been found, however it is important to note the limitations of our knowledge about these enzymes. With regard to PI3K-C2α, total body or endothelial-cell specific deficiency of PI3K-C2α in mice results in embryonic lethality due to defective angiogenesis and vascular maturation, implicating PI3K-C2α in vascular formation and barrier integrity (10). More recently, PI3K-C2α has been implicated in primary cilium function (11). Deregulation of these functions could be relevant in cancer progression, although they are still poorly understood.

In summary, hyperactivation of PI3K by upstream receptor tyrosine kinases, G-protein-coupled receptors or activating mutations, results in an accumulation of phosphatidylinositides, this in turn increases membrane recruitment and activation of AKT (also known as protein kinase B), a key mediator of the oncogenic effects of enhanced PI3K signaling. While the role of class I PI3Ks in cancer is well established, the link of class II and class III PI3Ks in cancer is not well defined.

## 1.2 AKT activation, functions and isoform specific distinctions

### 1.2.1 Mechanisms of AKT activation

The AKT protein kinase (also known as protein kinase B) has three highly homologous isoforms, namely AKT1, AKT2 and AKT3. AKT proteins are comprised of a Pleckstrin Homology (PH) domain and a carboxyl-terminal domain (Figure 1.2) (12). AKT is localized to the membrane by binding to PI(3,4,5)$P_3$ (13) and PI(3,4)$P_2$ (14) with its PH domain. AKT is subsequently activated via phosphorylation at Threonine 308 and Serine 473 by 3-phosphoinositide-dependent-kinase-1 (PDK1) (15) and mTORC2 (PDK2) (16) respectively. Although Thr308 phosphorylation is required and sufficient for AKT activation (17), phosphorylation on both Ser473 and Thr308 allows for maximal activation (15). Both PI(3,4,5)$P_3$ and PI(3,4)$P_2$ are required for the complete activation of AKT (14,18,19), and PI(3,4)$P_2$ levels correlate with phosphorylation of Ser473 and overall AKT activity (cytosolic), while PI(3,4,5)P3 determined Thr308 levels and the activity of membrane-associated AKT (19).

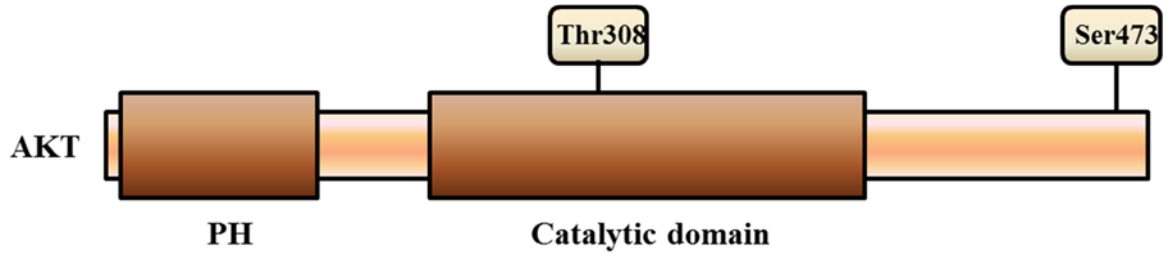


**Figure 1.2 Structure and domains of AKT**

AKT possesses a N-terminal PH domain and a catalytic domain. The main phosphorylation sites, Thr308 and Ser473, are depicted on the schematic.

### 1.2.2 AKT regulates cellular processes which are deregulated in cancer

Activated AKT regulates several cellular processes through phosphorylation of downstream substrates containing the R-X-R-X-X-S/T consensus motif (20). These proteins are part of cellular survival, cell cycle progression, protein translation and metabolic pathways, crucial for the survival of a cancer cell.

AKT also promotes cellular survival through inhibition of apoptosis. This is achieved by preventing cytochrome *c* release from the mitochondria, and by phosphorylating and inactivating proapoptotic factors like BAD and the FOXO family of transcription factors, which mediates the expression of pro-apoptotic genes like the Fas ligand gene (Figure 1.3) (21). In addition, AKT activation favors the phosphorylation and nuclear translocation of the E3 ubiquitin-protein ligase MDM2, thus antagonizing p53 control of the cell cycle (Figure 1.3) (22,23).

AKT activation also promotes cell cycle progression by positively regulating cyclin D1 expression through phosphorylating and inactivating glycogen synthase kinase 3β (GSK3β). In addition, AKT antagonizes the nuclear translocation of cell cycle inhibitors $p21^{WAFI}$ and $p27^{Kip1}$ by phosphorylating a site near their nuclear localization signal (NLS) (Figure 1.3) (24).

Activation of AKT promotes cell growth through activation of the mTOR kinase, by way of TSC2 phosphorylation, consequently inhibiting the formation of the TSC1/TSC2 complex (Figure 1.3) (24). The TSC1/TSC2 complex inhibits RHEB through the GTPase-activating protein (GAP) activity of TSC2 (25). Active RHEB activates mTOR, which stimulates protein synthesis through phosphorylation and activation of a number of targets including p70 S6 kinase (p70 S6K) and eIF4E binding proteins (4E-BPs) (Figure 1.3) (21). Additionally, mTOR also enhances the expression of the hypoxia-inducible transcription factor (HIF1) (26).

Furthermore, AKT also regulates metabolism and angiogenesis through the phosphorylation of endothelial nitric oxide synthase (eNOS) which increases nitric oxide production (Figure 1.3) (27,28). A role for AKT in tumor invasion and metastasis has also been established: AKT increases the secretion of matrix metalloproteinases (29) and induces epithelial-mesenchymal transition (EMT) (30). There has also been evidence linking AKT activation to chromosomal instability (31). Taken together, these studies implicate AKT functions in cellular processes crucial to cancer progression.

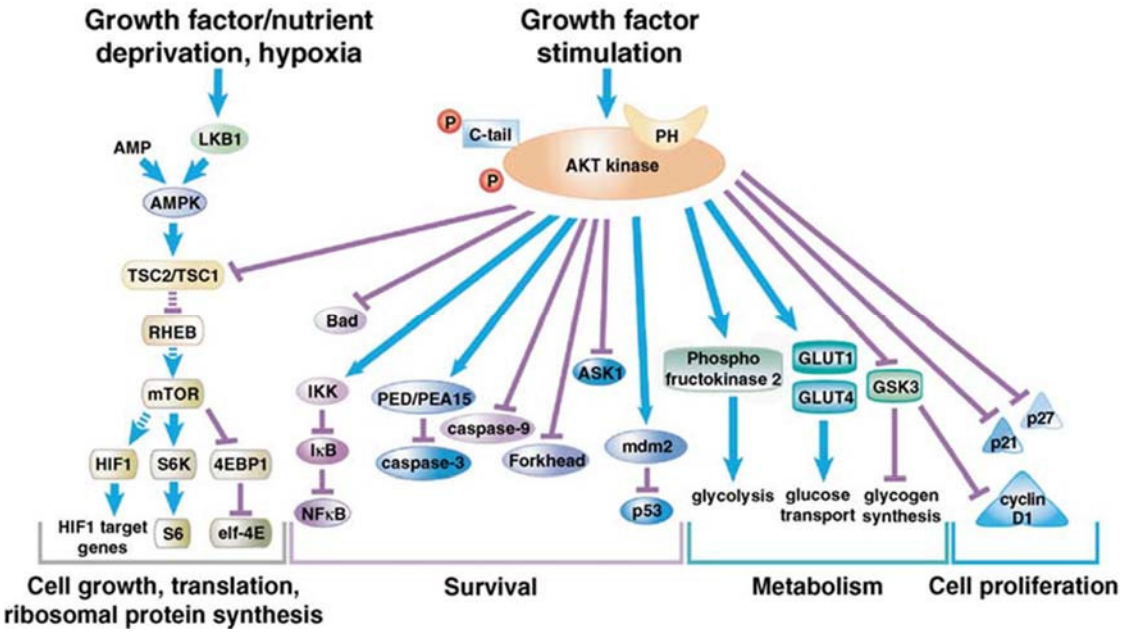


**Figure 1.3 Downstream substrates of AKT and their cellular functions**

Continuous lines represent direct phosphorylation of target proteins by AKT, leading to activation (arrow end) or inhibition (blunt end). Broken lines indicate indirect or unknown mechanisms of activation or inhibition. Figure adapted from Bellacosa, 2005.

### 1.2.3 Perturbations to AKT in human cancer

#### 1.2.3.1 Amplification and overexpression of AKT

*AKT*, in particular *AKT2*, has been found to be amplified in human cancer. *AKT2* amplification and overexpression was first discovered in a subset of ovarian carcinomas (32,33), and the higher frequency of *AKT2* amplification in undifferentiated ovarian tumors suggests a link with tumor aggressiveness (33). Subsequently, several studies have reported *AKT2* amplification in non-Hodgkin's lymphoma, primary pancreatic carcinomas, hepatocellular carcinomas and colorectal cancer (24).

While *AKT1* amplifications are rare genetic events (24), elevated AKT1 protein levels have been reported in one breast cancer study cohort (34). Another study cohort, however, revealed that HER-2/neu expression correlated with increased AKT2, but not AKT1 (24). Subsequently, the role of AKT2, but not AKT1 or AKT3, in mediating tumor invasion and metastasis was demonstrated through its ability to transform NIH3T3 fibroblasts (35), and to increase the invasiveness and metastatic potential of human breast and ovarian cell lines by upregulating β1 integrins (36). The frequent amplification of *AKT2*, but not *AKT1*, suggests that these isoforms are not equivalent in cancer signaling and progression.

#### 1.2.3.2 Hyperactivation of AKT in cancer

AKT is often found to be hyperactivated in a wide variety of cancers (Table 1.1) (24), furthermore, AKT activation has been correlated to advanced disease, poor prognosis, metastasis and radioresistance in certain cancers (21). Studies have also suggested that AKT activation is an early event in preneoplastic lesions, rendering it a potential target for chemoprevention (37).

Unlike PI3K, somatic mutations of *AKT* are not frequent. Recent exon sequencing of *AKT1* found an E17K somatic mutation in the PH domain of breast (8%), colorectal (6%) and ovarian (2%) cancer samples (38). This mutation favors the constitutive localization and activation of AKT1 at the plasma membrane (38). A subsequent study with a larger sample of tumors found the mutation in breast cancer samples (4%), but not in any colorectal, lung, gastric, hepatocellular carcinomas and acute leukemias (39). This observation points to the rarity of this genetic event, and suggests that it might not be an important driver mutation (Kim, 2008). Notably, however, the E17K mutation reduces the sensitivity of AKT to allosteric kinase inhibitors (38), presenting implications for personalized medicine.

**Table 1.1 Representation of frequency of AKT activation in human cancers**

Table is adapted from Altomore, 2005 and Bellacosa, 2005.

| *Tumor type* | *% Tumors with active AKT* |
|---|---|
| Glioma | ~55 |
| Thyroid carcinoma | 80–100 |
| Breast carcinoma | 20–55 |
| Small-cell lung carcinoma | ~60 |
| Non-small-cell lung carcinoma | 30–75 |
| Gastric carcinoma | ~80 |
| Gastrointestinal stromal tumors | ~30 |
| Pancreatic carcinoma | 30–70 |
| Bile duct carcinoma | ~85 |
| Ovarian carcinoma | 40–70 |
| Endometrial carcinoma | >35 |
| Prostate carcinoma | 45–55 |
| Renal cell carcinoma | ~40 |
| Anaplastic large-cell lymphoma | 100 |
| Acute myeloid leukemia | ~70 |
| Multiple myeloma | ~90 |
| Malignant mesothelioma[a] | ~65 |
| Malignant melanoma[b] | 43–67 |

### 1.2.4 Termination of AKT signaling through phosphatases

Phosphatase and tensin homolog deleted on chromosome ten (PTEN) is a dual lipid and protein phosphatase that antagonizes AKT activation. It specifically dephosphorylates the 3'-position of $PI(3,4,5)P_3$, consequently reducing membrane recruitment and activation of AKT (40). Its tumor suppressive function will be explored in detail in Section 1.3.

More recently, protein phosphatases that directly deactivate AKT through the dephosphorylation of either Thr308 or Ser473 have been characterized. Protein phosphatase 2 (PP2A) dephosphorylates Thr308 (41) while PHLPP dephosphorylates Ser473 (42). Interestingly, PHLPP1 and PHLPP2 display distinct preferences for the AKT isoforms – PHLPP1 is specific for AKT2 and AKT3, while PHLPP2 is specific for AKT1 and AKT3 (43). In light of this, it is intriguing to find that Phlpp1 cooperates with *Pten* heterozygosity in prostate cancer (CaP) progression in mice (44), suggesting a possible involvement of AKT2 signaling in CaP progression.

### 1.2.5 GEMMs of AKT

The use of GEMMs has allowed for a better understanding of the oncogenic function of AKT in tumorigenesis. Constitutive activation of Akt is achieved through myristoylation or mutation of the phosphorylation sites of Akt (Thr308 and Ser473) to aspartic acid (D) to mimic a phosphorylated residue (Akt1-DD) (45). The mouse mammary tumor virus long terminal repeat (MMTV-LTR) promoter has been used to induce the expression of Akt1-DD in the mammary epithelium (45). Although these mice do not develop mammary tumors, the authors note a cooperation of PI3K and Akt1 activation in driving mammary tumorigenesis (45).

Studies on knockout mouse models have elucidated the role and relative importance of the different Akt isoforms, in cellular survival and metabolism. Knockout of the *Akt1* gene (*Akt1*$^{-/-}$) in mice results in growth retardation and increased apoptosis (46). *Akt2* knockout (*Akt2*$^{-/-}$), on the other hand, results in insulin resistance, loss of adipose tissue and mild growth retardation (47,48). Finally, although Akt3 is not required for metabolism, *Akt3*$^{-/-}$ mice display reduced brain size due to reduction in both number and size of the cells (49). These discordant phenotypes suggest that despite high levels of sequence and structural homology in the PH and catalytic domains of the isoforms (12), these isoforms are not redundant, but instead play distinct roles in regulation of cellular survival, cell growth, and metabolism.

### 1.2.6 Specific localization and function of AKT and its isoforms

Despite structural similarities, there is increasing evidence that the AKT isoforms are not functionally equivalent, but instead promote distinct signaling outputs. While the limited availability of reagents hampered the initial studies on the distinct roles of the three AKT isoforms, development of isoform-specific antibodies and their phosphorylated counterparts have allowed for a better understanding of their localization, substrate specificity, tissue expression and activation.

#### 1.2.6.1 Distinct subcellular localization of AKT and its isoforms

Prior to the development of isoform-specific AKT antibodies, AKT function was explored using anti-“pan”-AKT-antibodies. These studies established a model in which AKT is localized in the cytoplasm and, upon PI3K activation, translocated to the plasma membrane where it is fully activated (50). However, this model did not communicate the complete story.

There is increasing evidence in support of distinct subcellular AKT localization. All three AKT isoforms have been found to localize in the nucleus, under steady state conditions or in response to growth factor stimulation (51,52). This nuclear localization is reportedly crucial for cell survival and proliferation, through phosphorylation of AKT targets, such as the FOXO family of transcription factors and p21, and increased cyclin D1 expression. Nuclear AKT also plays a role in DNA repair, RNA export and cellular differentiation (51). Notably, the promyelocytic leukemia protein (PML) tumor suppressor has been found to promote dephosphorylation of nuclear AKT by recruiting the phosphatase PP2A (53). *In vivo* studies have found an association between *Pml* loss and the development of colon and prostate adenocarcinomas, particularly in a *Pten* heterozygous context, highlighting the importance of targeting nuclear AKT for cancer therapy (53).

With the development of isoform-specific antibodies, it became clear that both AKT1 and AKT2 are largely cytoplasmic. AKT2 was, however, also found in the mitochondria, while AKT3 was largely localized to the nucleus (50). AKT2 has also been found to be associated with a distinct subset of the early endosomes via interaction with WDFY2, a FYVE domain-containing and PIP3 binding protein (54). The mitochondria and endosomal localizations of AKT2 (where it potentially contributes to sustained insulin signaling) are consistent with previous *in vivo* and *in vitro* studies that implicate AKT2 in regulation of energy metabolism.

#### 1.2.6.2 AKT isoforms and substrate specificity

While there is a certain degree of functional compensation amongst the AKT isoforms, *in vivo* studies with specific knockout of the distinct Akt isoforms in mouse models demonstrate that each isoform also performs distinct roles (46,48,49). The distinct subcellular localization of the three AKT isoforms suggests that they act to phosphorylate distinct substrates. For instance,

the Ankyrin repeat domain protein 2 (ARPP) is typically found in skeletal muscle cells where it regulates differentiation and where it has been identified as a novel AKT2 specific substrate (55). In addition, AKT1 but not AKT2 phosphorylates Palladin on Ser507 (56). Phospho-Palladin on Ser507 is required for F-actin bundling and maintenance of an organized actin cytoskeleton, thereby inhibiting migration of breast cancer cells (56).

#### 1.2.6.3 AKT isoform specificity in cancer progression

Studies using *in vivo* models have revealed isoform-specific functions of AKT in cancer progression. In the context of breast cancer, AKT1 has been found to promote tumor growth (57,58). This has been confirmed in myoblasts in which isoform specific knockdown of *AKT1* or *AKT2* showed that only AKT1 is specifically required for G1/S cell cycle transition (59). In addition, mouse genetic studies with Akt1 null mice have shown that Akt1 is associated with mammary tumor induction and growth (60). Despite a role for AKT1 in tumorigenesis, it is important to note that Akt1 activation also suppresses invasion (57), migration and epithelial-mesenchymal transition (EMT) (58).

On the other hand, overexpression of AKT2 promotes invasion (36), migration and EMT (58). Strikingly, overexpression of Akt2, but not Akt1, in a mouse model of breast cancer markedly increased the incidence of pulmonary metastases, implicating Akt2 in metastatic progression (61).

Although the role of AKT3 in breast cancer progression remains poorly understood, a recent study has found that AKT3 is amplified in basal-like triple negative breast cancer (TNBC) cell lines, and that it is required for TNBC growth *in vitro* and *in vivo* (62). Given that TNBC currently represents the only breast tumor subtype without effective therapy; this particular dependence on AKT3 provides an exciting new avenue for targeted therapy (62).

In summary, despite structural and sequence homology, *in vivo* and *in vitro* studies of AKT isoforms reveal very distinct functions of said isoforms. However, the mechanisms underlying specific AKT isoform activation, and downstream substrates of specific isoforms remains poorly understood.

### 1.3 PTEN function in tumor suppression

*PTEN* (phosphatase and tensin homolog deleted on chromosome 10) was first identified in 1997 as a novel tumor suppressor gene, mapping to chromosome 10q23. Two independent groups identified *PTEN* to be frequently disrupted in multiple tumor types and targeted by germline mutations of patients with Cowden disease (63,64).

#### 1.3.1 PTEN in tumor suppression and antagonizing AKT signaling

*PTEN* encodes a dual-specificity phosphatase that can dephosphorylate both phosphopeptide and phosphoinositide substrates. It consists of 9 exons, encompassing a phosphatase domain and a C2 lipid membrane-binding domain (Figure 1.4) (40). The PTEN phosphatase domain contains the catalytic motif HCXXGXXR found in protein tyrosine phosphatases (PTPs), where C represents the catalytic cysteine residue and X is any amino acid (Figure 1.4) (65).

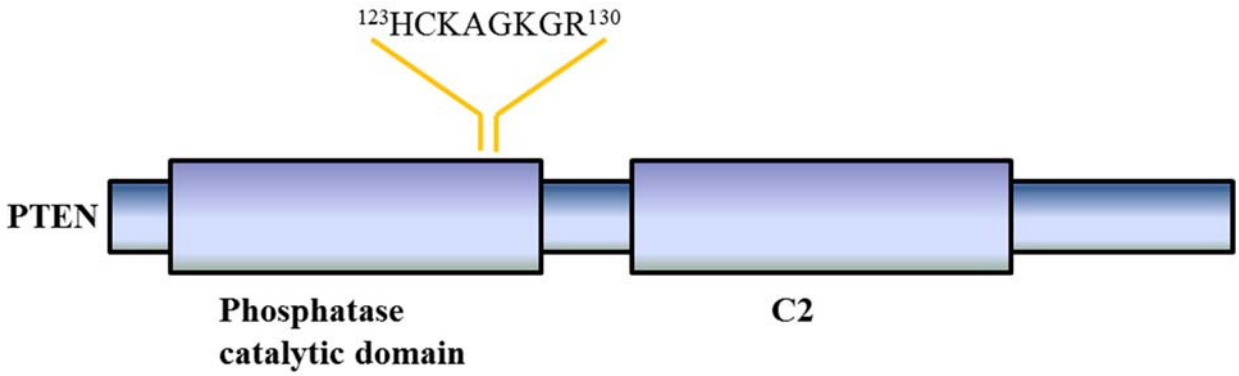


**Figure 1.4 Structure and domains of PTEN**

PTEN contains a N-terminal phosphatase catalytic domain (active site located from residues 123 to 130) and a C2 lipid membrane-binding domain. Both domains are essential for its tumor suppressive function.

Importantly, PTEN dephosphorylates $PI(3,4,5)P_3$ to $PI(4,5)P_2$ (66), antagonizing AKT signaling because $PI(3,4,5)P_3$ is required for the membrane recruitment and activation of AKT (13). Thus, PTEN negatively regulates AKT signaling, leading to decreased phosphorylation of downstream targets like PRAS40 and tuberous sclerosis 2 (TSC2) (40).

Although the lipid phosphatase function of PTEN is important in antagonizing AKT signaling, the protein phosphatase function of PTEN is also crucial in other aspects of tumor suppression like cell cycle arrest (40). PTEN can dephosphorylate phosphorylated Tyr-, Ser- and Thr- residues *in vitro* (67), and validated cellular protein targets include focal adhesion kinase, c-SRC, as well as PTEN itself (68–70), proving important in the regulation of cellular migration, invasion and autoregulation.

### 1.3.2 Pertubations to PTEN in human cancer

Germline mutations which eliminate PTEN function or reduce PTEN levels are found in approximately 80% of patients with Cowden syndrome (71). *PTEN* mutations have also been identified in sporadic tumors (72). Analysis of the Catalogue of Somatic Mutations in Cancer (COSMIC) reveals that while mutations can occur throughout the length of *PTEN*, mutation hotspots exist, particularly in exon5, which encodes the phosphatase catalytic domain of PTEN (40).

*PTEN* deletion or other alterations also occur (40); allelic or homozygous deletion of *PTEN* is frequent in breast and prostate cancer, melanoma and glioma (40). *PTEN* is transcriptionally silenced by promoter methylation in endometrial, gastric, lung, thyroid, breast and ovarian tumors, as well as in glioblastoma (40). Further, a subset of Cowden patients carry germline mutations in the promoter or in potential splice donor and acceptor sites, which can result in exon skipping, altering PTEN function (73).

PTEN hamartoma tumor syndrome (PHTS) is a group of syndromes characterized by benign growths and a high risk for cancers of the breast, endometrium and thyroid (40). Cowden syndrome is the best characterized PHTS, and germline *PTEN* mutations occur in 85% of these patients (71).

In the general population, *PTEN* loss has also been associated with increased risk of breast, endometrial and thyroid cancers, Lhermitte-Duclos disease and glioblastomas (40). In addition, *PTEN* is also frequently deleted in prostate cancer and found to be epigenetically silenced in melanoma and non-small-cell lung cancer (NSCLC). In pancreatic cancer, PTEN has been found to be aberrantly localized (74).

Subtle variation in PTEN levels is increasingly recognized as a factor that can affect tumor susceptibility. The first evidence of this emerged from studies of *Pten* hypermorphic ($Pten^{hy/+}$) mice which express 80% of normal levels of Pten (75). Notably, these mice develop a spectrum of tumors, in particular breast tumors (75), suggesting that mechanisms which regulate expression and function of PTEN can powerfully contribute to tumor suppression (76).

*PTEN* can be regulated post transcriptionally by microRNAs and competing endogenous RNAs (ceRNAs) (76). Notably, microRNA 21 (miR-21), miR-25a, miR-22 and the miR-106b-25 cluster have been found to regulate *PTEN* expression in human cancer (40). Post-translational regulation of PTEN, albeit lacking *in vivo* validation, includes phosphorylation, ubiquitylation, oxidation, acetylation, proteosomal degradation and subcellular localization (40). Nonetheless, Lys13 and Lys289, which are monoubiquitylated for nuclear import, have been found to be mutated in endometrial cancer and Cowden patients, as well as associated with nuclear exclusion (40).

### 1.3.3 GEMMs of PTEN

To study the effects of *Pten* loss *in vivo*, our lab has generated mouse models with constitutive and conditional *Pten* loss by targeted disruption of exons 4 and 5 of *Pten*, which encode the phosphatase catalytic domain (77,78). Together with others, we find that homozygous loss of *Pten* results in embryonic lethality, while *Pten* heterozygous ($Pten^{+/-}$) mice develop tumors of the breast, endometrium, prostate, adrenal, pituitary and lymphoma (77,79,80). Additionally, $Pten^{+/-}$ mice also develop benign polyps in the intestines (81). The penetrance and severity of breast and endometrial tumors in $Pten^{+/-}$ mice is highly dependent on the genetic background of the mice (81).

$Pten^{+/-}$ mice have been used to understand cooperativity between *Pten* and several other genes in tumor progression. *Pten* heterozygosity has been found to accelerate tumorigenesis in a Wnt-induced mammary tumor model (82), it also accelerates endometrial carcinoma in *Mlh1* deleted mice (83). In both examples of compound mutants, the tumors are associated with loss of heterozygosity (LOH) for the remaining *Pten* allele (40).

Because of the embryonic lethality of homozygous *Pten* loss, complete *Pten* loss can only be studied in a tissue specific manner with conditional *Pten* knockout mice. Tissue specific deletion of *Pten* in mice has been found to induce tumors in the prostate, thyroid, breast, lung, bladder and pancreas (40). It also results in early onset lymphoma and autoimmunity (84).

*Pten* knock-in mouse models have also been used to study the tumorigenic consequences of *Pten* loss of function mutations *in vivo*. The PTEN (C124S) and PTEN (G129E) are two mutations that are found in the germline of Cowden patients (85). Both of these mutations lie in the catalytic core of PTEN. The PTEN (C124S) mutation causes the missense substitution of the catalytic Cys124 to Ser. This results in a catalytically dead PTEN, with no phosphatase activity towards both phosphoinositide and phosphopeptide substrates. The PTEN (G129E) mutation

involves the missense substitution of Gly129 to Glu, which eliminates the phosphoinositide phosphatase function, but retains activity toward phosphopeptides (85). Compared to the *Pten*$^{+/-}$ mice, the *Pten*$^{C124S/+}$ and the *Pten*$^{G129E/+}$ had increased lymphoproliferation, and a greater proportion of the mice developed adenomas of the thyroid, adrenal and gallbladder. In addition, these mice developed large invasive adenocarcinomas of the breast that were not observed in the *Pten*$^{+/-}$ mice (85). The increased severity of tumorigenic phenotype in the *Pten* knock-in mice suggests a dominant negative effect of the PTEN (C124S) and PTEN (G129E) mutations, in line with the finding that PTEN homodimerization is critical for its lipid phosphatase function (85).

### 1.3.4 PTEN and thyroid cancer

In the specific context of thyroid cancer, homozygous deletion of *PTEN* is found in less than 10% of all human cases (86). Promoter methylation of *PTEN* was found in 46% of papillary thyroid carcinomas, but in more than 80% of follicular carcinomas and adenomas (87). Further, loss of heterozygosity of *PTEN* was found in 27% of follicular carcinoma (88). These indicate the importance of *PTEN* loss in follicular carcinoma initiation.

In line with the role of *PTEN* in the initiation of thyroid carcinoma, *Pten*$^{+/-}$ mice develop benign thyroid lesions with late onset and at low frequency (89). Surprisingly, homozygous deletion of *Pten* in the follicular cells of the thyroid led only to the development of goiters and benign follicular thyroid adenoma in mice 1 year old (90). Further, only a portion of older mice developed invasive and often metastatic thyroid follicular carcinomas. This suggests that *PTEN* loss alone is not sufficient enough to promote invasive thyroid tumor development, and that additional mutations must be selected in order for the cancer to progress to aggressive stages of disease (91).

### 1.3.5 Roles of PTEN

PTEN plays an integral role in regulating many of the cellular processes governed by the PI3K-AKT-mTOR signaling pathway. These processes include metabolism, cell motility and polarity, regulation of tumor microenvironment and cellular senescence (65). PTEN has also been found to have a role in the self-renewing activity of both normal and cancer stem cells (65).

In addition to its location in the cytoplasm where it dephosphorylates $PI(3,4,5)P_3$, PTEN has also been found to be localized and functional within the nucleus, where it controls genomic stability and cell cycle progression (65). Loss of nuclear PTEN is associated with more aggressive cancers, although nuclear pools of $PI(3,4,5)P_3$ are not sensitive to PTEN expression, suggesting a role for nuclear PTEN beyond its lipid phosphatase activity (65).

In summary, PTEN is an essential tumor suppressor because it regulates key signaling pathways such as the proto-oncogenic PI3K-AKT signaling pathway which is often hyperactivated in many cancers, like those of the breast, thyroid and prostate.

### 1.4 INPP4B function in cancer progression

#### 1.4.1 INPP4B structure and isoforms

INPP4B (inositol polyphosphate 4-phosphatase type II) was first cloned and characterized in 1997 (92). INPP4B is a 105kDa enzyme that is $Mg^{2+}$-independent, and INPP4B is a dual specificity phosphatase known to catalyze the hydrolysis of the 4-position phosphate of $PI(3,4)P_2$ (92). More recently, it has been shown to also act as a phosphatase for $PI(3,4,5)P_3$ that accumulates as a result of PTEN deficiency (93).

INPP4B has an N-terminal C2-lipid binding domain, and a C-terminal phosphatase catalytic domain (Figure 1.5) (94). Like PTEN, the phosphatase catalytic domain of INPP4B contains a $C(X)_5R$ catalytic motif that is characteristic of dual specificity phosphatases (Figure 1.5) (94). Specifically, the CKSAKDRT (aa 842-849) catalytic motif contains the catalytic cysteine residue that functions as the nucleophile for catalysis, and cysteine modifying reagents (e.g. N-ethymaleimide) can inactivate INPP4B (92).


**Figure 1.5 Structure and functional domains of INPP4B**

INPP4B consists a N-terminal C2 lipid membrane-binding domain, a NHR domain and a C-terminal 4-phosphatase catalytic domain.

Notably, INPP4B has a closely related isozyme, INPP4A (inositol polyphosphate 4-phosphatase type I), and both proteins are 37% identical in the rat (92). The phosphatase catalytic motif CKSAKDRT is completely conserved between both isozymes (Figure 1.6). Overall, the sequence similarity is much greater in the C-terminus of the proteins, which contains the phosphatase catalytic domain (Figure 1.6). A C-terminal anti-peptide antibody against INPP4A has been reported to also precipitate INPP4B (92).

Several splice variants of INPP4B have been reported, although the significance of these variants remains unclear. There are two major splice isoforms of INPP4B, INPP4Bα and INPP4Bβ. These isoforms differ at their C-terminus, with the α form containing a hydrophilic C-terminus and the β form containing a hydrophobic C-terminus, believed to be a transmembrane domain (92). Overexpressed EGFP-Inpp4bβ has been found to localize to the golgi in COS cells (95), but the significance of this is poorly understood. In addition, purified recombinant INPP4Bβ does not possess any detectable enzymatic activity towards phosphoinositides or soluble inositols, suggesting that additional factors or processing might be required for the function of this isoform (92,96).

### 1.4.2 INPP4B as a tumor suppressor

INPP4B was initially identified as a potential tumor suppressor in a shRNA-mediated genetic screen performed in HMEC cells. This genetic screen found that knockdown of INPP4B resulted in anchorage independent growth of these cells (97).

INPP4B preferentially hydrolyzes PI(3,4)$P_2$ to PI(3)P (98), and because direct interaction of PI(3,4)$P_2$ with the pleckstrin homology (PH) domain of AKT is required for membrane recruitment and full activation of AKT (15), INPP4B, like PTEN, is anticipated to act as a tumor suppressor by antagonizing PI3K/AKT signaling (98).

**Figure 1.6 Alignment of INPP4B and INPP4A**

Sequence alignment of amino acid sequences of INPP4B and INPP4A reveal a complete conservation of the phosphatase catalytic motif in both proteins (highlighted in yellow). Overall, there is higher conservation in the C-terminal region of both proteins.

**Figure 1.6 (continued)**

#### 1.4.2.1 INPP4B as a tumor suppressor in breast cancer

Evidence of INPP4B as a tumor suppressor was first provided by the lab of Dr. Lewis Cantley. Dr. Cantley's team found that INPP4B inhibits the PI3K-AKT signaling pathway, and knockdown of *INPP4B* in breast cancer cell lines increased cell proliferation, anchorage-independent growth, migration and *in vivo* tumor formation (98). Furthermore, loss of heterozygosity (LOH) of the *INPP4B* locus was found in approximately 60% of basal-like breast cancers, as well as a significant fraction of ovarian cancers, and correlated with lower overall patient survival (98,99). Indeed, in a survey of immunohistochemical biomarkers for basal-like breast cancers, INPP4B is found to have the strongest association with basal-like breast cancers, potentiating its use as a biomarker in the diagnosis and treatment of such cancers, which until now has remained a clinical challenge (100).

Interestingly, INPP4B expression correlates with ER expression (99), and re-expression of INPP4B in ER-negative, INPP4B-null human breast cancer cells reduced AKT activation and anchorage-independent growth (99). In addition, INPP4B protein loss is frequently observed in tumors that did not express PTEN (99), suggesting a potential cooperation between INPP4B and PTEN in tumor suppression.

#### 1.4.2.2 INPP4B as a tumor suppressor in prostate cancer

Recent concordant analyses of the prostate cancer (CaP) genome revealed that the PI3K, RAS/RAF and RB pathways are commonly altered, with frequencies ranging from 34% to 43% in primary tumors, and 74% to 100% in metastases (101). Taking into consideration deletions, mutations and/or loss of expression, the PI3K pathway is altered in nearly half of primaries and all metastases examined (101). Of note, while *INPP4B* is downregulated in 8% of primary CaP,

*INPP4B* is reduced in up to 47% of metastatic CaP (101), implicating the potential role of INPP4B in metastatic progression.

In addition, both INPP4B and PTEN are found to be substantially reduced in primary tumors compared to normal tissue (102,103). In androgen-dependent CaP, decreased expression of INPP4B reduced the time to biochemical recurrence, and increased the risk of clinical relapse (102,103). Of particular note, *INPP4B*, but not *PTEN*, has been found to be androgen responsive, with *INPP4B* increasing following androgen receptor (AR) activation (102). This has important implications for androgen ablation therapy, *INPP4B* downregulation would lead to AKT activation (102). This potentially reduces the antitumor effects of androgen ablation, and underscores the importance of AKT targeting therapies in combination with androgen deprivation (102).

Furthermore, INPP4B suppresses the invasion of prostate carcinoma PC-3 cells *in vitro*, and this is associated with suppression of IL-8 and induction of PAK6 expression (104).

#### 1.4.2.3 INPP4B as a tumor suppressor in other cancers

Decreased *INPP4B* expression has been found to correlate with tumor progression in melanocytic neoplasms, and INPP4B expression in melanoma cells decreases proliferation, invasion and tumorigenic capacity (105).

Downregulation of INPP4B is found in close to 50% of primary nasopharyngeal carcinoma (NPC) tumors (106). The *INPP4B* promoter has been shown to be hypermethylated, providing the mechanism for transcriptional silencing of *INPP4B* in NPC (106).

Recently, we describe a tumor suppressive role for INPP4B in metastatic follicular thyroid carcinoma, and provide evidence that it regulates AKT signaling in an isoform-specific manner at the endosomes (107). This is described in Chapter 2 of my thesis.

### 1.4.3 INPP4B as an oncogene

Interestingly, INPP4B has been found to mediate PI3K signaling through SGK3 in breast cancer cell lines, and this is required for 3D proliferation, invasive migration and tumorigenesis *in vivo* (108). SGK3 signaling has been found to be particularly important in a subset of breast cancers with oncogenic mutations in *PIK3CA*, yet exhibit only minimal AKT activation (109).

In addition, INPP4B overexpression is associated with poor clinical outcome and therapy resistance in acute myeloid leukemia (AML), reinforcing its unexpected role in oncogenesis (110,111). It is interesting to note that this oncogenic role of INPP4B appears to be independent of its phosphoinositide phosphatase function (110,111).

### 1.4.4 GEMMs of INPP4B

The first *Inpp4b* null mice were made with a mutation similar to the spontaneous *weeble* mutation in *Inpp4a* (112). The *weeble* mutation is a single nucleotide deletion in *Inpp4a* that is believed to result in truncation of Inpp4a (113). These $Inpp4b^{-/-}$ mice are deleted for exon 11, and display increased osteoclast differentiation rate and potential, resulting in decreased bone mass and osteoporosis (112). This is attributed to Inpp4b regulation of intracellular calcium levels, which modulate NFATc1 nuclear translocation and activation (112).

In order to evaluate the functional relevance of polymorphisms in INPP4B (S474R, H548P) associated with neuroinflammatory diseases like multiple sclerosis, a transgenic knock-in mouse model, $Inpp4b^{474R/548P}$ was generated. These mice exhibit significantly longer latencies of cortical

motor evoked potentials, suggesting that INPP4B plays a role in regulating nerve conduction velocity (114).

However, little is known about the *in vivo* role of INPP4B in tumorigenesis, and whether it cooperates with other tumor suppressors in cancer progression. In addition, the molecular mechanisms by which INPP4B exerts its tumor suppressive function remains poorly understood.

## 1.5 Endosome biology

### 1.5.1 The signaling endosome and cancer

Endocytosis is the process of internalizing cell surface components and extracellular molecules into lipid vesicles called endosomes (115). Endocytosis has been classically considered to be an effective mechanism of downregulating cellular signaling through internalizing receptors or ligand-receptor complexes for subsequent degradation by the lysosomes (115). However, there is increasing evidence in support of a signaling endosome hypothesis, where endosomes contribute actively to intracellular signaling (115), through spatial and temporal regulation of signaling, avoiding unspecific cross-talk between different pathways and regulating the duration of signaling (116).

The notion that signaling occurs only at the plasma membrane was challenged by the discovery that the majority of activated epidermal growth factor receptors (EGFRs) and their downstream signaling factors such as Shc, Grb2 and mSOS are found on the early endosomes, suggesting that EGFR signaling continues from this compartment (116,117). Nevertheless, the significance of signaling complexes on endosomes was not recognized because they could represent a transport intermediate on the way to lysosomal degradation (116). However, it was subsequently demonstrated that prolonged membrane retention of activated EGFR, as a result of impaired clathrin-mediated endocytosis, reduced the activity of downstream signaling components like ERK 1 / 2 or PI3K, supporting the notion that endocytosis of receptor tyrosine kinases was crucial in establishing and controlling specific signaling pathways (118).

Endosome-associated proteins can associate with the endosomes through direct interaction with the endosomal membrane or through binding an endosomal protein (115). These endosome proteins are capable of connecting proteins from different signaling pathways (Figure 1.7A)

(115). Two important endosome-associated proteins, APPL1 (adaptor protein containing PH domain, PTB domain, and leucine zipper motif) and EEA1 (early endosomal antigen-1), define the early endosomal membrane and have been shown to interact directly with AKT, mediating signaling cross-talk (119,120). In zebrafish development, APPL1-AKT signaling has been shown to be important in the specific phosphorylation of GSK3-β, but not TSC2 (Figure 1.7B) (119). EEA1-AKT interaction has been shown to be crucial for angiotensin II induced AKT activation by p38 of the mitogen-activated protein kinase (MAPK) pathway (Figure 1.7C) (120). This leads to the downstream activation of S6 kinase and mTOR, and the subsequent hypertrophy of vascular smooth muscle cells (Figure 1.7C) (120).

In addition to mediating signaling by receptor tyrosine kinases, there is emerging evidence that endocytosis is integral to cell motility and invasiveness (121). Endocytosis of receptor tyrosine kinases (RTKs) is essential for specific intracellular response to migratory guidance cues (122). Furthermore, the phosphorylation of endophilin-A2 by Src disrupts its association with dynamin, inhibiting endocytosis of matrix metalloproteinase MT1-MMP, contributing to tumor invasiveness (123). More recently, clathrin- and RAB5- mediated endocytosis have been shown to be required for the activation of RAC induced by motogenic stimuli (124). Subsequent endosomal recycling of RAC to the plasma membrane also ensures localized signaling, leading to the formation of actin-based migratory protrusions (124), supporting a role of endocytosis in mediating cellular migration and invasiveness. However, the significance of derailed endocytosis in human cancer is still poorly understood.

**Figure 1.7 Endosome-associated proteins mediate signaling specificity, localization and crosstalk**

Green color represents endosome-associated proteins; orange and yellow show interacting proteins; blue arrows represent crosstalk; black squares represent output function. (A) Endosome-associated proteins can localize two signaling pathways to the endosomes, mediating signaling crosstalk. (B) APPL mediates crosstalk between glycogen synthase 3 beta (GSK3- β) and AKT, but is not required for TSC2 activation. (C) EEA1 mediates crosstalk between p38 and AKT. Figure adapted from Palfy, 2012.

**Figure 1.7 (continued)**

**A**

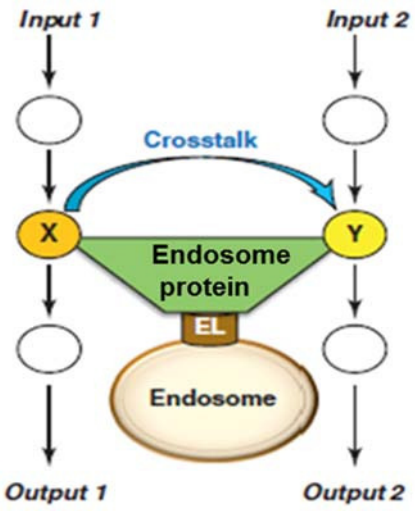


**B**

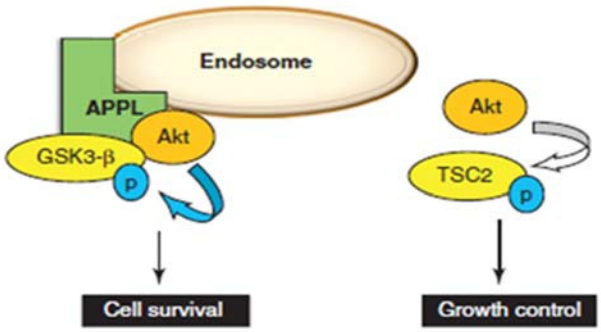

**Figure 1.7 (continued)**

**C**

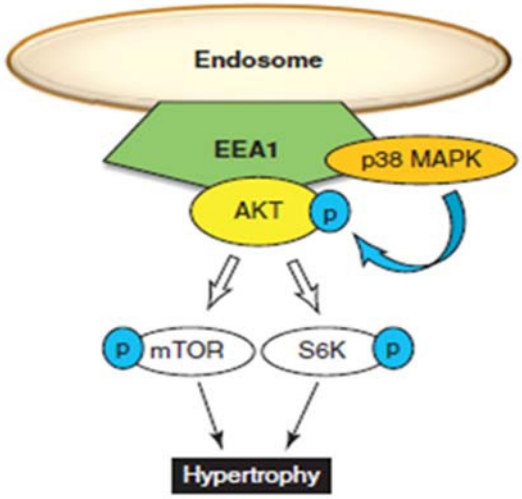

### 1.5.2 Membrane identity of endosome vesicles

One important aspect of endocytosis is the fusion and fission of endocytic vesicles to allow for the sorting of their cargo (125). As endosomal vesicles mature, they acquire membrane identities, defined by different species of phosphatidylinositol phosphates, distinct from the membrane from which they have emerged (125). While PI(4,5)$P_2$ is implicated in clathrin-mediated endocytosis, it remained unclear how subsequent endosome vesicles are dominated by PI(3)P (Figure 1.8) (126). Recently, PI3K-C2α is shown to mediate this conversion through catalyzing the formation of PI(3,4)$P_2$, which is subsequently converted to PI(3)P, potentially through the action of 4-phosphatases like INPP4A or INPP4B (Figure 1.8) (126). The depletion of PI(3,4)$P_2$ or PI3K-C2α impairs the maturation of clathrin-coated pits before fission, and inhibits the recruitment of SNX9 (126), reinforcing the importance of PI(3,4)$P_2$ in endocytosis. While the mechanism underlying the conversion of PI(3,4)$P_2$ to PI(3)P remains unclear, INPP4A/B, an effector of endosomal RAB5, would be an excellent candidate (126,127), potentially implicating INPP4B as an important regulator of endocytosis.

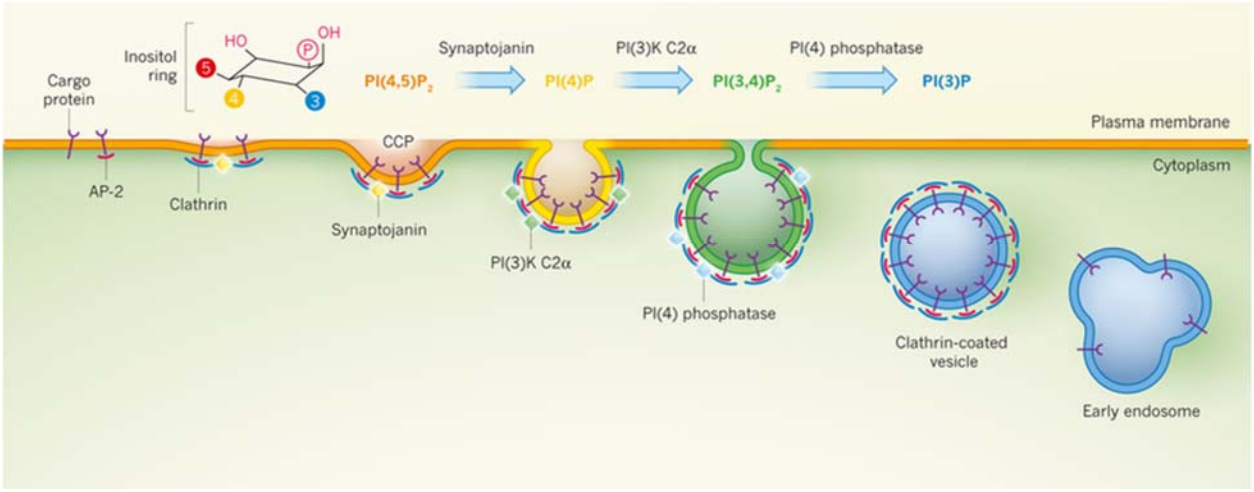


**Figure 1.8 Phosphoinositide conversion during clathrin-mediated endocytosis**

At the plasma membrane, AP-2 proteins mediates clathrin assembly to form clathrin-coated pits (CCPs). CCP maturation is accompanied by step-wise conversion of PI(4,5)$P_2$ to PI(4)P, and then to PI(3,4)$P_2$. This is mediated by synaptojanin and PI3K-C2α. 4-phosphatases are believed to mediate the subsequent conversion of PI(3,4)P2 to PI(3)P, which define endosome vesicles. (Figure adapted from Schmid, 2013).

## 1.6 Concluding remarks

While the function of PTEN has been extensively studied, little is known about the underlying molecular mechanisms by which INPP4B exerts its tumor suppressive function, and its role in tumorigenesis *in vivo* has not been studied. Thus, we seek to investigate the tumor suppressive functions of INPP4B – both *in vitro* and *in vivo* with knockout (KO) mouse models, and to investigate if *Inpp4b* loss cooperates with *Pten* heterogeneity in tumor progression.

## 1.7 References


1. Fruman D a, Rommel C. PI3K and cancer: lessons, challenges and opportunities. Nat Rev Drug Discov. 2014;13(2):140–56.

2. Vanhaesebroeck B, Guillermet-Guibert J, Graupera M, Bilanges B. The emerging mechanisms of isoform-specific PI3K signalling. Nat Rev Mol Cell Biol. 2010;11(5):329–41.

3. Samuels Y, Ericson K. Oncogenic PI3K and its role in cancer. Curr Opin Oncol. 2006;18(1):77–82.

4. Klarenbeek S, van Miltenburg MH, Jonkers J. Genetically engineered mouse models of PI3K signaling in breast cancer. Mol Oncol. 2013;7(2):146–64.

5. Adams JR, Xu K, Liu JC, Agamez NMR, Loch AJ, Wong RG, et al. Cooperation between Pik3ca and p53 mutations in mouse mammary tumor formation. Cancer Res. 2011;71(7):2706–17.

6. Bi L, Okabe I, Bernard DJ, Wynshaw-Boris a., Nussbaum RL. Proliferative Defect and Embryonic Lethality in Mice Homozygous for a Deletion in the p110-alpha Subunit of Phosphoinositide 3-Kinase. J Biol Chem. 1999;274(16):10963–8.

7. Foukas LC, Claret M, Pearce W, Okkenhaug K, Meek S, Peskett E, et al. Critical role for the p110alpha phosphoinositide-3-OH kinase in growth and metabolic regulation. Nature. 2006;441(7091):366–70.

8. Utermark T, Rao T, Cheng H, Wang Q, Lee SH, Wang ZC, et al. The p110α and p110β isoforms of PI3K play divergent roles in mammary gland development and tumorigenesis. Genes Dev. 2012;26(14):1573–86.

9. Zhao JJ, Cheng H, Jia S, Wang L, Gjoerup O V, Mikami A, et al. The p110alpha isoform of PI3K is essential for proper growth factor signaling and oncogenic transformation. Proc Natl Acad Sci U S A. 2006;103(44):16296–300.

10. Yoshioka K, Yoshida K, Cui H, Wakayama T, Takuwa N, Okamoto Y, et al. Endothelial PI3K-C2α, a class II PI3K, has an essential role in angiogenesis and vascular barrier function. Nat Med. 2012; 18(10):1560–9.

11. Franco I, Gulluni F, Campa CC, Costa C, Margaria JP, Ciraolo E, et al. PI3K class II α controls spatially restricted endosomal PtdIns3P and Rab11 activation to promote primary cilium function. Dev Cell. 2014;28(6):647–58.

12. Toker A, Marmiroli S. Signaling specificity in the Akt pathway in biology and disease. Adv Biol Regul. 2014;55:28–38.

13. Vivanco I, Sawyers CL. The phosphatidylinositol 3-Kinase AKT pathway in human cancer. Nat Rev Cancer. 2002;2(7):489–501.

14. Franke TF, Kaplan DR, Cantley LC, Toker A. Direct Regulation of the Akt Proto-Oncogene Product by Phosphotidylinositol-3,4-bisphosphate. Science; 1992;1041:665–8.

15. Alessi DR, James SR, Downes CP, Holmes AB, Gaffney PRJ, Reese CB, et al. Characterization of a 3-phosphoinositide-dependent protein kinase which phosphorylates and activates protein kinase Bα. Curr Biol. 1997; 7(4):261–9.

16. Sarbassov DD, Guertin DA, Ali SM. Phosphorylation and Regulation of Akt / PKB by the Rictor-mTOR Complex. Science. 2005;307:1098–102.

17. Stokoe D, Stephens LR, Copeland T, Gaffney PRJ, Reese CB, Painter GF, et al. Dual Role of Phosphatidylinositol-3 , 4 , 5- trisphosphate in the Activation of Protein Kinase B. Science. 1997;277:567–70.

18. Klippel A, Kavanaugh WM, Pot D, Williams LT. A Specific Product of Phosphatidylinositol 3-Kinase Directly Activates the Protein Kinase Akt through Its Pleckstrin Homology Domain. Mol Cell Biol. 1997;17(1):338–44.

19. Ma K, Cheung SM, Marshall AJ, Duronio V. PI(3,4,5)P3 and PI(3,4)P2 levels correlate with PKB/akt phosphorylation at Thr308 and Ser473, respectively; PI(3,4)P2 levels determine PKB activity. Cell Signal. 2008;20(4):684–94.

20. Alessi DR, Caudwell FB, Andjelkovic M, Hernmings BA, Cohen P. Molecular basis for the substrate specificity of protein kinase B ; comparison with MAPKAP kinase-1 and p70 S6 kinase. FEBS. 1996;399:333–8.

21. Altomare D, Testa JR. Perturbations of the AKT signaling pathway in human cancer. Oncogene. 2005;24(50):7455–64.

22. Mayo LD, Donner DB. A phosphatidylinositol 3-kinase /Akt pathway promotes translocation of Mdm2 from the cytoplasm to the nucleus. Proc Natl Acad Sci. 2001; 98:11598-603.

23. Ogawara Y, Kishishita S, Obata T, Isazawa Y, Suzuki T, Tanaka K, et al. Akt enhances Mdm2-mediated ubiquitination and degradation of p53. J Biol Chem. 2002;277(24):21843–50.

24. Bellacosa A, Kumar C. Activation of AKT kinases in cancer: implications for therapeutic targeting. Adv cancer res. 2005;4:29-86.

25. Inoki K, Li Y, Zhu T, Wu J, Guan K-L. TSC2 is phosphorylated and inhibited by Akt and suppresses mTOR signalling. Nat Cell Biol. 2002;4(9):648–57.

26. Hudson CC, Liu M, Chiang GG, Otterness DM, Loomis DC, Kaper F, et al. Regulation of Hypoxia-Inducible Factor 1 Expression and Function by the Mammalian Target of Rapamycin. Mol Cell Biol. 2002;22(20):7004–14.

27. Dimmeler S, Fleming I, Fisslthaler B, Hermann C, Busse R, Zeiher AM. Activation of nitric oxide synthase in endothelial cells by Akt-dependent phosphorylation. Nature. 1999;399:601–5.

28. Fulton D, Gratton J, Mccabe TJ, Fontana J, Fujio Y, Walsh K, et al. Regulation of endothelium- derived nitric oxide production by the protein kinase Akt. Nature. 1999;399:597–601.

29. Thant AA, Nawa A, Kikkawa F, Ichigotani Y, Zhang Y, Sein TT, et al. Fibronectin activates matrix metalloproteinase-9 secretion via the MEK1-MAPK and the PI3K-Akt pathways in ovarian cancer cells. Clin Exp Metastasis. 2001;18(423):423–8.

30. Grille SJ, Bellacosa A, Upson J, Klein-szanto AJ, Roy F Van, Lee-kwon W, et al. The Protein Kinase Akt Induces Epithelial Mesenchymal Transition and Promotes Enhanced Motility and Invasiveness of Squamous Cell Carcinoma Lines. Cancer Res. 2003;63:2172–8.

31. Aoki K, Tamai Y, Horiike S, Oshima M, Taketo MM. Colonic polyposis caused by mTOR-mediated chromosomal instability in Apc+/Delta716 Cdx2+/- compound mutant mice. Nat Genet. 2003;35(4):323–30.

32. Cheng JQ, Godwin AK, Bellacosa A, Taguchi T, Franke TF, Hamilton TC, et al. AKT2 , a putative oncogene encoding a member of a subfamily of protein-serine / threonine kinases , is amplified in human ovarian carcinomas. Proc Natl Acad Sci. 1992;89:9267–71.

33. Bellacosa N, Feo D, Godwin AK, Bell DW, Cheng JQ, Altomare DA, et al. Molecular alterations of the AKT2 oncogene in ovarian and breast carcinomas. Int J Cancer. 1995;285:280–5.

34. Stål O, Pérez-tenorio G, Åkerberg L, Olsson B, Nordenskjöld B, Skoog L, et al. Akt kinases in breast cancer and the results of adjuvant therapy. Breast Cancer Res. 2003;5(2):37–44.

35. Cheng JQ, Altomare D a, Klein M a, Lee WC, Kruh GD, Lissy N a, et al. Transforming activity and mitosis-related expression of the AKT2 oncogene: evidence suggesting a link between cell cycle regulation and oncogenesis. Oncogene. 1997;14(23):2793–801.

36. Arboleda MJ, Lyons JF, Kabbinavar FF, Bray MR, Snow BE, Ayala R, et al. Overexpression of AKT2 / Protein Kinase B beta Leads to Up-Regulation of β1 Integrins , Increased Invasion , and Metastasis of Human Breast and Ovarian Cancer Cells. Cancer Res. 2003;63:196–206.

37. Balsara BR, Pei J, Mitsuuchi Y, Page R, Klein-Szanto A, Wang H, et al. Frequent activation of AKT in non-small cell lung carcinomas and preneoplastic bronchial lesions. Carcinogenesis. 2004;25(11):2053–9.

38. Carpten JD, Faber AL, Horn C, Donoho GP, Briggs SL, Robbins CM, et al. A transforming mutation in the pleckstrin homology domain of AKT1 in cancer. Nature. 2007;448(7152):439–44.

39. Kim MS, Jeong EG, Yoo NJ, Lee SH. Mutational analysis of oncogenic AKT E17K mutation in common solid cancers and acute leukaemias. Br J Cancer. 2008;98(9):1533–5.

40. Hollander MC, Blumenthal GM, Dennis P a. PTEN loss in the continuum of common cancers, rare syndromes and mouse models. Nat Rev Cancer. 2011;11(4):289–301.

41. Kuo Y-C, Huang K-Y, Yang C-H, Yang Y-S, Lee W-Y, Chiang C-W. Regulation of phosphorylation of Thr-308 of Akt, cell proliferation, and survival by the B55alpha regulatory subunit targeting of the protein phosphatase 2A holoenzyme to Akt. J Biol Chem. 2008;283(4):1882–92.

42. Gao T, Furnari F, Newton AC. PHLPP: a phosphatase that directly dephosphorylates Akt, promotes apoptosis, and suppresses tumor growth. Mol Cell. 2005;18(1):13–24.

43. Brognard J, Sierecki E, Gao T, Newton AC. PHLPP and a second isoform, PHLPP2, differentially attenuate the amplitude of Akt signaling by regulating distinct Akt isoforms. Mol Cell. 2007;25(6):917–31.

44. Chen M, Pratt CP, Zeeman ME, Schultz N, Taylor BS, O'Neill A, et al. Identification of PHLPP1 as a tumor suppressor reveals the role of feedback activation in PTEN-mutant prostate cancer progression. Cancer Cell. 2011; (2):173–86.

45. Hutchinson J, Jin J, Cardiff RD, Woodgett JR, Muller WJ. Activation of Akt (protein kinase B) in mammary epithelium provides a critical cell survival signal required for tumor progression. Mol Cell Biol. 2001; 21(6):2203–12.

46. Chen WS, Xu P, Gottlob K, Chen M, Sokol K, Shiyanova T, et al. Growth retardation and increased apoptosis in mice with homozygous disruption of the Akt1 gene. Genes Dev. 2001;15(312):2203–8.

47. Garofalo RS, Orena SJ, Rafidi K, Torchia AJ, Stock JL, Hildebrandt AL, et al. Severe diabetes, age-dependent loss of adipose tissue, and mild growth deficiency in mice lacking Akt2/PKB. J Clin Invest. 2003;112(2):197–208.

48. Cho H, Mu J, Kim JK, Thorvaldsen JL, Chu Q, Crenshaw EB, et al. Insulin resistance and a diabetes mellitus-like syndrome in mice lacking the protein kinase Akt2 (PKB beta). Science. 2001;292(5522):1728–31.

49. Easton RM, Cho H, Roovers K, Shineman DW, Mizrahi M, Forman MS, et al. Role for Akt3/protein kinase Bgamma in attainment of normal brain size. Mol Cell Biol. 2005;25(5):1869–78.

50. Santi S, Lee H. The Akt isoforms are present at distinct subcellular locations. Am J Physiol Cell Physiol. 2010;298(3):C580–91.

51. Martelli AM, Tabellini G, Bressanin D, Ognibene A, Goto K, Cocco L, et al. The emerging multiple roles of nuclear Akt. Biochim Biophys Acta. 2012; 1823(12):2168–78.

52. Wan L, Singh A, Zhai B, Yuan M, Wang Z, Gygi SP. Cell-cycle-regulated activation of Akt kinase by phosphorylation at its carboxyl terminus. Nature. 2014;508(7497):541–5.

53. Trotman LC, Alimonti A, Scaglioni PP, Koutcher J a, Cordon-Cardo C, Pandolfi PP. Identification of a tumour suppressor network opposing nuclear Akt function. Nature. 2006; 441(7092):523–7.

54. Walz H a, Shi X, Chouinard M, Bue C a, Navaroli DM, Hayakawa A, et al. Isoform-specific regulation of Akt signaling by the endosomal protein WDFY2. J Biol Chem. 2010;285(19):14101–8.

55. Cenni V, Bavelloni A, Beretti F, Tagliavini F, Manzoli L, Lattanzi G, et al. Ankrd2/ARPP is a novel Akt2 specific substrate and regulates myogenic differentiation upon cellular exposure to H(2)O(2). Mol Biol Cell. 2011;22(16):2946–56.

56. Chin YR, Toker A. The Actin-Bundling Protein Palladin Is an Akt1-Specific Substrate that Regulates Breast Cancer Cell Migration. Mol Cell. 2010;38(3):333–44.

57. Hutchinson JN, Jin J, Cardiff RD, Woodgett JR, Muller WJ. Activation of Akt-1 ( PKB-α ) Can Accelerate ErbB-2-Mediated Mammary Tumorigenesis but Suppresses Tumor Invasion. Cancer Res. 2004;64:3171–8.

58. Irie HY, Pearline R V, Grueneberg D, Hsia M, Ravichandran P, Kothari N, et al. Distinct roles of Akt1 and Akt2 in regulating cell migration and epithelial-mesenchymal transition. J Cell Biol. 2005;171(6):1023–34.

59. Héron-Milhavet L, Franckhauser C, Rana V, Berthenet C, Fisher D, Hemmings B a, et al. Only Akt1 is required for proliferation, while Akt2 promotes cell cycle exit through p21 binding. Mol Cell Biol. 2006;26(22):8267–80.

60. Maroulakou IG, Oemler W, Naber SP, Tsichlis PN. Akt1 ablation inhibits, whereas Akt2 ablation accelerates, the development of mammary adenocarcinomas in mouse mammary tumor virus (MMTV)-ErbB2/neu and MMTV-polyoma middle T transgenic mice. Cancer Res. 2007;67(1):167–77.

61. Dillon RL, Marcotte R, Hennessy BT, Woodgett JR, Mills GB, Muller WJ. Akt1 and akt2 play distinct roles in the initiation and metastatic phases of mammary tumor progression. Cancer Res. 2009;69(12):5057–64.

62. Chin YR, Yoshida T, Marusyk A, Beck AH, Polyak K, Toker A. Targeting Akt3 signaling in triple-negative breast cancer. Cancer Res. 2014;74(3):964–73.

63. Steck AP, Pershouse, MA, Jasser, SA, Yung, WKA, Lin, H, Ligon, AH, Langford, LA, Baumgard, ML, Hattier, T, Davis, T, Frye, C, Hu, R, Sweldlund, B, Teng D and TS. Identification of a candidate tumor suppressor gene, MMAC1, at chromosome 10q23.3 that is mutated in multiple advanced cancers. Nat Genet. 1997;15:57–61.

64. Li J, Yen C, Liaw D, Podsypanina K, Bose S, Wang SI, et al. PTEN, a putative protein tyrosine phosphatase gene mutated in human brain, breast, and prostate cancer. Science. 1997;275(5308):1943–7.

65. Song MS, Salmena L, Pandolfi PP. The functions and regulation of the PTEN tumour suppressor. Nat Rev Mol Cell Biol.; 2012;13(5):283–96.

66. Maehama T and Dixon J. The tumor suppressor, PTEN/MMAC1, dephosphorylates the lipid second messenger, phosphatidylinositol 3,4,5-trisphosphate. J Biol Chem. 1998;273(22):13375–8.

67. Myers MP, Stolarov JP, Eng C, Li J, Wang SI, Wigler MH, et al. P-TEN, the tumor suppressor from human chromosome 10q23, is a dual-specificity phosphatase. Proc Natl Acad Sci U S A. 1997;94(17):9052–7.

68. Tamura M, Gu J, Takino T, Yamada KM. Tumor Suppressor PTEN Inhibition of Cell Invasion , Migration , and Growth : Differential Involvement of Focal Adhesion Kinase and p130 Cas. Cancer Res. 1999;4370(21):442–9.

69. Tibarewal P, Zilidis G, Spinelli L, Schurch N, Maccario H, Gray A, et al. PTEN protein phosphatase activity correlates with control of gene expression and invasion, a tumor-suppressing phenotype, but not with AKT activity. Sci Signal. 2012;5(213):ra18.

70. Zhang S, Huang W-C, Li P, Guo H, Poh S-B, Brady SW, et al. Combating trastuzumab resistance by targeting SRC, a common node downstream of multiple resistance pathways. Nat Med. 2011; 17(4):461–9.

71. Marsh DJ, Coulon V, Lunetta KL, Rocca-serra P, Patricia L, Dahia M, et al. Mutation spectrum and genotype-phenotype analyses in Cowden disease and Bannayan – Zonana syndrome , two hamartoma syndromes with germline PTEN mutation. Hum Mol Genet. 1998;7(3):507–15.

72. Chalhoub N, Baker SJ. PTEN and the PI3-kinase pathway in cancer. Annu Rev Pathol. 2009;4:127–50.

73. Pezzolesi MG, Li Y, Zhou X, Pilarski R, Shen L, Eng C. Mutation-positive and mutation-negative patients with Cowden and Bannayan-Riley-Ruvalcaba syndromes associated with distinct 10q haplotypes. Am J Hum Genet. 2006;79(5):923–34.

74. Perren a, Komminoth P, Saremaslani P, Matter C, Feurer S, Lees J a, et al. Mutation and expression analyses reveal differential subcellular compartmentalization of PTEN in endocrine pancreatic tumors compared to normal islet cells. Am J Pathol. 2000;157(4):1097–103.

75. Alimonti A, Carracedo A, Clohessy JG, Trotman LC, Nardella C, Egia A, et al. Subtle variations in Pten dose determine cancer susceptibility. Nat Genet. 2010;42(5):454–8.

76. Berger AH, Pandolfi PP. Haplo-insufficiency: A driving force in cancer. Journal of Pathology. 2011. 476: 137–46.

77. Cristofano A Di, Pesce B, Cordon-cardo C, Pandolfi PP. Pten is essential for embryonic development and tumour suppression. Nature. 1998;19:348–55.

78. Trotman LC, Niki M, Dotan Z a, Koutcher J a, Di Cristofano A, Xiao A, et al. Pten dose dictates cancer progression in the prostate. PLoS Biol. 2003;1(3):E59.

79. Suzuki a, de la Pompa JL, Stambolic V, Elia a J, Sasaki T, del Barco Barrantes I, et al. High cancer susceptibility and embryonic lethality associated with mutation of the PTEN tumor suppressor gene in mice. Curr Biol. 1998;8(21):1169–78.

80. Podsypanina K, Ellenson LH, Nemes A, Gu J, Tamura M, Yamada KM, et al. Mutation of Pten/Mmac1 in mice causes neoplasia in multiple organ systems. Proc Natl Acad Sci U S A. 1999;96(4):1563–8.

81. Stambolic V, Tsao MS, Macpherson D, Suzuki A, Chapman WB, Mak TW. High incidence of breast and endometrial neoplasia resembling human Cowden syndrome in pten(+/-) mice. Cancer Res. 2000;60(13):3605–11.

82. Li Y, Podsypanina K, Liu X, Crane A, Tan LK, Parsons R, et al. Deficiency of Pten accelerates mammary oncogenesis in MMTV- Wnt-1 transgenic mice. BMC Mol Biol. 2001; 2:2

83. Wang H, Douglas W, Lia M, Edelmann W, Kucherlapati R, Podsypanina K, et al. DNA mismatch repair deficiency accelerates endometrial tumorigenesis in Pten heterozygous mice. Am J Pathol. 2002;160(4):1481–6.

84. Liu X, Karnell JL, Yin B, Zhang R, Zhang J, Li P, et al. Distinct roles for PTEN in prevention of T cell lymphoma and autoimmunity in mice. J Clin Invest. 2010;120(7):2497–507.

85. Papa A, Wan L, Bonora M, Salmena L, Song MS, Hobbs RM, et al. Cancer-associated PTEN mutants act in a dominant-negative manner to suppress PTEN protein function. Cell; 2014;157(3):595–610.

86. Dahia PLM, Marsh DJ, Zheng Z, Zedenius J, Komminoth P, Frisk T, et al. Somatic deletions and mutations in Cowden Disease Gene, PTEN, in sporadic thyroid tumors. Cancer Res. 1997;57(617):4710–3.

87. Alvarez-Nuñez F, Bussaglia E, Mauricio D, Ybarra J, Vilar M, Lerma E, et al. PTEN promoter methylation in sporadic thyroid carcinomas. Thyroid. 2006;16(1):17–23.

88. Halachmi N, Halachmi S, Evron E, Cairns P, Okami K, Saji M, et al. Somatic mutations of the PTEN tumor suppressor gene in sporadic follicular thyroid tumors. Genes Chr. Cancer. 1998;23(3):239–43.

89. Cristofano A Di, Acetis M De, Koff A, Cordon-cardo C, Pandolfi PP. Pten and p27 KIP1 cooperate in prostate cancer tumor suppression in the mouse. Nat Genet. 2001;27:222–4.

90. Yeager N, Klein-Szanto A, Kimura S, Di Cristofano A. Pten loss in the mouse thyroid causes goiter and follicular adenomas: Insights into thyroid function and cowden disease pathogenesis. Cancer Res. 2007;67(3):959–66.

91. Antico-Arciuch VG, Dima M, Liao X-H, Refetoff S, Di Cristofano a. Cross-talk between PI3K and estrogen in the mouse thyroid predisposes to the development of follicular carcinomas with a higher incidence in females. Oncogene; 2010;29(42):5678–86.

92. Norris FA, Atkins RC, Majerus PW. The cDNA Cloning and Characterization of Inositol Polyphosphate 4-Phosphatase Type II. J Biol Chem. 1997;272(38):23859–64.

93. Kofuji S, Kimura H, Nakanishi H, Nanjo H, Takasuga S, Liu H, et al. INPP4B is a PtdIns(3,4,5)P3 phosphatase that can act as a tumor suppressor. Cancer Discov. 2015; CD-14-1329

94. Agoulnik IU, Hodgson MC, Bowden WA, Ittmann MM. INPP4B : the New Kid on the PI3K Block Abstract : Oncotarget. 2011;2(4):321–8.

95. Ferron M, Vacher J. Characterization of the murine Inpp4b gene and identification of a novel isoform. Gene, 2011;376(1):152–61.

96. Rynkiewicz NK, Liu H-J, Balamatsias D, Mitchell C a. INPP4A/INPP4B and P-Rex proteins: related but different? Adv Biol Regul. 2012; 52(1):265–79.

97. Westbrook TF, Martin ES, Schlabach MR, Leng Y, Liang AC, Feng B, et al. A genetic screen for candidate tumor suppressors identifies REST. Cell 2005;121(6):837–48.

98. Gewinner C, Wang ZC, Richardson A, Teruya-Feldstein J, Etemadmoghadam D, Bowtell D, et al. Evidence that inositol polyphosphate 4-phosphatase type II is a tumor suppressor that inhibits PI3K signaling. Cancer Cell; 2009;16(2):115–25.

99. Fedele CG, Ooms LM, Ho M, Vieusseux J, O'Toole S a, Millar EK, et al. Inositol polyphosphate 4-phosphatase II regulates PI3K/Akt signaling and is lost in human basal-like breast cancers. Proc Natl Acad Sci U S A. 2010;107(51):22231–6.

100. Won JR, Gao D, Chow C, Cheng J, Lau SYH, Ellis MJ, et al. A survey of immunohistochemical biomarkers for basal-like breast cancer against a gene expression profile gold standard. Mod Pathol; 2013; 26(11):1438–50.

101. Taylor BS, Schultz N, Hieronymus H, Gopalan A, Xiao Y, Carver BS, et al. Integrative genomic profiling of human prostate cancer. Cancer Cell 2010;18(1):11–22.

102. Hodgson MC, Shao L, Frolov A, Li R, Peterson LE, Ayala G, et al. Decreased expression and androgen regulation of the tumor suppressor gene INPP4B in prostate cancer. Cancer Res. 2011 Jan;71(2):572–82.

103. Rynkiewicz NK, Fedele CG, Chiam K, Gupta R, Kench JG, Ooms LM, et al. INPP4B is highly expressed in prostate intermediate cells and its loss of expression in prostate carcinoma predicts for recurrence and poor long term survival. Prostate 2015;75(1):92–102.

104. Hodgson MC, Deryugina EI, Suarez E, Lopez SM, Lin D, Xue H, et al. INPP4B suppresses prostate cancer cell invasion. Cell Commun Signal 2014;12:61.

105. Perez-Lorenzo R, Gill KZ, Shen C-H, Zhao FX, Zheng B, Schulze H-J, et al. A tumor suppressor function for the lipid phosphatase INPP4B in melanocytic neoplasms. J Invest Dermatol. 2014;134(5):1359–68.

106. Yuen JW-F, Chung GT-Y, Lun SW-M, Cheung CC-M, To K-F, Lo K-W. Epigenetic Inactivation of Inositol polyphosphate 4-phosphatase B (INPP4B), a Regulator of PI3K/AKT Signaling Pathway in EBV-Associated Nasopharyngeal Carcinoma. PLoS One. 2014;9(8):e105163.

107. Chew CL, Lunardi A, Gulluni F, Ruan DT, Chen M, Salmena L, et al. In vivo role of INPP4B in tumor and metastasis suppression through regulation of PI3K/AKT signaling at endosomes. Cancer Discov. 2015 CD-14-1347.

108. Gasser J a, Inuzuka H, Lau AW, Wei W, Beroukhim R, Toker A. SGK3 Mediates INPP4B-Dependent PI3K Signaling in Breast Cancer. Mol Cell. 2014;56(4):595–607.

109. Vasudevan KM, Barbie D a, Davies M a, Rabinovsky R, McNear CJ, Kim JJ, et al. AKT-independent signaling downstream of oncogenic PIK3CA mutations in human cancer. Cancer Cell. 2009;16(1):21–32.

110. Dzneladze I, He R, Woolley JF, Hi Son M, Sharobim MH, Greenberg S a, et al. INPP4B overexpression is associated with poor clinical outcome and therapy resistance in acute myeloid leukemia. Leukemia. 2015; doi10.1038.

111. Rijal S, Fleming S, Cummings N, Rynkiewicz NK, Ooms LM, Nguyen N-YN, et al. Inositol polyphosphate 4-phosphatase II (INPP4B) is associated with chemoresistance and poor outcome in AML. Blood. 2015. 2014-09-603555.

112. Ferron M, Boudiffa M, Arsenault M, Rached M, Pata M, Giroux S, et al. Inositol polyphosphate 4-phosphatase B as a regulator of bone mass in mice and humans. Cell Metab. 2011; 14(4):466–77.

113. Nystuen A, Legare ME, Shultz LD, Frankel WN, Street M, Harbor B. A Null Mutation in Inositol Polyphosphate 4-Phosphatase Type I Causes Selective Neuronal Loss in Weeble Mutant Mice. Neuron. 2001;32:203–12.

114. Lemcke S, Müller S, Möller S, Schillert A, Ziegler A, Cepok-Kauffeld S, et al. Nerve conduction velocity is regulated by the inositol polyphosphate-4-phosphatase II gene. Am J Pathol. 2014;184(9):2420–9.

115. Pálfy M, Reményi A, Korcsmáros T. Endosomal crosstalk: meeting points for signaling pathways. Trends Cell Biol. 2012;22(9):447–56.

116. Miaczynska M, Pelkmans L, Zerial M. Not just a sink: endosomes in control of signal transduction. Curr Opin Cell Biol. 2004;16(4):400–6.

117. Guglielmol GM Di, Baass PC, Ou W, Posner BI, Bergeron JJM. Compartmentalization of SHC , GRB2 and mSOS , and hyperphosphorylation of Raf-1 by EGF but not insulin in liver parenchyma. EMBO J. 1994;13(18):4269–77.

118. Vieira A V, Lamaze C, Schmid SL. Control of EGF Receptor Signaling by Clathrin-mediated Endocytosis. Science. 1996;274(5295):2086–9.

119. Schenck A, Goto-Silva L, Collinet C, Rhinn M, Giner A, Habermann B, et al. The endosomal protein Appl1 mediates Akt substrate specificity and cell survival in vertebrate development. Cell. 2008;133(3):486–97.

120. Nazarewicz RR, Salazar G, Patrushev N, San Martin A, Hilenski L, Xiong S, et al. Early endosomal antigen 1 (EEA1) is an obligate scaffold for angiotensin II-induced, PKC-alpha-dependent Akt activation in endosomes. J Biol Chem. 2011;286(4):2886–95.

121. Polo S, Di Fiore PP. Endocytosis conducts the cell signaling orchestra. Cell. 2006;124(5):897–900.

122. Jékely G, Sung H-H, Luque CM, Rørth P. Regulators of endocytosis maintain localized receptor tyrosine kinase signaling in guided migration. Dev Cell. 2005;9(2):197–207.

123. Wu X, Gan B, Yoo Y, Guan J-L. FAK-mediated src phosphorylation of endophilin A2 inhibits endocytosis of MT1-MMP and promotes ECM degradation. Dev Cell. 2005;9(2):185–96.

124. Palamidessi A, Frittoli E, Garré M, Faretta M, Mione M, Testa I, et al. Endocytic trafficking of Rac is required for the spatial restriction of signaling in cell migration. Cell. 2008;134(1):135–47.

125. Schmid SL, Mettlen M. Lipid switches and traffic control. Nature. 2013;499:161–2.

126. Posor Y, Eichhorn-Gruenig M, Puchkov D, Schöneberg J, Ullrich A, Lampe A, et al. Spatiotemporal control of endocytosis by phosphatidylinositol-3,4-bisphosphate. Nature. 2013;499(7457):233–7.

127. Posor Y, Eichhorn-Grünig M, Haucke V. Phosphoinositides in endocytosis. Biochim Biophys Acta. 2014;1851(6):794–804.

# CHAPTER 2

## *In vivo* role of INPP4B in tumor and metastasis suppression through regulation of PI3K/AKT signaling at endosomes

## Authors' Contributions

**Conception and design:** C.L. Chew, D.T. Ruan, A. Lunardi, L. Salmena, P.P. Pandolfi

**Development of methodology:** C.L. Chew, F. Gulluni, D.T. Ruan, A. Lunardi, M. Chen, L. Salmena, A. Papa

**Carried out experiments:** C.L. Chew, F. Gulluni, M. Chen, A. Lunardi

**Acquisition of data:** C.L. Chew, F. Gulluni, D.T. Ruan, M. Chen, C. Ng, J. Fung

**Analysis and interpretation of data (e.g. statistical analysis, H&E and IHC interpretation):** C.L. Chew, D.T. Ruan, A. Lunardi, M. Chen, M. Nishino, R.T. Bronson, E. Hirsch, P.P. Pandolfi

**Writing, review, and/or revision of the manuscript:** C.L. Chew, D.T. Ruan, A. Lunardi, M. Chen, P.P. Pandolfi

**Administrative, technical, or material support:** C.L. Chew, D.T. Ruan, A. Lunardi, A. Papa, J.G. Clohessy, J. Sasaki, T. Sasaki, L. Longo

**Study supervision:** C.L. Chew, A. Lunardi, D.T. Ruan, A. Papa, P.P. Pandolfi

**Provided histology and immunohistochemistry:** C. Ng, J. Fung

At the time of submission of this dissertation, work presented in this chapter has been published in *Cancer Discovery* as a manuscript entitled:

# *In vivo* role of INPP4B in tumor and metastasis suppression through regulation of PI3K/AKT signaling at endosomes

**Chen Li Chew[1], Andrea Lunardi[1*], Federico Gulluni[2*], Daniel T. Ruan[1], Ming Chen[1], Leonardo Salmena[1, 6], Michiya Nishino[3], Antonella Papa[1], Christopher Ng[1], Jacqueline Fung[1], John G. Clohessy[1], Junko Sasaki[4], Takehiko Sasaki[4], Roderick T. Bronson[5], Emilio Hirsch[2] and Pier Paolo Pandolfi[1]**

*[1]Cancer Research Institute, Beth Israel Deaconess Cancer Center, Department of Medicine and Pathology, Beth Israel Deaconess Medical Center, Harvard Medical School, Boston, MA 02215, USA. [2]Molecular Biotechnology Center, Department of Molecular Biotechnology and Health Sciences, University of Torino, Italy. [3]Department of Pathology, Beth Israel Deaconess Medical Center, Harvard Medical School, Boston, MA 02215. [4]Department of Medical Biology, Akita University Graduate School of Medicine and Research Center for Biosignal, Akita University, Akita 010-8543, Japan. [5]Department of Microbiology and Immunobiology, Harvard Medical School, Boston, MA 02215 USA. [6]Present address: Department of Pharmacology and Toxicology, University of Toronto and Princess Margaret Cancer Center, Toronto ON M5T 2M9, Canada.*

*These authors contributed equally to this article.

**Correspondence should be addressed to:** Pier Paolo Pandolfi

Beth Israel Deaconess Medical Center, CLS Building, Room 401
330 Brookline Avenue, Boston, MA 02215.
Phone: 617-735-2121; Email: ppandolf@bidmc.harvard.edu

**Running title**: INPP4B inhibits thyroid tumorigenesis and metastasis

**Keywords:** Cancer, metastasis, genetics, INPP4B, endosome, PI3K/AKT, thyroid

**Conflict of Interest:** None of the authors have anything to declare

## 2.1 ABSTRACT

The phosphatases PTEN and INPP4B have been proposed to act as tumor suppressors by antagonizing PI3K/AKT signaling, and are frequently dysregulated in human cancer. While PTEN has been extensively studied, little is known about the underlying mechanisms by which INPP4B exerts its tumor suppressive function and its role in tumorigenesis *in vivo*. Here, we show that a partial or complete loss of *Inpp4b* morphs benign thyroid adenoma lesions in *Pten* heterozygous mice into lethal and metastatic follicular-like thyroid cancer (FTC). Importantly, analyses of human thyroid cancer cell lines and specimens reveal INPP4B downregulation in FTC. Mechanistically, we find that INPP4B, but not PTEN, is enriched in the early endosomes of thyroid cancer cells, where it selectively inhibits AKT2 activation and in turn tumor proliferation and anchorage-independent growth. We therefore identify INPP4B as a novel tumor suppressor in FTC oncogenesis and metastasis through localized regulation of PI3K/AKT pathway at the endosomes.

## 2.2 SIGNIFICANCE

Although both PTEN and INPP4B can inhibit PI3K/AKT signaling through their lipid phosphatase activities, here we demonstrate lack of an epistatic relationship between the two tumor suppressors. Instead, the qualitative regulation of PI3K/AKT2 signaling by INPP4B provides a mechanism for their cooperation in suppressing thyroid tumorigenesis and metastasis.

## 2.3 INTRODUCTION

The phosphoinositide 3-kinase (PI3K)/AKT signaling pathway modulates important biological processes such as cell cycle, survival, metabolism and motility, which are often disrupted in cancer (1). Hyperactivation of the PI3K/AKT pathway leads to an accumulation of phosphatidylinositol (3,4,5)-trisphosphate ($PI(3,4,5)P_3$), which in turn increases the recruitment and activation of protein kinase AKT at the cytoplasmic membrane (1), a key mediator of the oncogenic effects of enhanced PI3K signaling.

The AKT protein kinase family is made up of three highly homologous isoforms, namely AKT1, AKT2 and AKT3 (2). Despite similarities in sequence and regulation, studies reveal isoform-specific functions in cancer progression. In the context of breast cancer, overexpression of AKT2 promotes metastasis (3), while AKT1 suppresses metastasis (4, 5). The distinct functions of the AKT isoforms could be explained, at least in part, through the association of the AKT isoforms with distinct organelles or subcellular compartments (2).

The tumor suppressor gene *PTEN* (the phosphatase and tensin homolog), encoding a lipid-phosphatase, dephosphorylates $PI(3,4,5)P_3$ to $PI(4,5)P_2$ to antagonize PI3K/AKT signaling. To study the effects of *Pten* loss *in vivo*, we previously generated mouse models with constitutive and conditional *Pten* loss (6). We found that homozygous loss of *Pten* results in embryonic lethality, while *Pten* heterozygous ($Pten^{+/-}$) mice develop tumors of the breast, endometrium, prostate, adrenal, pituitary and lymphoma (7). More recently, INPP4B (inositol polyphosphate-phosphatase type II), another dual specificity and lipid phosphatase, has emerged as a putative tumor suppressor in the suppression of the PI3K/AKT signaling pathway. *INPP4B* was initially identified as an anchorage independent growth suppressor in a shRNA-mediated genetic screen performed in HMEC cells (8), and was found to inhibit PI3K signaling and to display tumor

suppressive activity in breast tumor cell lines (9). In agreement with these findings, INPP4B expression was found to be reduced in basal-like breast cancers (9, 10), melanoma (11), nasopharyngeal carcinoma (12), and prostate cancer (13). Furthermore, expression-profiling analyses revealed that INPP4B mRNA expression is reduced in up to 47% of metastatic prostate cancer cases (14), implicating the potential role of INPP4B in metastatic progression.

INPP4B converts $PI(3,4)P_2$ to PI(3)P and because direct interaction of $PI(3,4)P_2$ with the pleckstrin homology (PH) domain of AKT is required for membrane recruitment and full activation of AKT (15), INPP4B, like PTEN, is anticipated to act as a tumor suppressor by antagonizing PI3K/AKT signaling (9). However, unlike PTEN, the underlying molecular mechanisms by which INPP4B exerts its tumor suppressive function are poorly understood. Additionally it is not known whether INPP4B acts as a tumor suppressor *in vivo*.

We therefore sought to investigate the tumor suppressive functions of INPP4B *in vivo* in Knock-out (KO) mouse models. Surprisingly, we found that INPP4B exerts a specific role in the suppression of thyroid tumorigenesis and metastasis *in vivo* through the inhibition of PI3K-C2α mediated AKT2 activation at endosomes.

## 2.4 RESULTS

### Inpp4b knockout (*Inpp4b*$^{-/-}$) mice do not develop the tumorigenic phenotype of Pten haploinsufficient mice.

To determine the *in vivo* tumor suppressive function of INPP4B, we took advantage of Inpp4b knockout mice (*Inpp4b*$^{-/-}$) generated by using a homologous recombination targeting strategy in which the conditional targeting vector was constructed to delete exon 21 of the mouse *Inpp4b* gene, which encodes the phosphatase catalytic domain (Figure 2.1A-B). Unlike *Pten*$^{-/-}$ mice, *Inpp4b*$^{-/-}$ mice were viable and born in accordance to Mendelian frequencies (Figure 2.1C). Furthermore, *Inpp4b*$^{+/-}$ and *Inpp4b*$^{-/-}$ mice did not develop any of the tumors or the lymphoproliferative disease characteristic of *Pten*$^{+/-}$ mice in a 16-24 months follow-up (16). Aggressive and fatal, albeit sporadic, histiosarcomas were observed after a very long latency in *Inpp4b*$^{-/-}$ mice (data not shown). These results demonstrate unequivocally that the role of PTEN and INPP4B in tumorigenesis could be very distinct.

### Loss of *Inpp4b* in a *Pten* heterozygous background leads to metastatic follicular-like thyroid carcinoma.

We next sought to determine if loss of Inpp4b cooperated with Pten loss to promote tumor progression. We hypothesized that loss of Inpp4b would accelerate overall tumor progression in *Pten*$^{+/-}$ mice, keeping with their reported epistatic relationship in the suppression of PI3K/AKT signaling. To this end, we crossed *Pten*$^{+/-}$ mice with *Inpp4b*$^{-/-}$ mice. The resulting *Pten*$^{+/-}$*Inpp4b*$^{+/-}$ mice were then crossed with *Inpp4b*$^{+/-}$ littermates to generate wild type, *Pten*$^{+/-}$, *Pten*$^{+/-}$*Inpp4b*$^{+/-}$ and *Pten*$^{+/-}$*Inpp4b*$^{-/-}$ mice (Supplmentary Figure S2.1A). These mice were, once

**Figure 2.1. Generation and Characterization of *Pten*$^{+/-}$*Inpp4b*$^{+/-}$ and *Pten*$^{+/-}$*Inpp4b*$^{-/-}$ mice.** **A.** Diagram representing the structure of INPP4B, which contains an N-terminus C2 domain and a C-terminus phosphatase domain harboring the phosphatase catalytic motif CX5R. **B.** Schematic map of the WT Inpp4b locus (top), targeting vector (upper middle) and predicted targeted allele (lower middle) and knockout allele (bottom). **C.** Table depicting the observed versus the expected numbers of mice of the respective genotypes from a *Pten*$^{+/-}$*Inpp4b*$^{+/-}$ and *Inpp4b*$^{+/-}$ cross. These values gave a $\chi^2$ of 3.26, which is lower than the critical value of 11.070 which would yield an $\alpha$=0.05. Thus, we conclude that the mutants were born following Mendelian frequencies.

**Figure 2.1 (continued)**

**A**

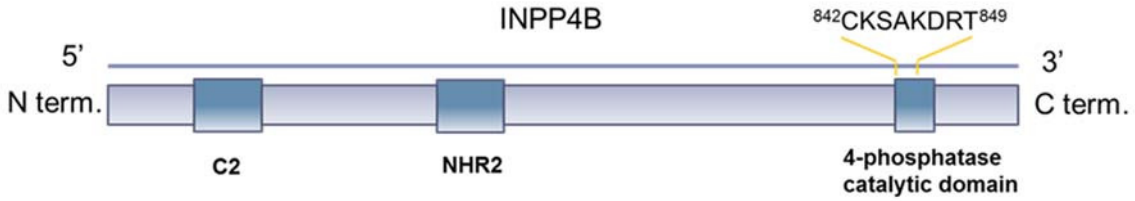


**B**

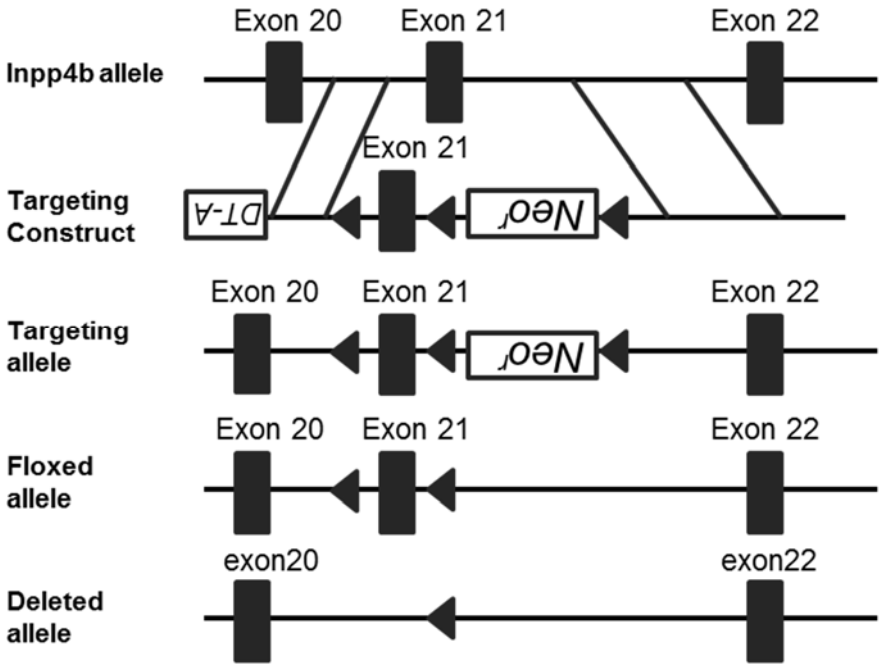


**C**

| | Observed | Expected | $(O-E)^2$ | $\chi^2$ |
|---|---|---|---|---|
| WT | 20 | 17 | 9 | 0.52941 |
| $Inpp4b^{+/-}$ | 33 | 34 | 1 | 0.02941 |
| $Inpp4b^{-/-}$ | 18 | 17 | 1 | 0.05882 |
| $Pten^{+/-}$ | 20 | 17 | 9 | 0.52941 |
| $Pten^{+/-}Inpp4b^{+/-}$ | 26 | 34 | 64 | 1.88235 |
| $Pten^{+/-}$ $Inpp4b^{-/-}$ | 19 | 17 | 4 | 0.23529 |
| TOTAL | 136 | 136 | | **3.26471** |

again, viable and born following the expected Mendelian frequencies (Figure 2.1C). The lack of embryonic lethality in any of the two compound *Pten*$^{+/-}$*Inpp4b*$^{+/-}$ and *Pten*$^{+/-}$*Inpp4b*$^{-/-}$ genetic make-ups further underscore the fact that PTEN and INPP4B might exert distinct roles in signaling since the progressive PI3K/AKT elevation should result in embryonic lethality as previously reported (6).

However, *Pten*$^{+/-}$*Inpp4b*$^{-/-}$ mice did not survive beyond 5-6 months of age, while the majority *Pten*$^{+/-}$*Inpp4b*$^{+/-}$ mice died between 8 and 14 months of age (Figure 2.2A). Gross anatomical analyses showed that the *Pten*$^{+/-}$*Inpp4b*$^{-/-}$ mice developed large multinodular goiters (Figure 2.2B). These mice died, or were euthanized, after developing compressive airway and esophageal obstruction as a consequence of the mass effect from thyroid enlargement. Histopathological analyses revealed that most of the thyroid tumors developed in the *Pten*$^{+/-}$*Inpp4b*$^{-/-}$ mice had variable degrees of encapsulation (Figure 2.2C and 2.2D, top left), microfollicular architecture (Figure 2.2C, left middle panel) and many showed impressive vascular invasion closely resembling follicular thyroid carcinoma (FTC) in human. High-grade features were commonly seen, including significant mitotic activity and necrosis, while some portion of the tumors showed nuclear features of follicular variant papillary thyroid carcinoma (FV-PTC), such as nuclear contour irregularity, nuclear grooves, intranuclear pseudoinclusions and chromatin pallor (Figure 2.2C, right panels). Collectively, the majority of tumors in *Pten*$^{+/-}$*Inpp4b*$^{-/-}$ mice displayed histological and pathological features of FTC and FV-PTC in human (Figure 2.2C and 2.2D, top). Importantly, 50% of *Pten*$^{+/-}$*Inpp4b*$^{-/-}$ mice developed diffuse pulmonary metastases (Figure 2.2D, top right). These metastases had the histologic appearance of thyroid tissue with follicular architecture, colloid, and also stained positive for thyroglobulin, a thyroid specific marker (Figure 2.2D, middle panel). Necropsy did not reveal

**Figure 2.2. Loss of Inpp4b in *Pten*$^{+/-}$ mice leads to follicular thyroid carcinoma. A.** Kaplan-Meier survival curve of *Pten*$^{+/-}$, *Pten*$^{+/-}$*Inpp4b*$^{+/-}$ and *Pten*$^{+/-}$*Inpp4b*$^{-/-}$ mice. **B.** *Top panel*: gross anatomy of representative thyroids from mice of the indicated genotypes. White arrows point to the location of the thyroid. *Bottom panel*: dissected thyroids from mice of the indicated genotypes; Scale bar, 2mm. WT: 12 month-old, *Pten*$^{+/-}$: 14 month-old, *Pten*$^{+/-}$*Inpp4b*$^{+/-}$: 8 month-old, *Pten*$^{+/-}$*Inpp4b*$^{-/-}$: 5 month-old. **C.** *Left panel:* H&E staining of a follicular thyroid carcinoma (FTC)-like thyroid tumor which is thinly encapsulated with microfollicular architecture. *Right panel:* H&E staining of a follicular variant of papillary thyroid carcinoma (FV-PTC)-like thyroid tumor. Middle and bottom panels highlight nuclear atypia characteristic of FV-PTC, including intranuclear pseudoinclusions (arrow). Scale bars, top and middle panels:100μm, bottom panel: 20 μm, **D.** *Top panel*: H&E staining of thyroid tumor and lung metastases from *Pten*$^{+/-}$*Inpp4b*$^{-/-}$ mice; *middle & bottom panel*: thyroglobulin and p-Akt (Ser473) staining. Scale bar, 100μm. Insets show thyroid cancer cells. Blue arrows point to the location of the metastases in the lungs.

**Figure 2.2 (continued)**

**A**

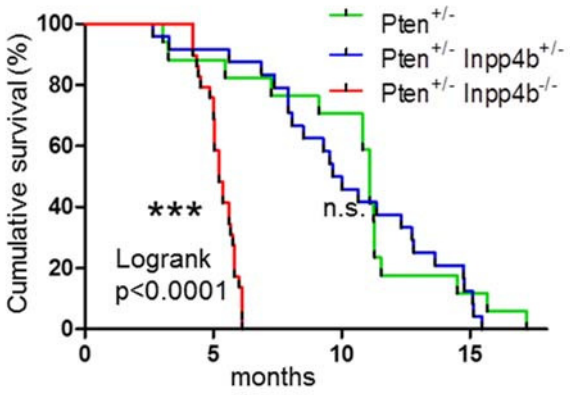


**B**

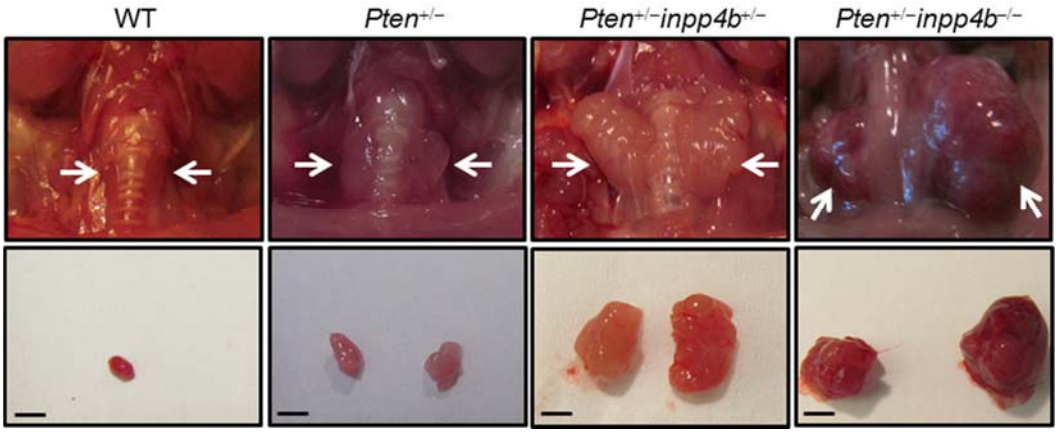

**Figure 2.2 (continued)**

**C**

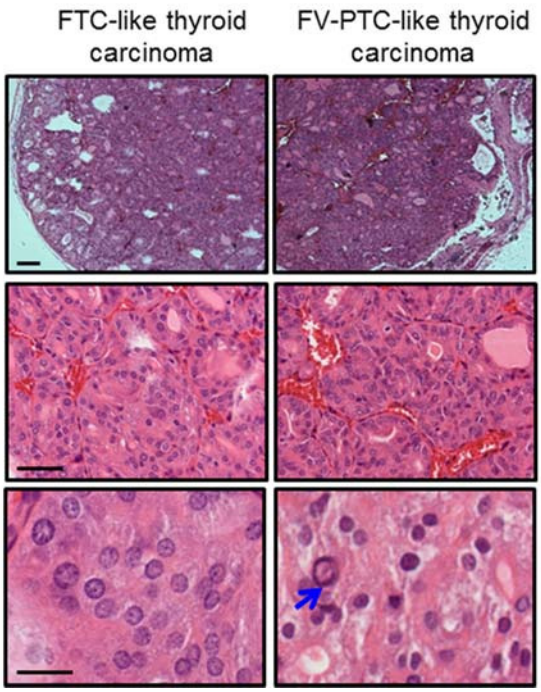

**Figure 2.2 (continued)**

**D**

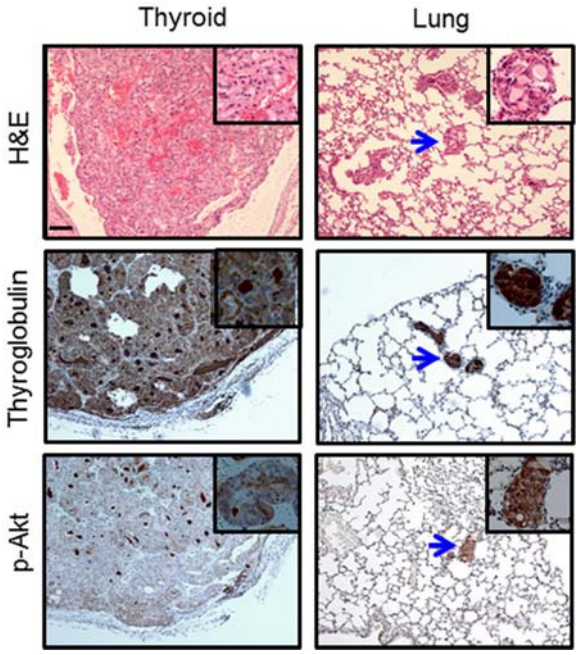

metastases in other regional and distant sites. Akt activation was observed by immunohistochemistry in both the thyroid tumors and the metastases (Figure 2.2D, bottom panel). Serum TSH levels of *Pten*$^{+/-}$*Inpp4b*$^{+/-}$ and *Pten*$^{+/-}$*Inpp4b*$^{-/-}$ mice did not differ significantly from that in *Pten*$^{+/-}$ mice (Supplementary Figure S2.1B). Additionally, we examined the thyroids from a cohort of *Pten*$^{+/-}$*Inpp4b*$^{+/-}$ mice. Histopathological analyses revealed that *Pten*$^{+/-}$*Inpp4b*$^{+/-}$ mice developed benign goiter and FVPTC/FTC, and presented with pulmonary metastases of thyroid carcinoma at a similar penetrance to *Pten*$^{+/-}$*Inpp4b*$^{-/-}$ mice (Supplementary Figurer S2.1C). Furthermore, *Pten*$^{+/-}$*Inpp4b*$^{+/-}$ and *Pten*$^{+/-}$*Inpp4b*$^{-/-}$ mice did not display accelerated tumorigenesis in other tissues as compared to *Pten*$^{+/-}$ mice by 5-8 months follow-up (data not shown). However, we did note a non-significant increased incidence of breast adenocarcinoma in *Pten*$^{+/-}$*Inpp4b*$^{+/-}$ mice (p=0.16, 37.5% in *Pten*$^{+/-}$*Inpp4b*$^{+/-}$ vs 15.5% in *Pten*$^{+/-}$ mice). Therefore, *Inpp4b* loss cooperates with *Pten* haploinsufficiency to promote thyroid cancer progression and metastasis.

**Human follicular thyroid cancer cell lines and tissues display low INPP4B expression.**

To assess the relevance of our mouse model findings to human FTC, we evaluated the status of INPP4B in human thyroid cancer cells. To this end we utilized seven thyroid cell lines, namely Nthy-Ori 3, Htori (SV40-immortalized primary thyroid follicular epithelial cells), FTC133, FTC236, FTC238 (follicular thyroid carcinoma), TPC1 (thyroid papillary carcinoma), and 8505C (anaplastic carcinoma). We first determined the relative expression levels of *INPP4B* in these thyroid cell lines. We observed very low expression of INPP4B at both protein (Figure 2.3A, Supplementary Figure S2.2) and mRNA transcript levels (Figure 2.3B) in the FTC cell

lines FTC133, FTC236 and FTC238 compared to SV40-immortalized human thyroid follicular cells Nthy-Ori-3 and Htori or the TPC1 thyroid cancer cell line. We also noted that PTEN protein expression was not detectable in the FTC cell lines (Figure 2.3A). A search using the Broad CCLE database revealed that the FTC cell lines harbor the PTEN R130* nonsense mutation. This concomitant loss of PTEN and INPP4B in our human FTC cell lines is faithfully modelled by our *Pten*$^{+/-}$*Inpp4b*$^{-/-}$ mice. Finally, we observed an increase in the activation of AKT in these cell lines, as indicated by higher levels of AKT phosphorylation at both Threonine 308 and Serine 473 residues (Figure 2.3C).

Importantly, *INPP4B* transcript expression was significantly downregulated in human FTC samples when compared to normal tissue samples (Figure 2.3D). Because of the infrequency of INPP4B deletions or mutations in human cancers, we further hypothesized that its loss in FTC cell lines might be due to aberrant gene methylation. Indeed, treatment of these cell lines with 5-Aza-2'-deoxycytidine (5-Aza), which inhibits DNA methylation, increased INPP4B expression approximately 4-fold (Figure 2.3E). Upregulation of INPP4B by 5-Aza decreased activation of both AKT1 and AKT2 (Serine 473 and Serine 474 respectively), (Figure 2.3F) with a much greater effect on p-AKT2 than on p-AKT1 (Figure 2.3F). However, bisulfite sequencing indicated that this upregulation is potentially indirect (Supplementary Figure S2.3), mediated via the upregulation of yet to be defined transcription factors. Overall, the downregulation of INPP4B in human FTC strongly supports its tumor suppressive role in this aggressive tumor type of the thyroid.

**Figure 2.3. INPP4B expression is reduced in human follicular thyroid cell lines and human surgical specimens. A.** Western blot analysis of thyroid cancer cell lines for INPP4B and PTEN expression. Arrow indicates specific band. The arrowhead indicates the specific band of INPP4B protein. **B.** RT-qPCR analysis of thyroid cancer cell lines for INPP4B transcript levels. **C.** Western blot analysis of thyroid cancer lines for AKT activation on both Serine 473 and Threonine 308 residues. **D.** RT-qPCR analysis of *INPP4B* in unmatched normal versus FTC patient tumor samples. **E-F.** Thyroid cancer cell lines were treated with 3uM 5-Aza-2'-deoxycytidine for 5 days. Panel shows transcript (**E**) and protein analysis of INPP4B expression and AKT activation levels in DMSO versus 5-Aza treated FTC cells. (**F**). Arrows indicate specific band (see also Methods).

**Figure 2.3 (continued)**

**A**

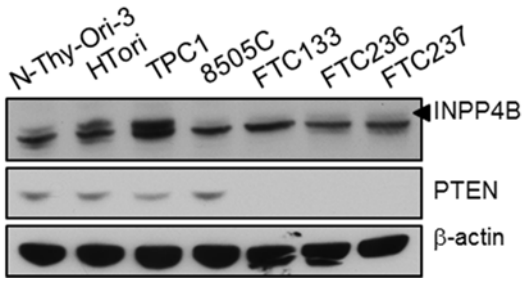


**B**

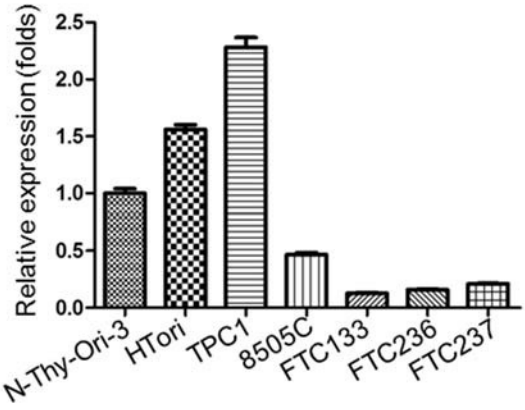

**Figure 2.3 (continued)**

**C**

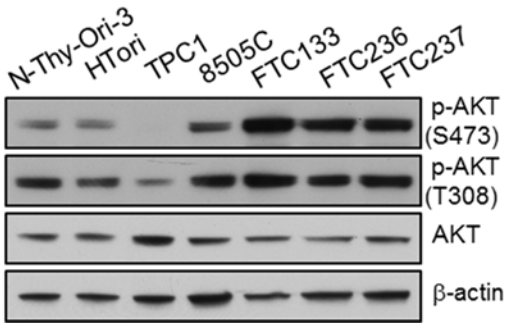


**D**

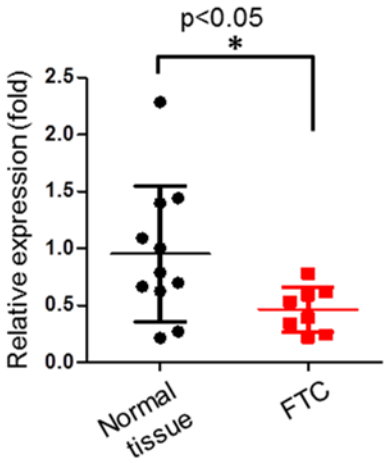

**Figure 2.3 (continued)**

**E**

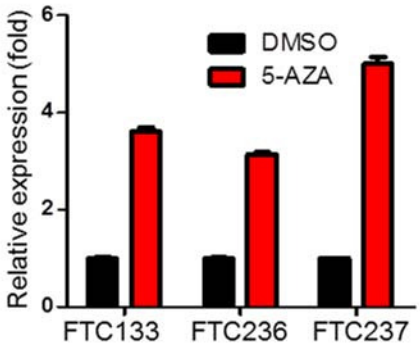


**F**

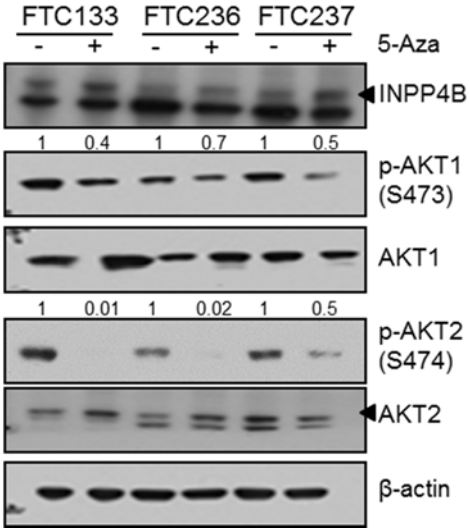

**Loss of Inpp4b increases Akt activation.**

We previously demonstrated that INPP4B knock down enhanced AKT activation (9). To gain insight into the mechanisms by which Inpp4b might promote thyroid tumor development, we analyzed thyroid tumor lysates from *Pten*$^{+/-}$, *Pten*$^{+/-}$*Inpp4b*$^{+/-}$ and *Pten*$^{+/-}$*Inpp4b*$^{-/-}$ mice for Akt activation via Western blotting. In agreement with previous findings, tumors from *Pten*$^{+/-}$*Inpp4b*$^{-/-}$ mice showed higher levels of Akt phosphorylation (monitored through p-Akt1 Serine 473 and p-Akt2 Serine 474) when compared to thyroid tumors obtained from *Pten*$^{+/-}$ or *Pten*$^{+/-}$*Inpp4b*$^{+/-}$ mice (Figure 2.4A). We also isolated primary mouse embryonic fibroblasts (MEFs) of all genetic combinations – wildtype, *Inpp4b*$^{flox/flox}$; *Inpp4b*$^{flox/+}$; *Pten*$^{+/-}$, *Pten*$^{+/-}$*Inpp4b*$^{+/-}$, and *Pten*$^{+/-}$*Inpp4b*$^{-/-}$. We found that MEFs with Inpp4b deletion displayed increased Akt activation, monitored through the phosphorylation of both Serine 473 and Threonine 308 at different time points after serum stimulation (Supplementary Figure S2.4). In addition, although *Pten*$^{+/-}$, *Pten*$^{+/-}$*Inpp4b*$^{+/-}$, and *Pten*$^{+/-}$*Inpp4b*$^{-/-}$ MEFs did not display much higher initial Akt activation upon serum starvation-restimulation (Figure 2.44B, t=5 mins and 15 mins), there was a prolonged Akt-1 and Akt2 activation in *Pten*$^{+/-}$*Inpp4b*$^{+/-}$, and *Pten*$^{+/-}$*Inpp4b*$^{-/-}$ MEFs when compared to *Pten*$^{+/-}$ MEFs (Figure 2.4B, t=30 mins). Furthermore, we found that human thyroid cancer cell lines with lower INPP4B displayed higher levels of AKT phosphorylation (Figure 2.3C and 2.4C). Notably, both AKT1 and AKT2 were activated to a similar extent in total cell lysates (Figure 2.4A, 2.4B and 2.4C). Therefore, loss of both lipid phosphatases, INPP4B and PTEN, resulted in an additive activation of AKT in thyroid tissue, MEFs and cancer cell lines.

**INPP4B suppresses PI3K-C2α mediated AKT2 activation at early endosomes in thyroid cancer cells.**

The observation that complete inactivation of Pten in mouse thyroid results mainly in follicular adenoma within 12 months of age (17) and that Inpp4b loss does not accelerate the entire tumor spectrum of *Pten*$^{+/-}$ mice raised the possibility that loss of Inpp4b specifically cooperates with *Pten* loss for tumor progression and metastasis in thyroid, not through a generic elevation of PI3K/AKT signaling, but potentially by deregulating the PI3K pathway in a more selective manner. Previous studies have shown that Akt2 deficiency had little-to-no effect on the tumor spectrum in *Pten*$^{+/-}$ mice, and only specifically significantly decreased the incidence of thyroid tumors in *Pten*$^{+/-}$ mice (18), suggesting that AKT2 might play an oncogenic role in thyroid cancer. Recent studies have shown that AKT2 phosphorylates its substrates on both endosomes and the plasma membrane (19). Strikingly, subcellular fractionation experiments showed that INPP4B, but not PTEN, was expressed in the Rab5-positive early endosomal (EE) fraction together with AKT2 in thyroid cancer cells (Figure 2.4D and 2.4E). Although AKT1 was also localized in the EE fraction (Figure 2.4D), surprisingly, knockdown of INPP4B selectively activated AKT2, but not AKT1 in the EE (Figure 2.4F). Consistent with this result, thyroid cancer cell lines with lower INPP4B expression display higher endosomal AKT2 activation (Supplementary Figure S5A). Furthermore, increasing INPP4B expression with 5-Aza in FTC236 cells resulted in a greater decrease in p-AKT2 in the EE fraction compared to p-AKT1 (Figure 2.4G). Collectively, these results lend support to the selective activation of AKT2 at the early endosomes by INPP4B.

In line with class II PI3K kinase α (PI3K-C2α ) producing PI(3,4)$P_2$ and being selectively activated in endocytosis as well as endocytic recycling (20, 21), we also found PI3K-

**Figure 2.4. Loss of Inpp4b in *Pten*$^{+/-}$ cells leads to increased Akt activation. A-B.** Western blot analysis of lysates from *Pten*$^{+/-}$ (n=3; ~10-11months), *Pten*$^{+/-}$*Inpp4b*$^{+/-}$ (n=2; ~6-8months) and *Pten*$^{+/-}$*Inpp4b*$^{-/-}$ (n=3; ~6 months) thyroid tissues (**A**), lysates from immortalized MEFs after serum starvation-restimulation. The MEFs were stimulated with serum for the indicated amount of time. (**B**). **C.** Western blot analysis of total lysate from different thyroid cancer cells. Please note that the AKT2 antibody used in **A-B** is different from **C**, resulting in the appearance of different unspecific bands. Arrows indicate specific band (see also Methods). **D-E.** Western blot analysis of cell fractions from TPC1 cells. HM: cytosolic/heavy membranes; EE: early endosome: LE: late endosome; PNS: postnuclear supernatant. Arrow indicates specific band. **F.** Western blot analysis of phosphorylated Akt1 and phosphorylated Akt2 in different cell fractions derived from TPC1 cells infected with either a non-targeting shRNA or an shRNA that targets INPP4B. **G.** Western blot analysis of phosphorylated Akt1 and phosphorylated Akt2 in different cell fractions derived from FTC236 cells treated with either DMSO or 3uM 5-Aza for 5days. **H.** Immunofluorescence of PI(3,4)$P_2$ and tubulin in TPC1 cells infected with either a non-targeting shRNA or an shRNA that targets INPP4B. Scale bars, 20 μm. **I.** Immunofluorescence of INPP4B, AKT2, PI3K-C2α and RAB5 in TPC1 cells. Scale bars, 5μm. **J.** Immunofluorescence of PI(3,4)$P_2$ and SNX9 in TPC1 and FTC236 cells. Scale bars, 20 μm.

**Figure 2.4 (continued)**

**A**

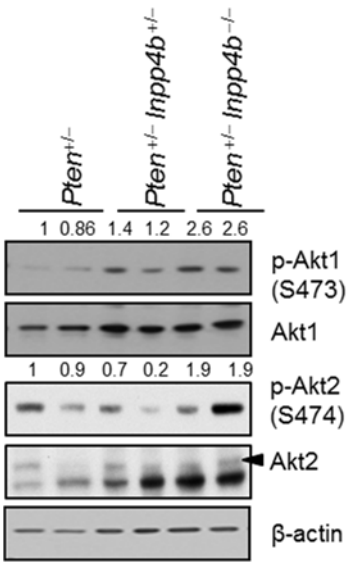


**B**

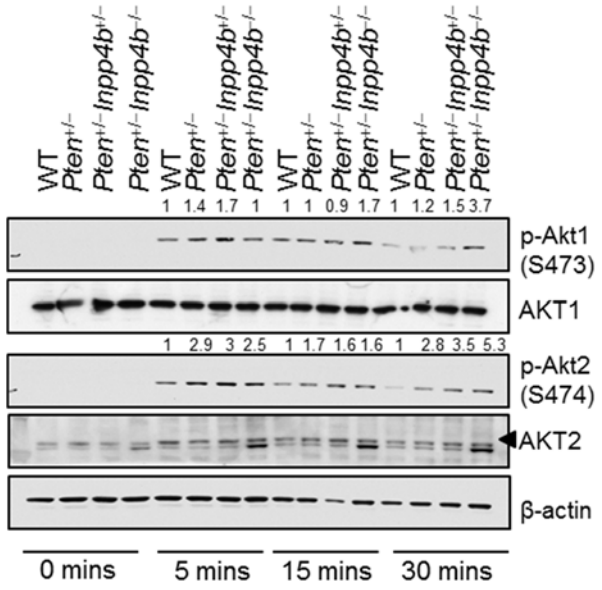

**Figure 2.4 (continued)**

**C**

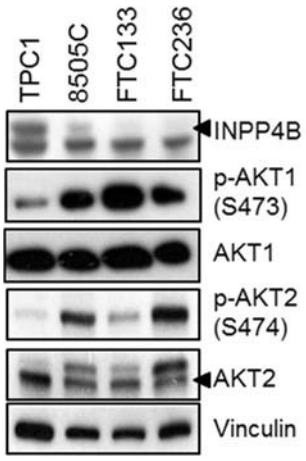


**D**

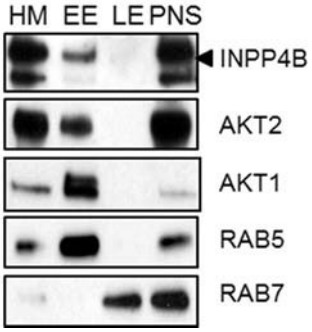

**Figure 2.4 (continued)**

**E**

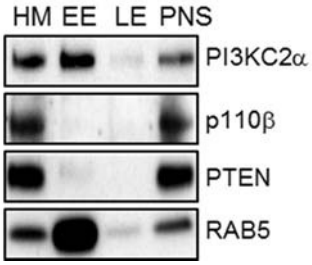


**F**

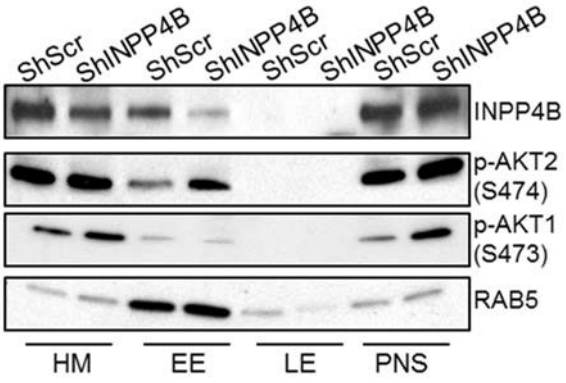


**G**

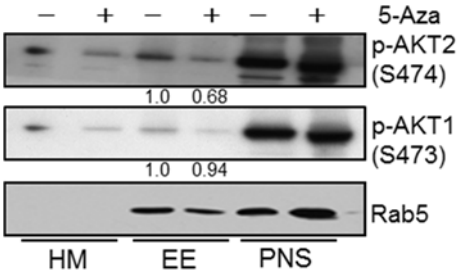

**Figure 2.4 (continued)**

**H**

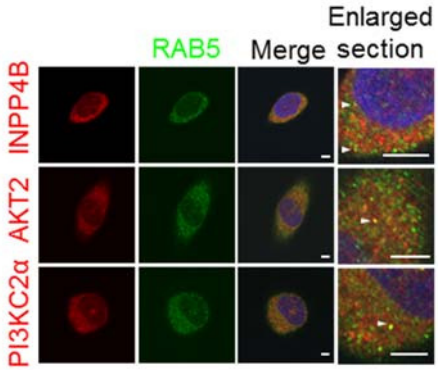


**I**

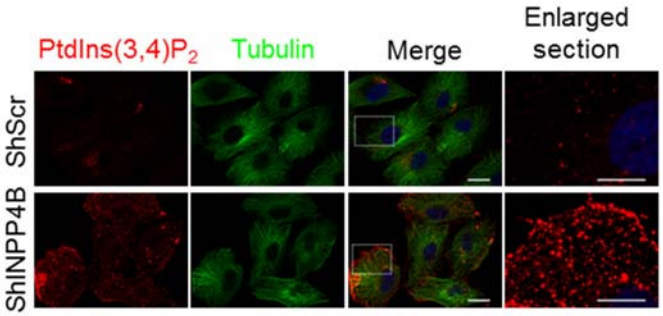


**J**

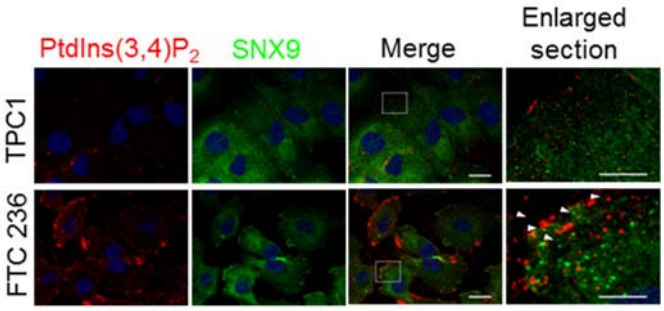

C2α expressed in the thyroid cancer cells and enriched in EE fraction, along with INPP4B and AKT2 (Figure 2.4E). The association of INPP4B, AKT2 and PI3K-C2α with EE was also confirmed by immunofluorescence, in which INPP4B, AKT2 and PI3K-C2α were co-localized with RAB5-positive punctate structures in the cells (Figure 2.4H). Notably, INPP4B loss was associated with increased abundance of $PI(3,4)P_2$ (Figures 2.4I and 2.4J), but not $PI(3,4,5)P_3$ (Supplementary Figure S2.5B). Consequently, there was an accumulation of the $PI(3,4)P_2$-binding protein SNX9 in vesicles near the plasma membrane (Figure 2.4J). Taken together, these results suggest that INPP4B negatively regulates PI3K-C2α signaling at the EE. Furthermore, loss of PI3K-C2α decreased AKT2 activation to a greater extent than that of AKT1 in total cell lysates (Supplementary Figure S2.6A and S2.6B) and significantly inhibited cell proliferation in FTC 236 cells (Supplementary Figure S2.6C), underscoring the functional relevance of enhanced PI3K-C2α signaling in cells with lower INPP4B. Taken together, our results strongly suggests that INPP4B inhibits PI3K-C2α mediated AKT2 activation in the early endosomes of thyroid cancer cells, even though they obviously do not rule out the possible involvement of other PI3K isoforms in AKT activation at the EE.

**Knockdown of INPP4B in thyroid cell lines provide an advantage for anchorage independent growth.**

To assess INPP4B dependent cellular processes *in vitro*, we next conducted cell proliferation and soft agar colony formation assays in two of the non-FTC thyroid cell lines, namely TPC1 and 8505C, in which we stably knocked down INPP4B (Figures 2.5A and 2.5B). We found that the knockdown of INPP4B did not confer a growth advantage for thyroid cell lines in full or 1% serum growth conditions, but did in 5% serum growth conditions (Figure 2.5C and Supplementary Figure S2.7A), suggesting that under specific conditions of nutrients or growth

factor amounts, INPP4B loss determines a growth advantage in thyroid cell lines, mirroring the *in vivo* phenotype. In addition, INPP4B knock down did not result in any change in TPC1 cell morphology, nor did it alter the morphology of *Pten*$^{+/-}$*Inpp4b*$^{-/-}$ MEFs compared to *Pten*$^{+/-}$ MEFs (Supplementary Figures S2.7B and S2.7C). Furthermore, INPP4B loss did not alter the distribution or arrangement of tubulin in the cytoskeleton of these cells (Supplementary Figures S2.7B and S2.7C). Instead, INPP4B loss provided a marked advantage for anchorage independent growth, a functional indicator of tumorigenicity and invasiveness (Figures 2.5D and 2.5E).

**Figure 2.5. Knockdown of INPP4B in thyroid cancer cells provides an advantage for anchorage independent growth. A.** RT-qPCR analysis of *INPP4B* upon shRNA-mediated knockdown. **B.** Western blot analysis of INPP4B levels in TPC1 and 8505C cell lines after shRNA-mediated knockdown. **C.** Proliferation of TPC1 and 8505C cell lines infected with either a non-targeting shRNA or a shRNA that targets INPP4B. Cells were cultured in complete media (10% serum), stained with crystal violet, and lysed. Absorbance was measured at OD595nm. **D-E.** Soft agar colony formation assay of cells infected with either a non-targeting shRNA or an shRNA which targets INPP4B. Cells were grown in soft agar for 2 weeks before being photographed (**D**) and the number of colonies was then counted (**E**).

**Figure 2.5 (continued)**

**A**

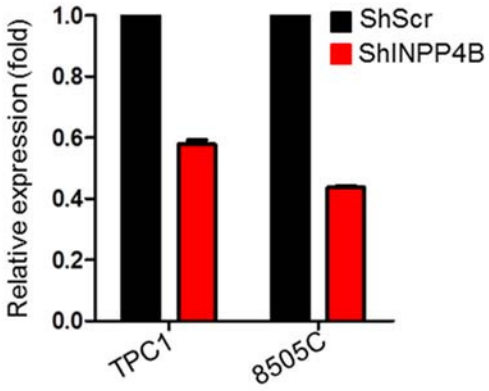


**B**

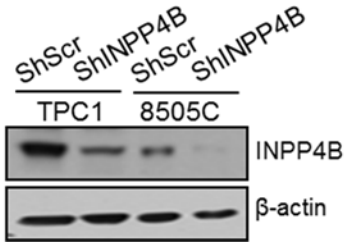

**Figure 2.5 (continued)**

**C**

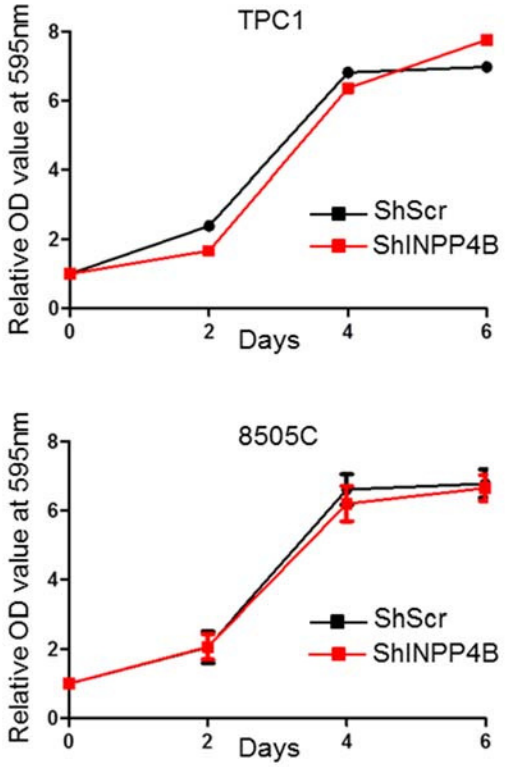

**Figure 2.5 (continued)**

**D**

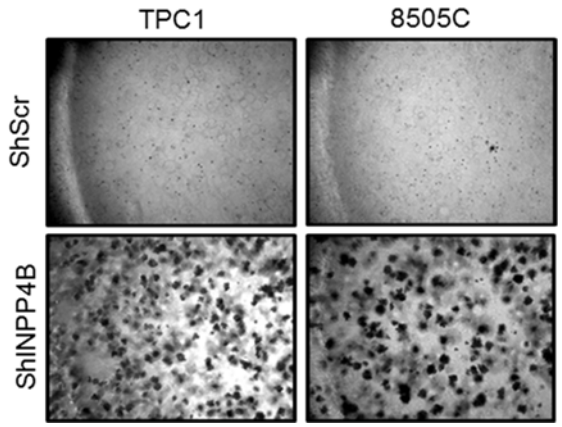


**E**

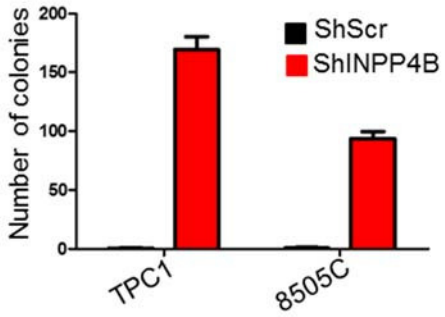

## 2.5 DISCUSSION

This study allowed us to reach three important conclusions:

First, INPP4B is a novel tumor suppressor in FTC. Through our mouse model, we demonstrated that either a partial or complete loss of Inpp4b in a *Pten* heterozygous background accelerates thyroid carcinoma progression, resulting in metastatic disease that recapitulates the hematogenous pulmonary metastases characteristic of advanced FTC in humans. The evidence that INPP4B is a relevant tumor suppressor in FTC is further supported by the observation that INPP4B expression is markedly reduced in human FTC, as compared to a normal thyroid and other subtypes of thyroid cancer.

Our findings lend further support to the notion that PI3K-AKT activation plays a central role in FTC oncogenesis. Multiple lines of evidence corroborate this notion: 1) AKT activation and expression is higher in FTC as compared to normal tissues and other thyroid tumors (22), 2) Cowden syndrome patients, with germline mutations in PTEN, have an increased incidence of FTC (23), 3) transgenic mice engineered to hyperactivate PI3K/AKT form FTCs (24, 25), and 4) in a mouse model of FTC, metastatic potential is Akt-dependent (26). This evidence underscores the importance of AKT hyperactivation in the initiation and progression of FTC, and also suggests that the pathogenesis of FTC is distinct from other forms of well-differentiated thyroid carcinoma, which are driven primarily via activation of the MAPK signaling pathway. Nevertheless, mutations in the RAS pathway and PAX8/PPARγ rearrangements are also found in FTC (27). While the specific pathogenic mechanisms contributed by these alterations remain unclear, there are indications that they too converge on the PI3K-AKT pathway (28). Therefore, it will be therefore interesting to understand in future studies whether these represent cooperative or mutually exclusive events.

Second, we observed that INPP4B is not solely epistatic to PTEN. PTEN and INPP4B are generally thought to be cooperative phosphatases that proximally regulate PI3K at the lipid level. On this basis, we anticipated that *Inpp4b*$^{-/-}$ mice would have a phenotype reminiscent of *Pten*$^{+/-}$ mice with increased susceptibility to epithelial tumors. Surprisingly, *Inpp4b*$^{-/-}$ mice were tumor free and had a tumor free survival of 16-24 months. In addition, crossing *Inpp4b*$^{-/-}$ mice with *Pten*$^{+/-}$ mice did not accelerate the entire tumor spectrum of *Pten*$^{+/-}$ mice by 5-8 months follow-up. Rather, we only observed a significant acceleration of thyroid tumorigenesis. Due to the early mortality that occurred in the *Pten*$^{+/-}$*Inpp4b*$^{-/-}$, further studies in conditional Pten and Inpp4b knockout mice will be needed in order to determine the potential cooperative effect between Pten and Inpp4b on tumor suppression in other tissues.

Despite the importance of PI3K-AKT signaling in the pathogenesis of FTCs, *Pten*$^{+/-}$ mice do not develop FTC. By 10 months of age, they instead develop benign adenomas that do not invade or metastasize. One might speculate that the extent of AKT activation accounts for the difference in thyroid carcinoma aggressiveness. Indeed, we observed increased Akt activation in *Pten*$^{+/-}$*Inpp4b*$^{-/-}$ thyroids when compared to *Pten*$^{+/-}$ or *Pten*$^{+/-}$*Inpp4b*$^{+/-}$ thyroids. However, in a previous study, we found that thyroid lesions in *Pten* knock-in mutant mice harboring specific lipid and phosphatase dead *Pten* mutations also demonstrated higher levels of Akt activation than *Pten*$^{+/-}$ thyroids similar to *Pten*$^{+/-}$*Inpp4b*$^{-/-}$ thyroids (29). Nevertheless, only 7 – 8 % of these mice developed aggressive thyroid adenocarcinoma, and importantly, there was no occurrence of lung metastasis (29). Furthermore, conditional loss of function of both copies of *Pten* in the thyroid results mainly in follicular adenoma within 12 months of age, which only progresses to invasive FTC at advanced ages, suggesting that even in a setting of maximal activation of PI3K-AKT signaling, other events are needed to trigger FTC (17). In contrast, the *Pten*$^{+/-}$*Inpp4b*$^{-/-}$

mice developed aggressive, often metastatic, and always lethal follicular-like carcinoma by 5-6 months of age. The shorter latency to a more aggressive follicular-like carcinoma in *Pten*$^{+/-}$*Inpp4b*$^{-/-}$ mice further support the notion that while increased Akt activation does play a role in follicular-like thyroid tumorigenesis, it is insufficient in mediating progression and metastases, and that the tumor suppressive function of INPP4B therefore extends beyond its role in suppressing the overall level of PI3K-AKT pathway activation. In this respect, the striking difference between PTEN and INPP4B that emerges from our study is their differential localization at the early endosome where INPP4B but not PTEN could regulate signaling in a localized and specialized fashion.

Beyond the level of AKT activation, isoform-specific AKT signaling plays an important role in mediating cancer progression. In the context of breast cancer, AKT2 has been implicated in metastasis, whereas AKT1 suppresses metastatic dissemination (30). Interestingly, signaling through AKT2 is critical for the development of thyroid neoplasms in *Pten*$^{+/-}$ mice (18). Specifically, loss of Akt2 in *Pten*$^{+/-}$ mice rescues the development of thyroid adenomas in this model (18). Furthermore, genomic amplification of AKT2 is frequently observed in FTC, but not in anaplastic thyroid carcinoma (31). These findings indicate that AKT2 activation is particularly important in follicular thyroid carcinoma progression and metastasis. Our finding that INPP4B, but not PTEN, localizes to the early endosomes to selectively regulate AKT2 identifies a novel and specific role for INPP4B in the regulation of PI3K-AKT signaling. INPP4B loss could therefore increase the $PI(3,4)P_2$ pool in the early endosomes, regulate endocytic trafficking and contribute to prolonged AKT2 signaling from the endocytic membranes, through which it mediates its effects on thyroid carcinoma initiation, migration and invasion. Our findings are also in line with recent observation that activation of the endocytic trafficking pathways is critical for

tumor cell migration (32). Therefore, it is possible that the aberrant activation of AKT2 at endosomes might represent the molecular mechanism underlying the characteristic metastatic propensity of FTCs. Intriguingly, although AKT1 is also localized at the early endosomes, INPP4B does not appear to regulate its activation. The exact mechanism underlying the selective regulation of AKT2 by INPP4B remains to be elucidated. Our study nevertheless represents an important first step in the understanding of the mechanism underlying isoform specific and localized AKT regulation.

In conclusion, our study provides strong evidence that INPP4B is not epistatic to PTEN and that INPP4B loss, although insufficient to initiate cancer in the thyroid, can promote FTC progression and metastasis in the context of PTEN haploinsufficiency through the isoform-specific regulation of AKT signaling at the endosomes (Figure 2.6). More generally, our findings provide compelling evidence for the critical role of a qualitative regulation of signal transduction in tumorigenesis.

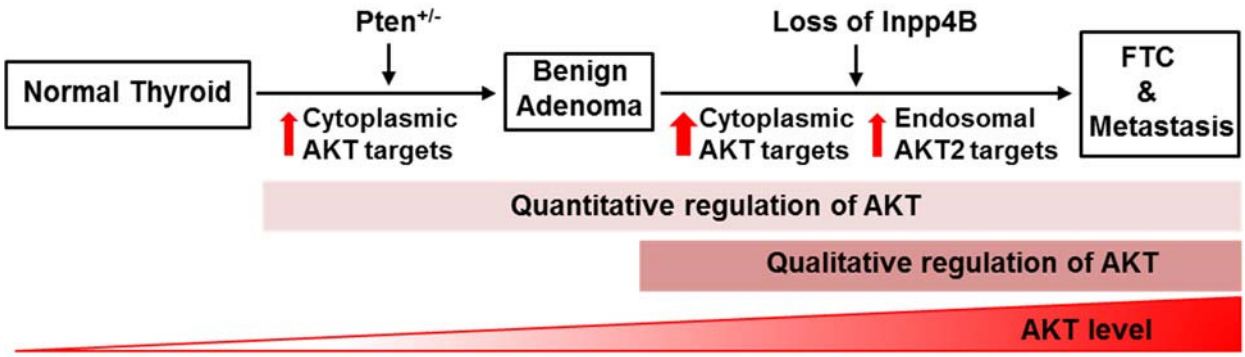


**Figure 2.6. Model for the role of INPP4B and PTEN loss in FTC progression and metastasis.** INPP4B and PTEN control both activation level and subcellular localization of PI3K/AKT signalling to oppose thyroid tumorigenesis.

## 2.6 METHODS

### Mice and histopathological analyses

Inpp4b knockout mice were generated by Sasaki and colleagues in the C57BL/6J background. *Pten*$^{+/-}$ mice used in the study are in the C57BL/6J background. Total body necropsy and histopathological analyses were performed on cohorts of male and female mice from 4-15 months of age. Mouse tissues were fixed in 4% paraformaldehyde and embedded in paraffin. They were then sectioned and stained with hematoxylin and eosin (H&E) for pathological analyses. The use of these mice and procedures performed were in accordance to NIH-approved guideline, and the Institutional Animal Care and Use Committee (IACUC) ate Beth Israel Deaconess Medical Center approved the studies.

### Studies with Primary cells

Mouse embryonic fibroblasts (MEFs) were isolated at day E13.5, immortalized with SV40 large T antigen, and maintained in DMEM supplemented with 10% fetal bovine serum, 2mM glutamine, 100 U/ml penicillin and streptomycin (Invitrogen).

### Cell lines

All cells were maintained in DMEM or RPMI supplemented with 10% fetal bovine serum, 2 mM glutamine, 100 U/ml penicillin and streptomycin (Invitrogen). N-Thy-Ori-3 cells were purchased from Sigma. Htori and 8505C cells were kindly provided by Dr. Sareh Parangi (MGH); FTC and TPC1 cells were kindly provided by Dr. Orlo H. Clark (UCSF). N-Thy-Ori-3 and Htori cells are the same cell line but different culturing conditions have caused them to diverge, as indicated by different INPP4B expression levels. FTC cell lines were derived from the same patient (FTC133 – primary tumor, FTC 236 – lymph node metastasis and FTC 237 – lung metastasis) (33). Cell lines were tested for specific markers by Western blot and qRT-PCR in our laboratory, routinely

tested for *Mycoplasma* (MycoAlert; Lonza), but not further authenticated.

**Human tissue collection**

The Committee for Human Research at Brigham and Women's Hospital approved this study. Thyroid tumors and normal tissue were discarded specimens obtained from patients undergoing thyroidectomy. The specimens were snap-frozen in the operating room suite with liquid nitrogen and were maintained at -80C until analysis. An endocrine pathologist, who confirmed the histologic diagnosis, evaluated the specimens.

**Western blotting and immunohistochemistry**

Cells and tissues were lysed with RIPA buffer (50mM Tris [pH8], 150mM NaCl, 0.1% SDS, 0.5% sodium deoxycholate, 1% NP40, 1mM EDTA and protease and phosphatase inhibitor cocktail [Roche]). For western blotting, the following antibodies were used: anti-AKT (9272), anti-Phospho-AKT (pSer473, 9271; pThr308, 9275), anti-AKT1(2938), anti-AKT2(3063 and 5239), anti-p-AKT1 (pSer473)(9018), anti-p-AKT2 (pSer474)(8599), anti-PTEN (9559), anti-INPP4B(8450) were from Cell Signaling Technology. Please note that anti-AKT2 (3063) and (5239) cross-reacted with different unspecific bands, with a lower AKT2 specific band for (3063) and an upper specific band for (5239) as indicated. Anti-INPP4B (81269) was from Epitomics. Anti-HSP90 (610419) was from BD Biosciences anti-β-actin (A3853) was from Sigma. The characterization of anti-INPP4B (81269) has been shown in the Supplementary Figure 2. For immunohistochemistry, anti-INPP4B antibody (81269) was from Epitomics and anti-phospho-Akt (pSer473, 4060) was from Cell Signaling Technology.

**Immunofluorescence**

Cells were grown on coverslips, fixed with 4% paraformaldehyde and permeabilized with 0.3% Triton or pre-chilled methanol. Cells were rinsed with PBS, blocked and then incubated with

primary antibody, followed by incubation with Alexa Fluor conjugated secondary antibodies (Life Techonologies). Coverslips were mounted with ProLong Gold Antifade reagent with DAPI (Life Technologies). Confocal images of cells were acquired with LSM510META Confocal Laser System (BIDMC) and Zeiss Observer-Z1 microscope equipped with Apotome (University of Torino). Primary antibodies used: anti-INPP4B (Atlas, 37682), anti-PI3K-C2α (anti-p170) (BD, 611046) anti-γ-tubulin (Sigma, GTU-88), anti-Rab5 (BD, 610261 and Cell Signaling Technology, 3547) anti-α-tubulin (Sigma, T6074), anti-PtdIns(3,4P)$_2$ and anti-PtdIns(3,4,5)P$_3$ (Echelon, Z-P034b and Z-P345), anti-SNX9 (Proteintech, 15721-1-AP), and anti-AKT2 (Cell Signaling Technology, 2964).

**Early endosome purification**

Cells were gently homogenized in the homogenization buffer (250mM sucrose, 3mM imidazole, pH 7.4 with protease inhibitor cocktail). The samples were centrifuged at 3000 rpm to remove nuclei and cell debris. Postnucelar supernatant (PNS) was subsequently separated by sucrose gradient centrifugation into different cellular fractions. In detail, the PNSs were adjusted to 40.6% sucrose using a stock solution (62% sucrose, 3mM imidazole pH 7.4), loaded at the bottom of centrifugation tubes (SW55), then sequentially overlaid with 1.5 ml 35% sucrose solution (35% sucrose, 3mM imidazole pH 7.4) followed by 1ml 25% solution (25% sucrose, 3mM imidazole pH 7.4) and 1ml of homogenization buffer on top of the load. After 1hour centrifugation, at 35000 rpm 4$^o$C, early endosomes (EE) were recovered from interphase between 35% and 25% layers, late endosomes (LE) were recovered from uppermost portion of 25% phase, and heavy membranes (HM) including ER, Golgi and plasma membranes were recovered from lowest interphase. EE, LE and HM were then precipitated with methanol/chloroform loaded in SDS-PAGE for western blot analyses.

**RNA isolation and RT-qPCR**

Total RNA was purified from cell lines and tissues using the PureLink RNA Mini Kit (Invitrogen). For qPCR analysis, 2ug of total RNA was reverse transcribed into cDNA using the High Capacity cDNA Reverse Transcription Kit (Applied Biosystems). SYBR-Green qPCR analysis was then performed using Applied Biosystems StepOnePlus in accordance to the manufacturer's protocol. Each target was run in triplicate, and expression levels were normalized to mouse hypoxanthine-guanine phosphoribosyltransferase (*HPRT*) or human porphobilinogen (PBGD).

**Genotyping**

The following genotyping primers were used:

Inpp4b del1: GTTTACATTTGACAGGGTGGTTGG

Inpp4b del2: TGCTGTCGCCGAAGAAGTTA

Inpp4b del3: CCTGCCATGGGTAGATTTCT

Pgen-1: TGGGAAGAACCTAGCTTGGAGG

Pgen-3: ACTCTACCAGCCCAAGGCCCGG

3193: CGAGACTAGTGAGACGTGCTACTTCC

**5-Aza-2'-deoxycytidine treatment**

Cells were briefly treated with 3uM of 5-Aza-2'-deoxycytidine for 5 days. After that, the cells were harvested for RNA and protein analysis.

**Growth proliferation assay**

Cells were plated at a density of $2.5x10^4$ cells/well in 12-well plates and each sample was plated in triplicate. Plates were collected on day 0, day 2, day 4 and day 6. The wells were washed with

PBS and cells were fixed with 4% paraformaldehyde (Santa Cruz Biotechnology). Wells were stained with 0.1% Crystal Violet solution, washed and dried. The absorbed stained was then solubilized with 10% acetic acid, and the absorbance was measured at 595nm.

**Soft-agar colony formation assay**

Soft-agar colony formation assay was performed by first plating 6-well tissue culture plates with 0.6% Noble agar/growth media and allowed to solidify at room temperature. $1x10^5$ thyroid cancer cell lines in 0.3% Noble agar/growth media were then seeded as the top layer. Each cell line was seeded in triplicate. The soft agar was allowed to solidify at room temperature, then placed in the incubator at 37°C. Fresh growth media was added every week, and colonies were counted and photographed after 2 weeks.

**Measurement of TSH levels**

Serum was collected from, *Pten*$^{+/-}$, *Pten*$^{+/-}$*Inpp4b*$^{+/-}$ and *Pten*$^{+/-}$*Inpp4b*$^{-/-}$ mice. The mice were between 3-5 months of age, and at least 4 mice in each genotype were tested. Briefly, blood was allowed to clot at 4°C for at least 2 hours. It was then centrifuged at 1000xg for 15 minutes. The serum was carefully removed and frozen at -20°C. For testing, we used the ultrasensitive thyroid-stimulating hormone (U-TSH) ELISA kit from MyBioSource (MBS042764).

**Bisulfite sequencing**

Genomic DNA samples were collected and treated with bisulfite using the EpiTect Bisulfite kit (Qiagen) according to the manufacturer's recommendations. PCR amplification was performed with primers specific for the methylated and unmethylated alleles, as described in Yuen et al. (12).

**Statistical analysis**

For quantitative data, data sets were generally analyzed using the unpaired, two-tailed Student's *t* tests (GraphPad Prism, GraphPad Software). $p<0.05$ was considered significant.

## 2.7 Acknowledgements

The authors thank all members of the Pandolfi laboratory for critical discussion, Lauren Fawls for editing the manuscript, Kelsey Berry for technical assistance and Justine Barletta for help with histopathological interpretation. The authors are grateful to Min Sup Song and Su Jung Song for insightful discussion.

## 2.8 Grant Support

This work has been supported by NIH grant U01 CA141496 to P.P.P. C.L.C. was supported by the A*STAR National Science Scholarship (Singapore).

## 2.9 References


1. Fruman DA, Rommel C. PI3K and cancer: lessons, challenges and opportunities. Nature reviews Drug discovery. 2014;13:140-56.

2. Toker A, Marmiroli S. Signaling specificity in the Akt pathway in biology and disease. Advances in biological regulation. 2014;55:28-38.

3. Arboleda MJ, Lyons JF, Kabbinavar FF, Bray MR, Snow BE, Ayala R, et al. Overexpression of AKT2/protein kinase Bbeta leads to up-regulation of beta1 integrins, increased invasion, and metastasis of human breast and ovarian cancer cells. Cancer research. 2003;63:196-206.

4. Hutchinson JN, Jin J, Cardiff RD, Woodgett JR, Muller WJ. Activation of Akt-1 (PKB-alpha) can accelerate ErbB-2-mediated mammary tumorigenesis but suppresses tumor invasion. Cancer research. 2004;64:3171-8.

5. Irie HY, Pearline RV, Grueneberg D, Hsia M, Ravichandran P, Kothari N, et al. Distinct roles of Akt1 and Akt2 in regulating cell migration and epithelial-mesenchymal transition. The Journal of cell biology. 2005;171:1023-34.

6. Di Cristofano A, Pesce B, Cordon-Cardo C, Pandolfi PP. Pten is essential for embryonic development and tumour suppression. Nature genetics. 1998;19:348-55.

7. Hollander MC, Blumenthal GM, Dennis PA. PTEN loss in the continuum of common cancers, rare syndromes and mouse models. Nature reviews Cancer. 2011;11:289-301.

8. Westbrook TF, Martin ES, Schlabach MR, Leng Y, Liang AC, Feng B, et al. A genetic screen for candidate tumor suppressors identifies REST. Cell. 2005;121:837-48.

9. Gewinner C, Wang ZC, Richardson A, Teruya-Feldstein J, Etemadmoghadam D, Bowtell D, et al. Evidence that inositol polyphosphate 4-phosphatase type II is a tumor suppressor that inhibits PI3K signaling. Cancer cell. 2009;16:115-25

10. Fedele CG, Ooms LM, Ho M, Vieusseux J, O'Toole SA, Millar EK, et al. Inositol polyphosphate 4-phosphatase II regulates PI3K/Akt signaling and is lost in human basal-like breast cancers. Proceedings of the National Academy of Sciences of the United States of America. 2010;107:22231-6.

11. Perez-Lorenzo R, Gill KZ, Shen CH, Zhao FX, Zheng B, Schulze HJ, et al. A tumor suppressor function for the lipid phosphatase INPP4B in melanocytic neoplasms. The Journal of investigative dermatology. 2014;134:1359-68.

12. Yuen JW, Chung GT, Lun SW, Cheung CC, To KF, Lo KW. Epigenetic inactivation of inositol polyphosphate 4-phosphatase B (INPP4B), a regulator of PI3K/AKT signaling pathway in EBV-associated nasopharyngeal carcinoma. PloS one. 2014;9:e105163.

13. Hodgson MC, Shao LJ, Frolov A, Li R, Peterson LE, Ayala G, et al. Decreased expression and androgen regulation of the tumor suppressor gene INPP4B in prostate cancer. Cancer research. 2011;71:572-82.

14. Taylor BS, Schultz N, Hieronymus H, Gopalan A, Xiao Y, Carver BS, et al. Integrative genomic profiling of human prostate cancer. Cancer cell. 2010;18:11-22.

15. Franke TF, Kaplan DR, Cantley LC, Toker A. Direct regulation of the Akt proto-oncogene product by phosphatidylinositol-3,4-bisphosphate. Science (New York, NY). 1997;275:665-8.

16. Di Cristofano A, Kotsi P, Peng YF, Cordon-Cardo C, Elkon KB, Pandolfi PP. Impaired Fas response and autoimmunity in Pten+/- mice. Science (New York, NY). 1999;285:2122-5.

17. Antico-Arciuch VG, Dima M, Liao XH, Refetoff S, Di Cristofano A. Cross-talk between PI3K and estrogen in the mouse thyroid predisposes to the development of follicular carcinomas with a higher incidence in females. Oncogene. 2010;29:5678-86.

18. Xu PZ, Chen ML, Jeon SM, Peng XD, Hay N. The effect Akt2 deletion on tumor development in Pten(+/-) mice. Oncogene. 2012;31:518-26.

19. Walz HA, Shi X, Chouinard M, Bue CA, Navaroli DM, Hayakawa A, et al. Isoform-specific regulation of Akt signaling by the endosomal protein WDFY2. The Journal of biological chemistry. 2010;285:14101-8.

20. Franco I, Gulluni F, Campa CC, Costa C, Margaria JP, Ciraolo E, et al. PI3K class II alpha controls spatially restricted endosomal PtdIns3P and Rab11 activation to promote primary cilium function. Developmental cell. 2014;28:647-58.

21. Posor Y, Eichhorn-Gruenig M, Puchkov D, Schoneberg J, Ullrich A, Lampe A, et al. Spatiotemporal control of endocytosis by phosphatidylinositol-3,4-bisphosphate. Nature. 2013;499:233-7.

22. Ringel MD, Hayre N, Saito J, Saunier B, Schuppert F, Burch H, et al. Overexpression and overactivation of Akt in thyroid carcinoma. Cancer research. 2001;61:6105-11.

23. Ngeow J, Mester J, Rybicki LA, Ni Y, Milas M, Eng C. Incidence and clinical characteristics of thyroid cancer in prospective series of individuals with Cowden and Cowden-like syndrome characterized by germline PTEN, SDH, or KLLN alterations. The Journal of clinical endocrinology and metabolism. 2011;96:E2063-71.

24. Furuya F, Hanover JA, Cheng SY. Activation of phosphatidylinositol 3-kinase signaling by a mutant thyroid hormone beta receptor. Proceedings of the National Academy of Sciences of the United States of America. 2006;103:1780-5.

25. Pringle DR, Vasko VV, Yu L, Manchanda PK, Lee AA, Zhang X, et al. Follicular thyroid cancers demonstrate dual activation of PKA and mTOR as modeled by thyroid-specific deletion of Prkar1a and Pten in mice. The Journal of clinical endocrinology and metabolism. 2014;99:E804-12.

26. Kim CS, Vasko VV, Kato Y, Kruhlak M, Saji M, Cheng SY, et al. AKT activation promotes metastasis in a mouse model of follicular thyroid carcinoma. Endocrinology. 2005;146:4456-63.

27. Nikiforova MN, Lynch RA, Biddinger PW, Alexander EK, Dorn GW, 2nd, Tallini G, et al. RAS point mutations and PAX8-PPAR gamma rearrangement in thyroid tumors: evidence for distinct molecular pathways in thyroid follicular carcinoma. The Journal of clinical endocrinology and metabolism. 2003;88:2318-26.

28. Diallo-Krou E, Yu J, Colby LA, Inoki K, Wilkinson JE, Thomas DG, et al. Paired box gene 8-peroxisome proliferator-activated receptor-gamma fusion protein and loss of phosphatase and tensin homolog synergistically cause thyroid hyperplasia in transgenic mice. Endocrinology. 2009;150:5181-90.

29. Papa A, Wan L, Bonora M, Salmena L, Song MS, Hobbs RM, et al. Cancer-associated PTEN mutants act in a dominant-negative manner to suppress PTEN protein function. Cell. 2014;157:595-610.

30. Dillon RL, Marcotte R, Hennessy BT, Woodgett JR, Mills GB, Muller WJ. Akt1 and akt2 play distinct roles in the initiation and metastatic phases of mammary tumor progression. Cancer research. 2009;69:5057-64.

31. Liu Z, Hou P, Ji M, Guan H, Studeman K, Jensen K, et al. Highly prevalent genetic alterations in receptor tyrosine kinases and phosphatidylinositol 3-kinase/akt and mitogen-activated protein kinase pathways in anaplastic and follicular thyroid cancers. The Journal of clinical endocrinology and metabolism. 2008;93:3106-16.

32. Palamidessi A, Frittoli E, Garre M, Faretta M, Mione M, Testa I, et al. Endocytic trafficking of Rac is required for the spatial restriction of signaling in cell migration. Cell. 2008;134:135-47.

33. Hoelting T, Siperstein AE, Clark OH, Duh QY. Epidermal growth factor enhances proliferation, migration and invasion of follicular and papillary thyroid cancer in vitro and in vivo. J. Clin Endocrinol Metab. 1994; 79(2):401-8.

# CHAPTER 3

## INPP4B loss and its role in prostate cancer progression

**Author contributions**

Several people contributed to the work presented in this chapter. **Chen Li Chew**, **Leonardo Salmena**, **Andrea Lunardi** and **Pier Paolo Pandolfi** developed hypotheses and designed experiments. **Chen Li Chew** carried out experiments and established study cohorts of mice. **Leonardo Salmena** and **George Poulogiannis** performed bioinformatics analyses. Pathologists **Sabina Signoretti** and **Roderick Bronson** performed histopathological analyses and scoring of PIN developed in prostates of experimental mice. **Christopher Ng** and **Jacqueline Fung** performed H&E and immunohistochemistry staining.

## 3.1 Introduction

### 3.1.1 Prostate cancer

The signaling pathways associated with prostate cancer progression are an area of extensive study, in part because gaining an understanding of the pathways gone awry may facilitate targeted cancer therapies. These therapeutic implications are important because more than 200,000 American men are diagnosed with prostate cancer (CaP) each year, making it the most common cancer and the second leading cause of cancer-related deaths in American men, trailing behind only lung cancer.

CaP may have some hereditary etiology; however, somatic mutations play a major part in the pathogenesis of this disease. Epidemiologic and twin studies have found that somatic gene defects can account for about half of the CaP cases (1). Such gene alterations include hypermethylation of *GSTP1*, allelic loss of *NKX3.1*, *PTEN* or *p27*, and increased expression of the androgen receptor (1).

The PI3K-AKT pathway is deregulated in 42% of primary CaP, and 100% of metastatic CaP (2), underscoring the importance of PI3K-AKT signaling in CaP tumorigenesis. Although PTEN is expressed in healthy prostate epithelium and prostatic intraepithelial neoplasia (PIN), it is often lost as these lesions become cancerous (3). Indeed, loss of PTEN expression is observed in 30-60% of all CaP (3). Further, a continuum of functional PTEN loss exists, and high grade CaP often has a higher degree of PTEN loss (3). While it is well established that loss of PTEN can lead to localized prostate cancer, the molecular mechanisms underlying metastatic CaP progression remains poorly understood (Figure 3.1).

Because of the importance of the PI3K-AKT signaling pathway in CaP progression (2), coupled with the fact that INPP4B, like PTEN, antagonizes PI3K-AKT signaling, we hypothesize that INPP4B cooperates with PTEN in suppressing prostate cancer progression.

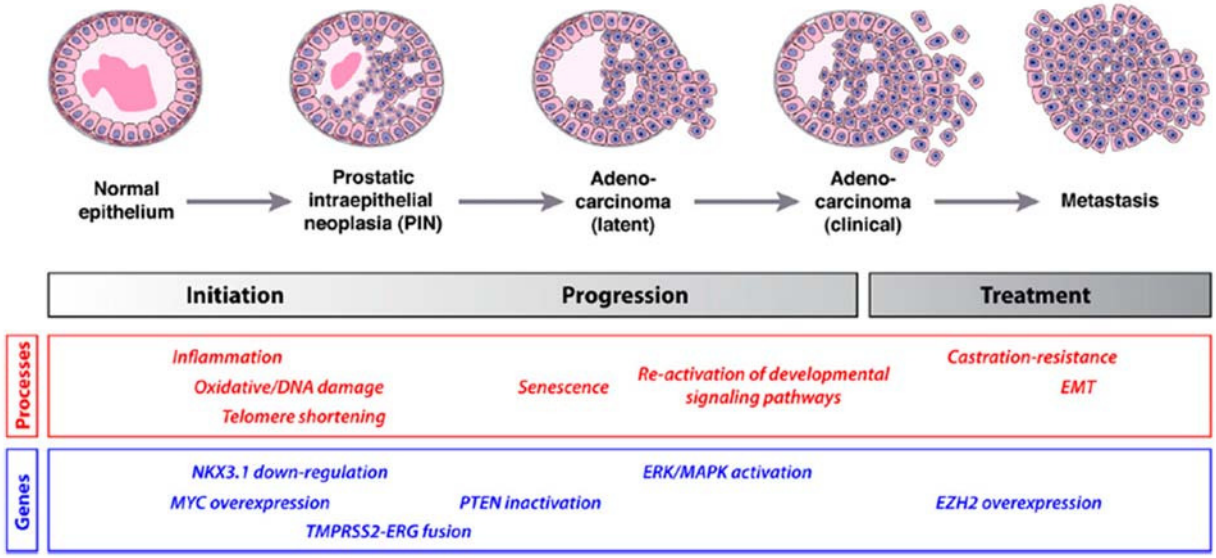


**Figure 3.1 The molecular pathogenesis of prostate cancer**

Flow chart depicting the stages in prostate cancer development, and the molecular mechanisms accounting for each transformation. The mechanisms underlying localized prostate cancer progression to metastatic prostate cancer remain poorly understood. Figure adapted from Shen and Abate-Shen, 2010.

### 3.1.2 GEMMs of prostate cancer

To date, several GEMMs of CaP have been generated in a bid to faithfully mimic prostate tumorigenesis in humans. Faithful modeling of human CaP allows us to gain a better understanding of the molecular mechanisms underlying CaP progression, and for pre-clinical trials of targeted therapies.

One of the first CaP models is the TRAMP (transgenic adenocarcinoma mouse prostate) model, where the prostate specific expression of SV40 T antigen oncoprotein is driven by the rat probasin promoter to disrupt critical tumor suppressor genes in human CaP, such as p53 and Rb (4). In the C57BL/6 genetic background, all male TRAMP mice develop PINs by 2 and 3 months of age, which progresses to poorly differentiated neuroendocrine carcinoma by 4-7 months, when distant metastases can primarily be detected in the lymph nodes and lung (TABLE) (5). Nonetheless, there are drawbacks to the clinical use of the TRAMP model. One such drawback is that a viral protein, whose role in the generation of human CaP is unknown, drives CaP in the TRAMP model (6). In addition, TRAMP mice develop neuroendocrine carcinoma, which rarely occurs in humans (5).

One of the most frequent genetic alterations in human CaP is deletion or mutation of *PTEN* (6). Thus, mouse models with loss of function of Pten would prove relevant in understanding the pathogenesis of CaP. Total body knock-out of *Pten* is embryonically lethal, thus, precluding the study of CaP progression in null mutants (7). Nevertheless, $Pten^{+/-}$ mice develop PINs by 8-10 months, while invasive adenocarcinoma is not observed (7). Compound mutant mouse models have been generated to investigate genetic alterations that can cooperate with *Pten* heterozygosity to modulate PIN formation and/or cancer progression (6). Notably, deficiency of Akt1 markedly attenuates the development of high-grade PIN in $Pten^{+/-}$ mice (8). Further, in

*Pten*$^{+/-}$*p27*$^{-/-}$ mice, loss of *p27* results in CaP at complete penetrance by 3 months of age, although no metastasis is observed (9). Loss of *Nkx3.1* in *Pten* heterozygous mice also results in invasive CaP in mice greater than 1 year of age, with metastases to the lymph nodes occurring with a 25% penetrance (10).

In order to study the tissue specific effect of the loss of a particular gene, conditional gene knockout systems based on the bacteriophage P1 Cre recombinase are widely used, where recombination between two LoxP sites results in deletion or inversion of intervening sequences (6). Conditional inactivation of a gene is achieved by flanking one or several exons of interest with LoxP sites, expressing Cre recombinase in a tissue specific manner using appropriate promoters, thus allowing the targeted exon(s) to be excised in a spatially-controlled manner (6).

To study the effect of complete *Pten* loss in the prostate, our lab utilizes *Pten*$^{loxP}$ mice crossed with the *PB-Cre4* transgenic line, in which *Cre* is under the control of a composite promoter, *ARR*$_2$*PB*, a derivative of the rat *Probasin* (*PB*) promoter (11). The *PB* gene is androgen responsive and is expressed at high levels in the epithelium of the prostate post-puberty (12). Therefore, excision of exons 4-5 of *Pten* would only occur in the prostate epithelium of the mice (12) It is important to note that the excision of *Pten* occurs post-puberty; eliminating any effect *Pten* loss has on prostate organogenesis that would confound analyses of cancer progression (12).

*Pten*$^{lx/lx}$-*PB-Cre*4 (*Pten*$^{pc-/-}$) mice display severe prostate enlargement and disorganized hyperplastic glands in all lobes with cellular dysplasia and cryptic glandular formation (12). These mice develop invasive and diffuse CaP in more than one prostate lobe and the tumor origin is multifocal (12). Although these prostate tumors are high-grade, undifferentiated lesions that are highly proliferative, metastasis is never observed (12). Strikingly, inactivation of both

*Pten* and *Trp53* results in invasive CaP by 10 weeks of age, in contrast to $Pten^{pc-/-}$ mice that presented with CaP after only 4-6 months of latency (13). More importantly, this mouse model reveals that acute *Pten* inactivation induces growth arrest through the p53-dependent cellular senescence pathway, thereby restricting prostate tumorigenesis in $Pten^{pc-/-}$ mice, which can be fully rescued through the combined loss of *Trp53* (13). More recently, loss of *Zbtb7a* has been shown to also promote *Pten*-null driven prostate tumorigenesis through Rb downregulation (14). We note that these mice do not present with lymph node or lung metastases. However, two studies find that loss of *Smad4* in $Pten^{pc-/-}$ mice or telomerase reactivation in the context of telomere dysfunction can result in aggressive CaP with metastases to the lymph nodes and the bone respectively (15,16).

As described in section 1.4.2.2 and section 3.1.1, genomic and transcriptional data in CaP reveal that *INPP4B*, together with *PTEN*, is down-regulated in metastatic CaP. However how INPP4B expression leads to CaP progression is still largely unknown. Additionally, a mouse model of CaP that would allow the *in vivo* study of *INPP4B* function is also lacking. Although PTEN loss leads to PIN and the formation of prostate tumors *in vivo*, these tumors often remain primary or localized in the prostate. Thus, my thesis aims to characterize the tumor suppressive function of INPP4B and its potential cooperation with PTEN in CaP progression *in vivo*, with the hypothesis that INPP4B might be a potential 'second-hit' required for CaP metastasis.

## 3.2 Results and discussion

### 3.2.1 *INPP4B* is reduced in metastatic prostate cancer in humans

To explore the possibility that the tumor suppressive functions of INPP4B counteracts the metastatic potential of primary prostate tumors, Dr. Leonardo Salmena and Dr. George Poulogiannis compared *INPP4B* expression between primary and metastatic samples in publicly available CaP databases – Lapointe (17), Taylor (2), Vanaja (18) and Varambally (19). As depicted in Figure 3.2 our analysis clearly shows that expression of INPP4B is significantly reduced in metastatic CaP when compared to localized CaP. This provides preliminary support for a role of INPP4B in metastatic progression of CaP.

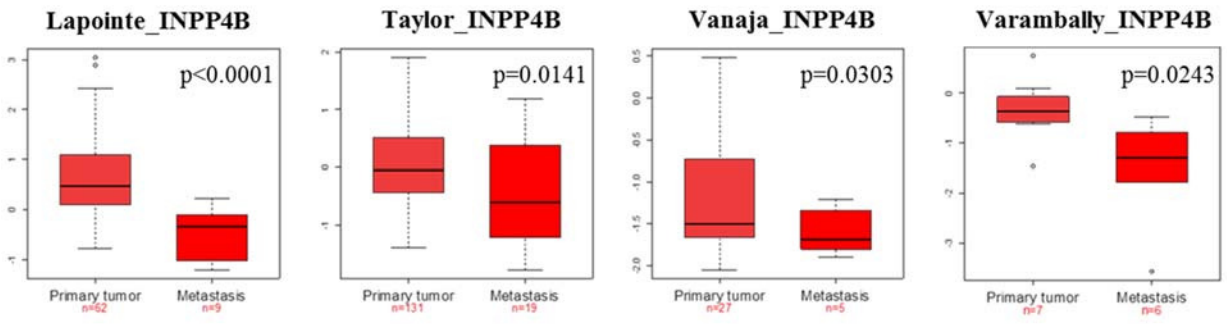


**Figure 3.2 *INPP4B* is significantly decreased in metastatic prostate cancer**

Bioinformatic analyses on four CaP datasets – Lapointe, Taylor, Vanaja and Varambally - show that INPP4B expression is significantly decreased in metastatic prostate cancer compared to primary tumors. *Salmena, L. and Poulogiannis, G.*

### 3.2.2 Characterization and validation of *Inpp4b* knockout (*Inpp4b*$^{-/-}$) mice

As described in Chapter 2, *Inpp4b* knockout mouse lines were obtained from Dr. Takehiko Sasaki (Akita University, Japan). These mice constitute a functional knockout of the phosphatase catalytic domain of Inpp4b (Figure 2.1A).

We first wanted to validate and characterize the mouse model. One approach I took was to look at the effect of Inpp4b loss of function in *Inpp4b*$^{fl/fl}$ mouse embryonic fibroblasts (MEFs). I isolated wildtype, *Inpp4b*$^{fl/+}$ and *Inpp4b*$^{fl/fl}$ MEFs, immortalized them with SV40 T-large antigen and then infected them with Cre-recombinase to knockout the phosphatase catalytic domain.

To find out if the mouse *Inpp4b* transcript was destabilized and degraded upon deletion of the floxed exon, I designed primers spanning the entire length of the mouse *Inpp4b* transcript (Figure 3.3A). Importantly, one primer pair was designed to amplify exons 19 to 23 (Figure 3.3A). Using this primer pair, wildtype *Inpp4b* would give an amplicon that is 628 base pairs in length. However, because *Inpp4b* knockout mice are deleted for exon 22, *Inpp4b*$^{+/-}$ and *Inpp4b*$^{-/-}$ mice would give a band that is 473 base pairs in length. Using semi-quantitative PCR, I am now confident that, on a transcript level, the knockout mouse model is indeed lacking the catalytic domain and that *Inpp4b* is not destabilized (Figure 3.3B).

**A**

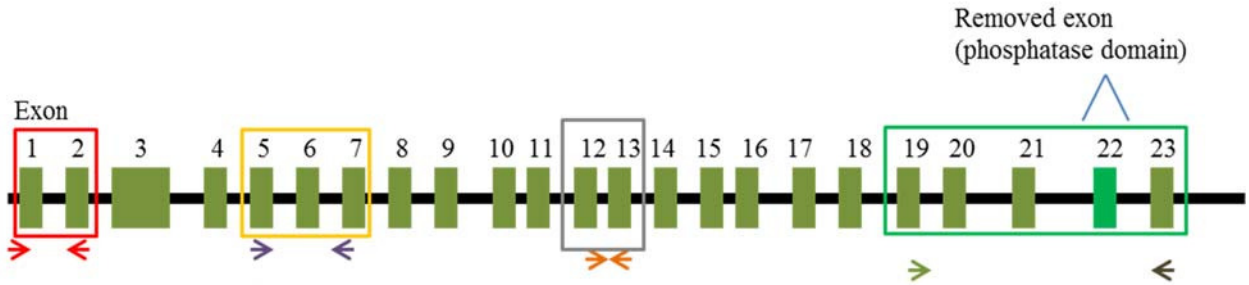


**B**

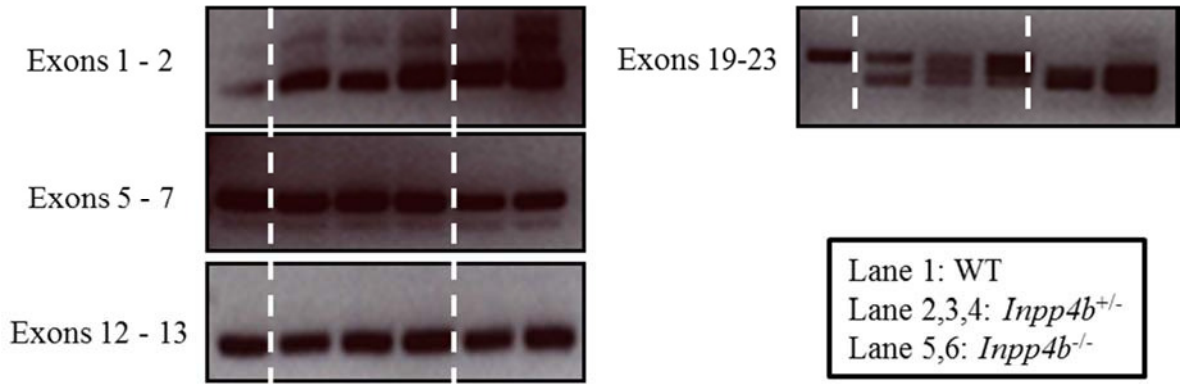


**Figure 3.3 *Inpp4b*$^{-/-}$ mice express *Inpp4b* lacking exon encoding phosphatase domain**

(A) Schematic depicting primer design over the entire length of *Inpp4b.* (B) Semi-quantitative PCR of *Inpp4b* in wildtype, *Inpp4b*$^{+/-}$ and *Inpp4b*$^{-/-}$ mice. Primer pair which amplifies Exons 19 to 23 indicate the presence of a shorter 473 base pairs band in the *Inpp4b*$^{+/-}$ and *Inpp4b*$^{-/-}$ mice.

Accordingly, we decided to check whether the loss of the catalytic domain could be detected on a protein level by the presence of a shorter, carboxyl-terminal deleted form of Inpp4b, since this truncated form of Inpp4b, though catalytically dead, might retain other functions or otherwise affect the normal activity of wildtype Inpp4b in *Inpp4b*$^{+/-}$ conditions, a key point for the correct interpretation of the data. However, I struggled with setting up the detection of mouse

Inpp4b protein levels at that point in time, given the lack of specific antibodies against the mouse protein that were commercially available then. Dr. Takehiko Sasaki has recently raised a specific antibody that detects mouse Inpp4b. This would be useful in further characterizing the *Inpp4b* knockout mouse model.

As described in Chapter 2, we found that MEFs with *Inpp4b* deletion displayed increased Akt activation, monitored through the phosphorylation of both Serine 473 and Threonine 308 at different time points after serum restimulation (Fig. S2.4A). This is in agreement with previous findings that Inpp4b loss results in increased Akt activation (20), providing functional support of the validity of *Inpp4b* knockout in the mouse model.

To further confirm that the increase in Akt activation was indeed due to Inpp4b loss of function in the MEFs, I re-expressed mouse Inpp4b in MEFs where *Inpp4b* has been floxed-out. Expression of Inpp4b was confirmed via western blotting with an antibody obtained in March 2015 from Dr. Takehiko Sasaki (Fig. 3.4A). This antibody was raised against a purified recombinant human INPP4B fragment (amino acids 2 – 235). The western blotting also confirmed the absence of full length mouse Inpp4b in *Inpp4b*$^{fl/fl}$ MEFs. Nonetheless, this does not preclude the existence of a stable, truncated protein lacking the catalytic domain of Inpp4b. Upon serum starvation-restimulation, expression of Inpp4b rescued Akt activation in *Inpp4b*$^{fl/fl}$ MEFs (Figure 3.4A). This provides additional support that Inpp4b antagonizes Akt activation. A future experiment would be to overexpress Inpp4b where the catalytic cysteine residue is mutated to alanine, thereby abrogating its catalytic activity (20). Efforts are underway to characterize Akt signaling in this mutant.

Since activation of Akt signaling is frequently associated with cellular proliferation, we analyzed the effect of Inpp4b loss of function by performing growth proliferation assays. We

**Figure 3.4 Functional characterization of *Inpp4b* knockout MEFs**

(A) Western blot analysis of lysates from immortalized *Inpp4b*$^{-/-}$ MEFs infected with either an empty vector or a vector that overexpresses Inpp4b. MEFs were serum starved and then restimulated with sfor the indicated amount of time. Arrowhead indicates specific band of INPP4B protein. (B) Proliferation of immortalized wildtype, *Inpp4b*$^{+/-}$ and *Inpp4b*$^{-/-}$ mouse embryonic fibroblasts (MEFs) upon Cre-mediated deletion. Cells were cultured in complete media (10% serum), stained with crystal violet, and lysed. Absorbance was measured at OD595nm.

**Figure 3.4 (continued)**

**A**

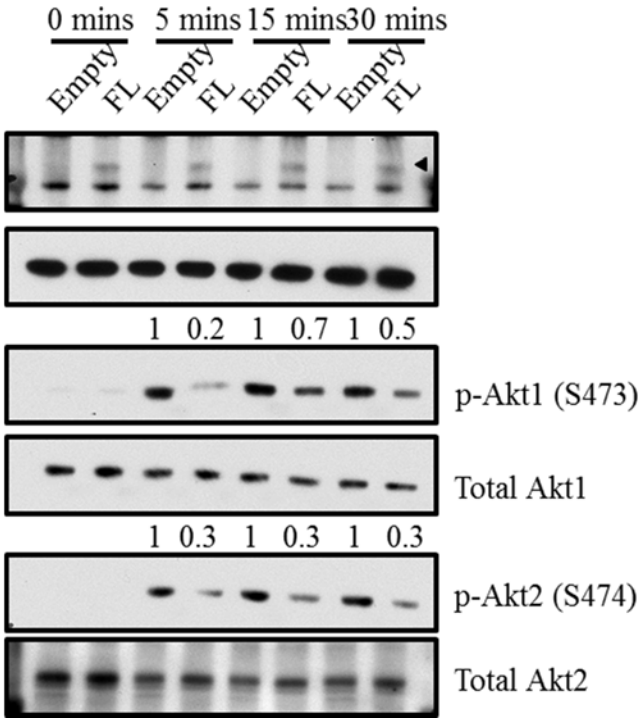


**B**

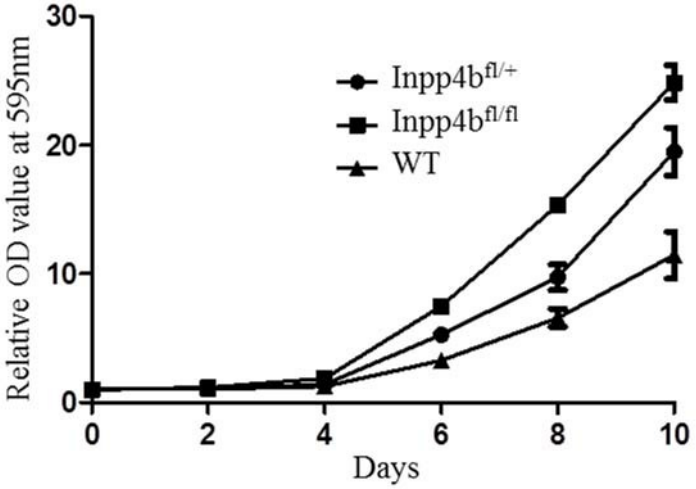

found that *Inpp4b*$^{fl/fl}$ MEFs had the highest proliferation rate, followed by *Inpp4b*$^{fl/+}$, and finally wildtype MEFs (Figure 3.4B).

### 3.2.3 *Inpp4b* knockout (*Inpp4b*$^{-/-}$) mice do not develop prostate intraepithelial neoplasia (PIN) characteristic of *Pten* haploinsufficient mice

To determine the possible tumor suppressive function of *INPP4B* in prostate tissue, we analyzed the prostates from *Inpp4b*$^{+/-}$ and *Inpp4b*$^{-/-}$ mice at different time points, up to 20 months old. Unlike *Pten*$^{+/-}$ mice which develop high-grade PIN (HGPIN) by 9 months of age (9), we found that partial or complete loss of *Inpp4b* in the prostate epithelium was insufficient to trigger any neoplastic transformation (Figure 3.5A-B). This demonstrates a possible distinction in the role of PTEN and INPP4B in prostate tumorigenesis.

### 3.2.4 Loss of Inpp4b in a *Pten* heterozygous background leads to prostate cancer progression

We next wanted to determine if Inpp4b loss cooperated with *Pten* heterozygosity to promote prostate cancer (CaP) progression. In keeping with genomic data from human CaP, we hypothesized that loss of *Inpp4b* would accelerate prostate cancer progression in *Pten*$^{+/-}$ mice. As described in Chapter 2, we crossed *Pten*$^{+/-}$ mice with *Inpp4b*$^{-/-}$ mice. The resulting *Pten*$^{+/-}$ *Inpp4b*$^{+/-}$ mice were then crossed with *Inpp4b*$^{+/-}$ littermates to generate wild type, *Pten*$^{+/-}$, *Pten*$^{+/-}$ *Inpp4b*$^{+/-}$ and *Pten*$^{+/-}$*Inpp4b*$^{-/-}$ mice (Figure S2.1A). To analyze the consequence of Inpp4b loss of CaP progression, we followed experimental cohorts of mice divided into three age groups – 6 to 8 months, 9 to 11 months and 12 to 15 months. Because *Pten*$^{+/-}$*Inpp4b*$^{-/-}$ mice developed metastatic, lethal follicular-like thyroid carcinoma and did not survive beyond 6 months of age

**Figure 3.5 *Inpp4b* knockout mice do not display any signs of prostate neoplasia**

(A) Hematoxylin and eosin (H&E) of Anterior, Ventral and Dorso-Lateral prostate lobes of WT, *Inpp4b*$^{+/-}$ and *Inpp4b*$^{-/-}$ mice at 6 months and (B) 20 months. Scale bars represent 50μm.

**Figure 3.5 (continued)**

**A**

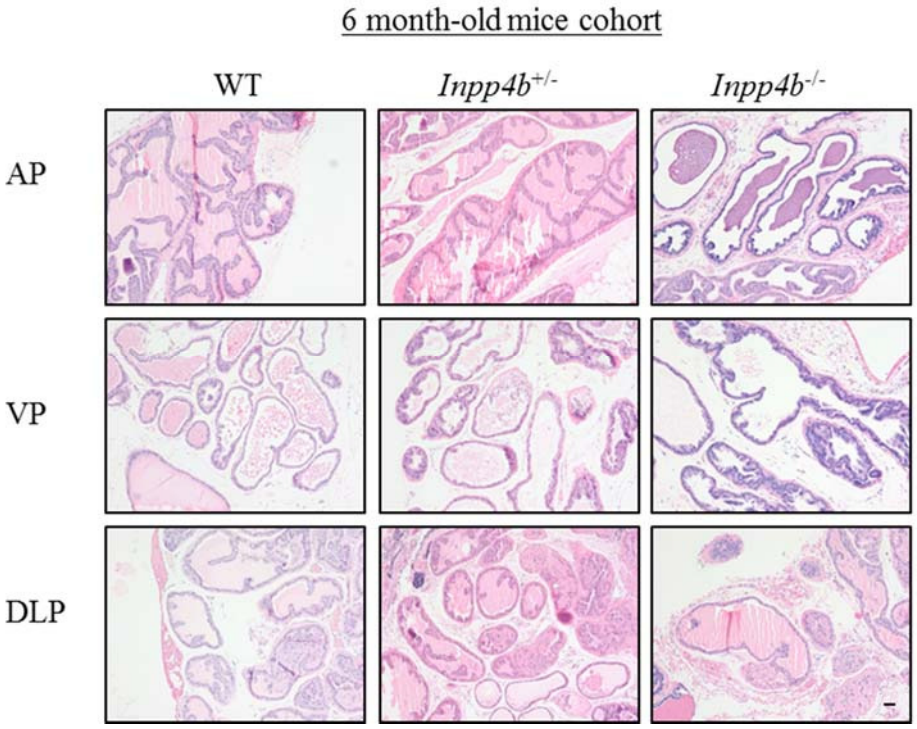


B

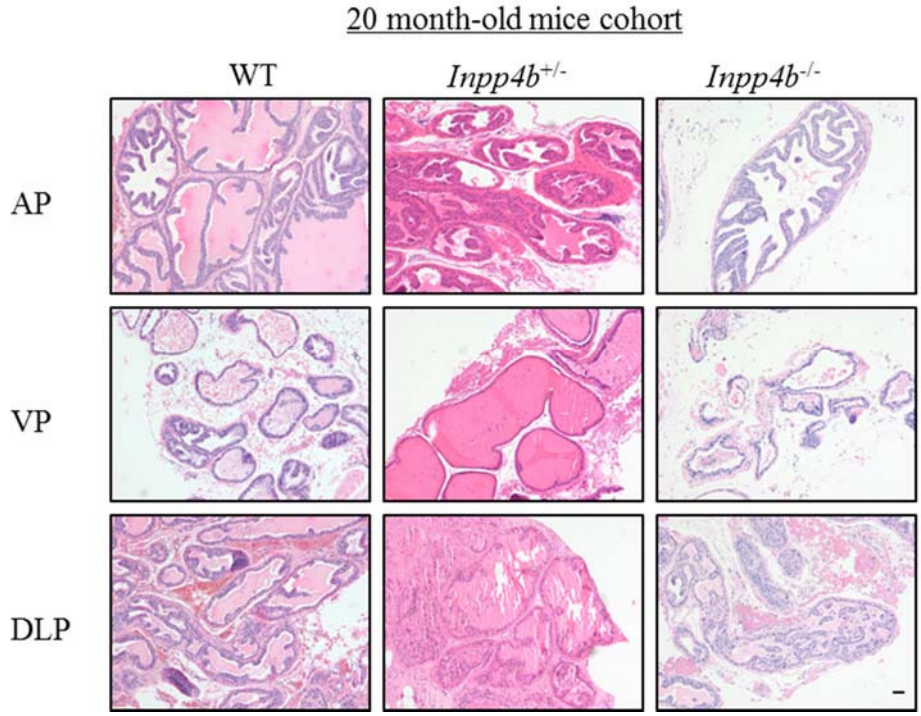

(Figure 2.2A), it precluded our use of these mice in studying the effect of complete *Inpp4b* loss on prostate tumorigenesis in the latter two age groups.

Histopathological analyses of wild type, *Pten*$^{+/-}$, *Pten*$^{+/-}$*Inpp4b*$^{+/-}$ and *Pten*$^{+/-}$*Inpp4b*$^{-/-}$ mice from 6 to 8 months of age revealed that there was no observable difference in the PIN developed (as a percentage of normal epithelium) in the ventral (VP), anterior (AP) or dorsolateral (DLP) lobes of the prostate (Figure 3.6A-B).

However, analyses of mice between 9-11 months of age reveal that partial loss of *Inpp4b* in *Pten*$^{+/-}$ mice resulted in an apparent increase in the percentage of PIN developed in all three lobes, with the most significant increase in the AP (Figure 3.7A-B).

Although there was no significant difference in total PIN development between wild type, *Pten*$^{+/-}$ and *Pten*$^{+/-}$*Inpp4b*$^{+/-}$ mice between 12 to 15 months of age (Figure 3.8A-B), analyses of these mice was complicated by architectural remodeling and the development of invasive carcinoma and cystic lesions in a number of *Pten*$^{+/-}$*Inpp4b*$^{+/-}$ mice precluded the scoring of these prostates for percentage of PIN developed. Nonetheless, in the prostate lesions that could be scored, we observed a general increase in the amount of high-grade PIN lesions developed in both the VP and AP (Figure 3.8C).

Strikingly, in the VPs of the *Pten*$^{+/-}$*Inpp4b*$^{+/-}$ mice, we observed microinvasion at a 56% penetrance and the development of invasive carcinoma in 25% of the mice (Figure 3.9A and 3.9B). Neoplastic lesions have never been reported in the ventral prostates of *Pten*$^{+/-}$ mice (9), nor were they observed in the *Pten*$^{+/-}$ mice of our experimental cohort. Furthermore, we observed a high degree of advanced remodeling and cystic lesions in the AP in 33% of *Pten*$^{+/-}$ *Inpp4b*$^{+/-}$ mice, which has never been described in *Pten*$^{+/-}$ mice (Figure 3.9A and 3.9C). Immunohistochemical analysis revealed an increased percentage of prostate epithelial cells with

**Figure 3.6 Analysis of 6 to 8 month-old cohort of *Pten*$^{+/-}$, *Pten*$^{+/-}$*Inpp4b*$^{+/-}$ and *Pten*$^{+/-}$*Inpp4b*$^{-/-}$ mice for prostatic intraepithelial neoplasia**

(A) Hematoxylin and eosin (H&E) of Anterior, Ventral and Dorso-Lateral prostate lobes of *Pten*$^{+/-}$, *Pten*$^{+/-}$ *Inpp4b*$^{+/-}$ and *Pten*$^{+/-}$ *Inpp4b*$^{-/-}$ mice at 6 to 8 months of age. Scale bar represents 50μm. (B) Incidence of PIN as a percentage of normal epithelium is reported in the dot plot.

**Figure 3.6 (continued)**

**A**

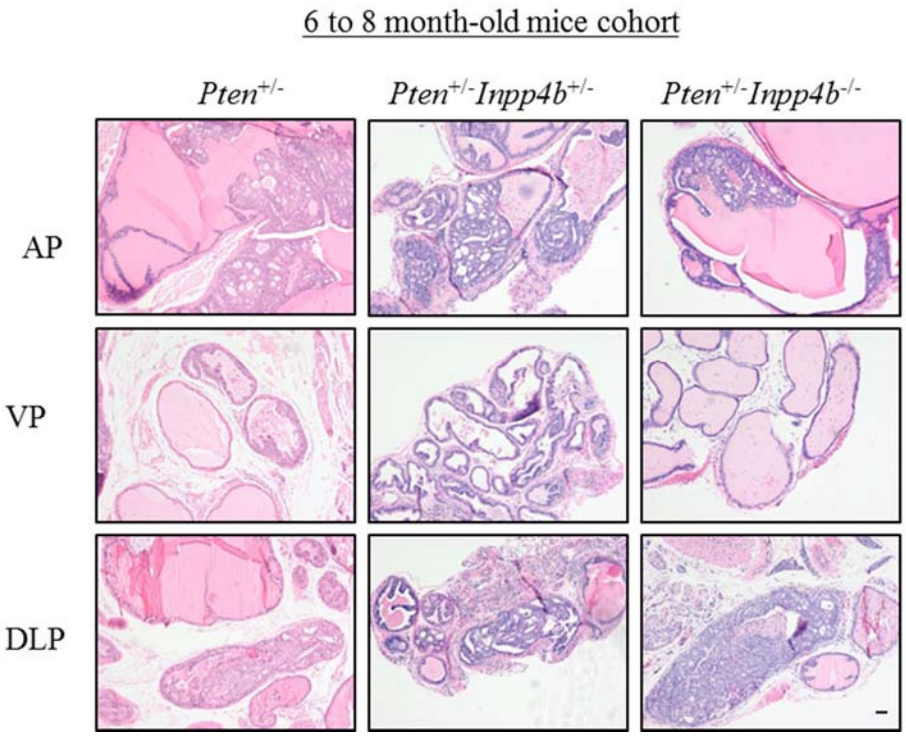


**B**

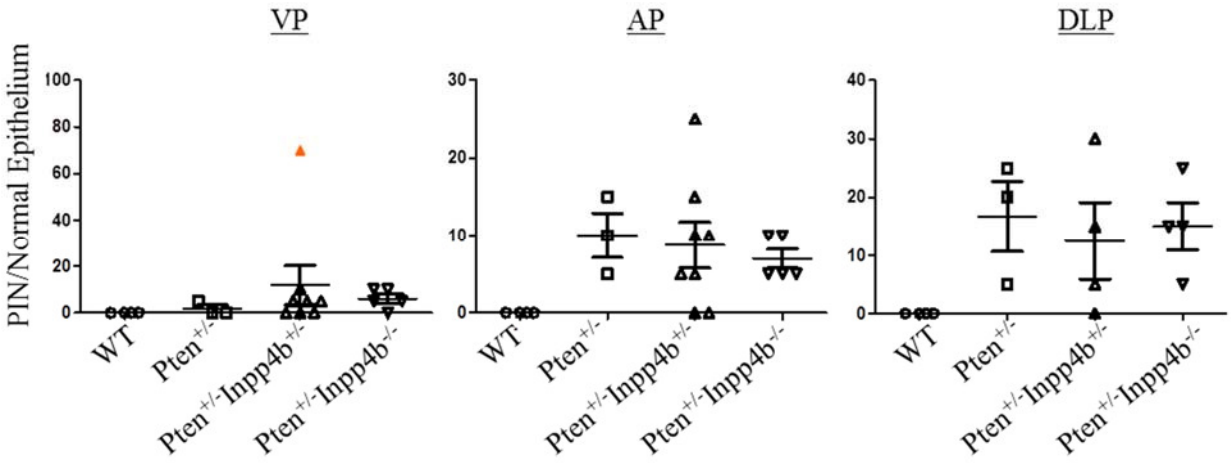

**Figure 3.7 Analysis of 9 to 11 month-old cohort of *Pten*$^{+/-}$, *Pten*$^{+/-}$*Inpp4b*$^{+/-}$ and *Pten*$^{+/-}$*Inpp4b*$^{-/-}$ mice for prostatic intraepithelial neoplasia**

(A) H&E of Anterior, Ventral and Dorso-Lateral prostate lobes of *Pten*$^{+/-}$ and *Pten*$^{+/-}$ *Inpp4b*$^{+/-}$ mice at 9 to 11 months of age. Scale bar represents 50μm. (B) Incidence of PIN as a percentage of normal epithelium is reported in the dot plot.

**Figure 3.7 (continued)**

**A**

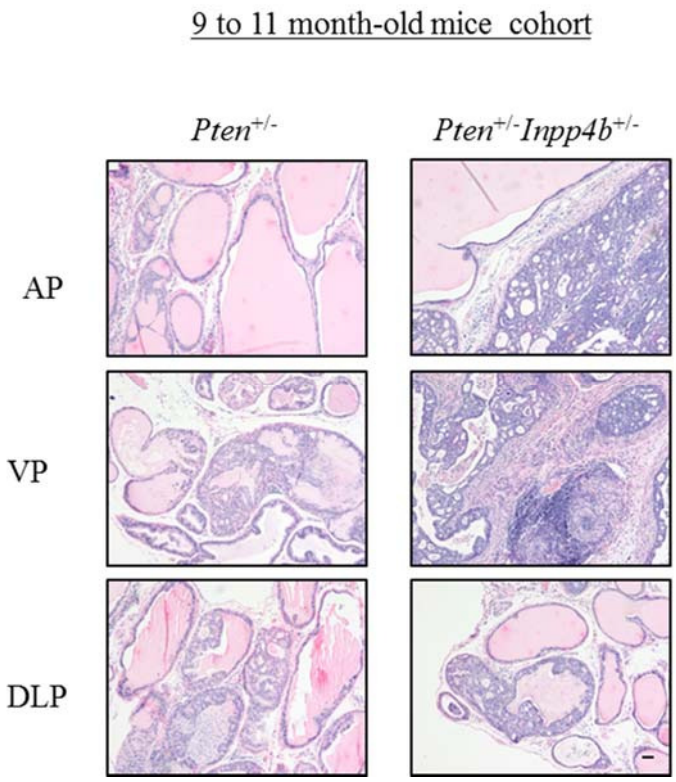


**B**

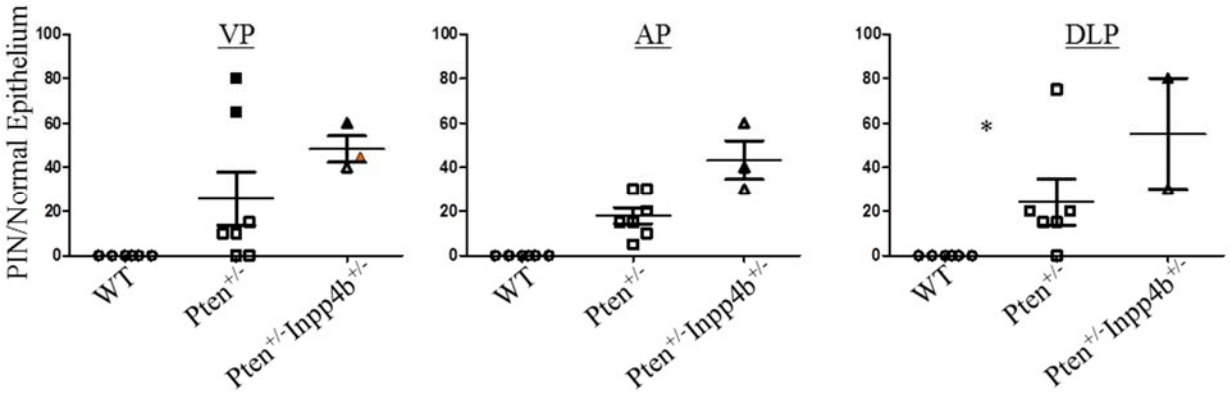

**Figure 3.8 Analysis of 12 to 15 month-old cohort of *Pten*$^{+/-}$, *Pten*$^{+/-}$*Inpp4b*$^{+/-}$ and *Pten*$^{+/-}$ *Inpp4b*$^{-/-}$ mice for prostatic intraepithelial neoplasia**

(a) H&E of Anterior, Ventral and Dorso-Lateral prostate lobes of *Pten*$^{+/-}$ and *Pten*$^{+/-}$ *Inpp4b*$^{+/-}$ mice at 12 to 15 months of age. Scale bar represents 50μm. (b) Incidence of PIN as a percentage of normal epithelium is reported in the dot plot. (c) Incidence of high-grade PIN (HGPIN) as a percentage of normal epithelium is reported in the dot plot.

**Figure 3.8 (continued)**

**A**

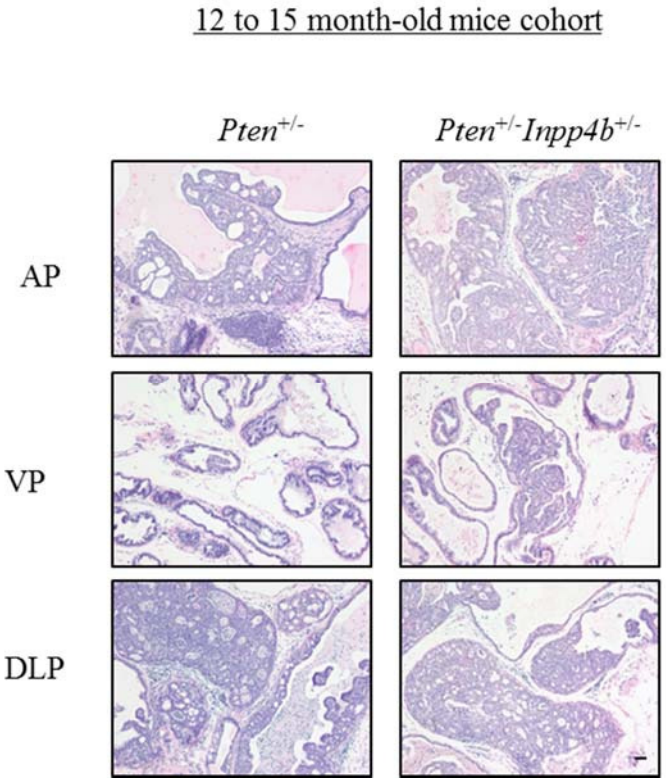


**B**

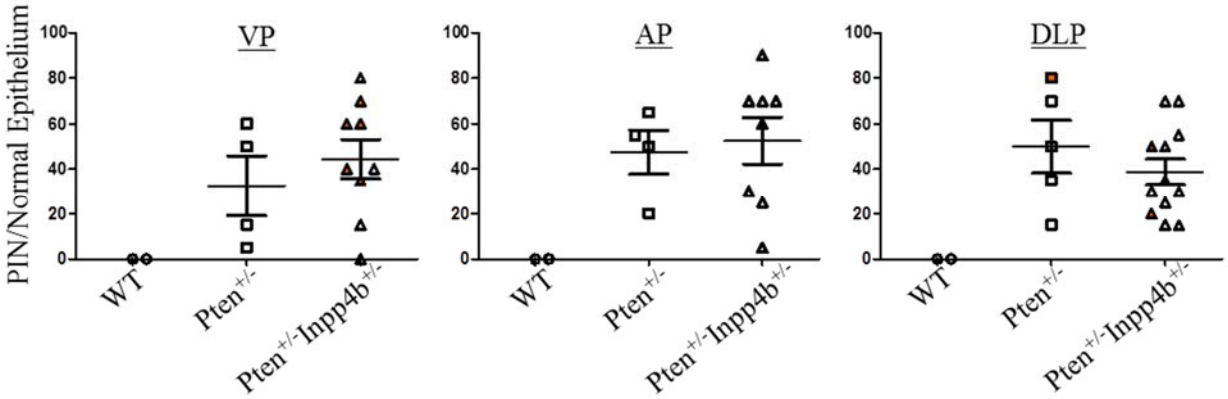

**Figure 3.8 (continued)**

**C**

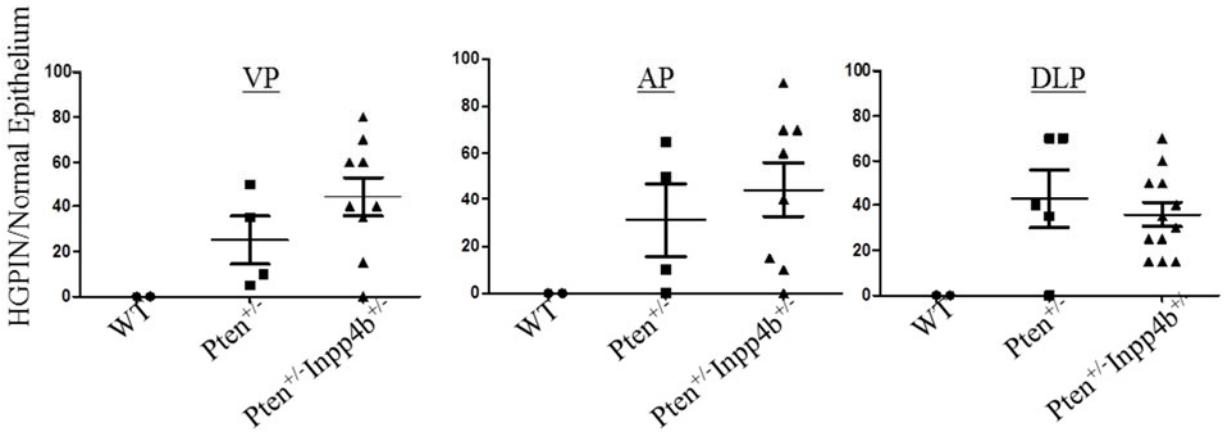

Akt activation (monitored through phosphorylation of Ser473) in both the ventral and anterior prostates of *Pten*$^{+/-}$*Inpp4b*$^{+/-}$ mice, compared to that of *Pten*$^{+/-}$ mice (Figure 3.9D and 3.9E, top panels). To assess any differences in the proliferation of the prostate epithelium, we performed immunostaining for the Ki-67 proliferation antigen. Ki-67 positive cells were rarely observed in the ventral and anterior prostate epitheliums of *Pten*$^{+/-}$ mice (Figures 3.9D and 3.9E, left panels), in line with previous reports that neoplastic transformation was rarely detected in these lobes (9). In contrast, there was a stark increase in the number of Ki67-positive prostate cells in both the ventral and anterior prostates of the *Pten*$^{+/-}$*Inpp4b*$^{+/-}$ mice (Figure 3.9D middle panel and 3.9E bottom panel). This indicates increased proliferation of prostate cells in the ventral and anterior prostates upon partial loss of *Inpp4b* in *Pten*$^{+/-}$ mice. Smooth muscle actin (SMA) staining of ventral prostate sections revealed development of invasive prostatic adenocarcinoma in the ventral prostate of *Pten*$^{+/-}$*Inpp4b*$^{+/-}$ mice (Figure 3.9D, bottom panel). Taken together, these suggest that *Inpp4b* loss can cooperate with *Pten* heterozygosity to promote prostate cancer progression.

### 3.2.5 *In vitro* detection of INPP4B with antibodies, and the identification of a novel isoform of INPP4B

We next wanted to characterize effects of INPP4B loss *in vitro* using human prostate cancer cell lines. However, we first needed to optimize systems for the analysis of endogenous INPP4B. We obtained two commercially available antibodies against INPP4B – Epitomics (EPR3108Y) and Cell Signaling Technologies (#8450). Anti-INPP4B (EPR3108Y) is raised against a synthetic peptide corresponding to human INPP4B from amino acids 1 to 100 (N-terminus), while anti-INPP4B (#8450) was raised against a synthetic peptide corresponding to residues near the C-terminus of human INPP4B (according to datasheet of antibody). The relative positions of

**Figure 3.9 *Inpp4b* heterozygosity accelerates prostate cancer in *Pten*$^{+/-}$ mice**

(A) Percentage of invasive prostate cancer (Ventral lobe), microinvasion (Ventral lobe) and cystic lesions (Anterior lobe) observed in the prostates of *Pten*$^{+/-}$ and *Pten*$^{+/-}$*Inpp4b*$^{+/-}$ mice. (B-C) *Left panels:* H&E of prostates from *Pten*$^{+/-}$*Inpp4b*$^{+/-}$ mice with invasive prostate cancer in the Ventral lobe (B), and cystic lesions in the Anterior lobe (C). *Right panels:* Higher magnifications regions within the black squares. Scale bars represent 50μm, except in left panel of (C), where it represents 250um. (D-E) Ki67, smooth muscle actin (SMA) and p-Akt (Ser473) staining of prostate sections from *Pten*$^{+/-}$ (*left panels*) and *Pten*$^{+/-}$*Inpp4b*$^{+/-}$ mice (*right panels*). Arrowheads indicate sites of tumor invasion. Scale bars, top panels: 250μm, middle and bottom panels: 50μm.

**Figure 3.9 (continued)**

**A**

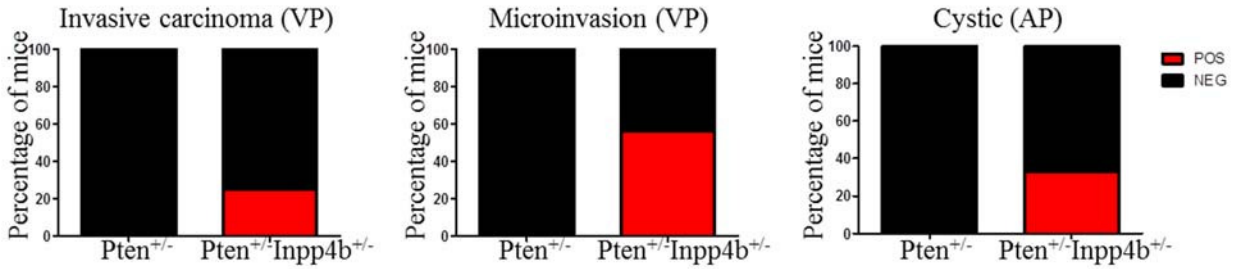


**B**

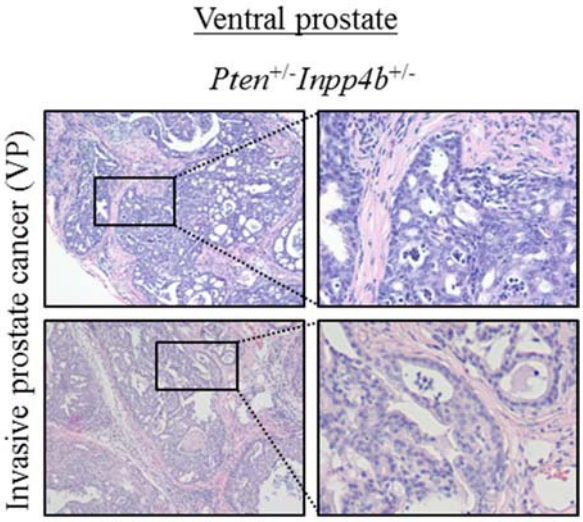

**Figure 3.9 (continued)**

**C**

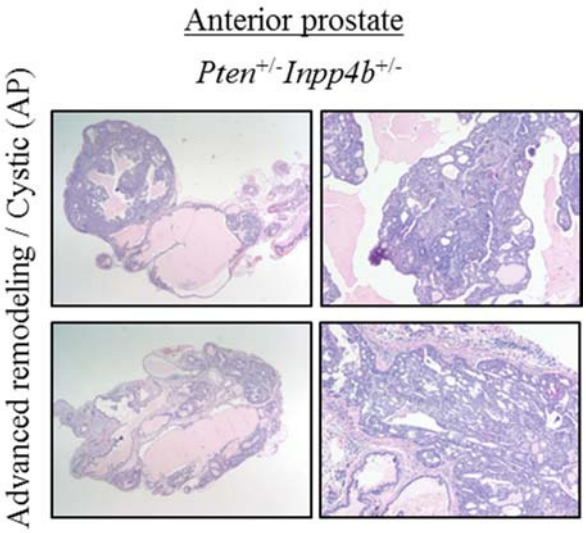


**D**

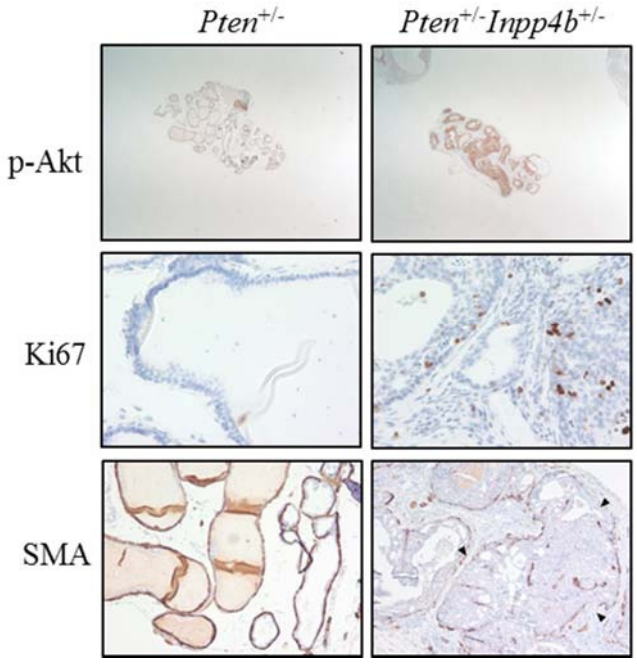

**Figure 3.9 (continued)**

**E**

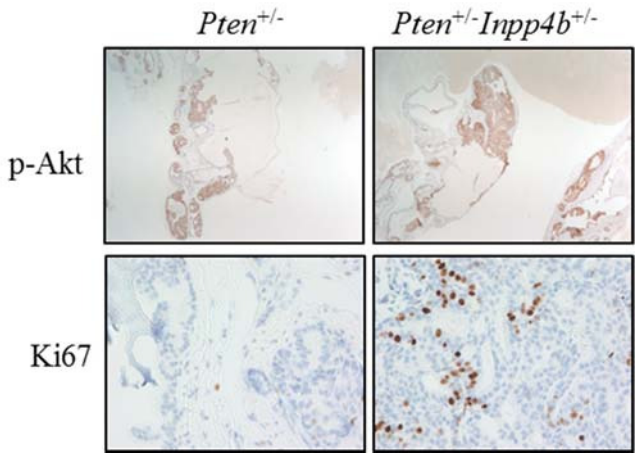

the epitopes recognized by both antibodies are represented in Figure 3.10A. Although I too grappled with setting up the detection of INPP4B protein levels, through extensive troubleshooting efforts using *in vitro* knockdown of INPP4B in various prostate cell lines (PWR1E, RWPE1, DU145) and a breast cancer cell (HMEC) as positive control, I am now confident of specifically detecting INPP4B in our human cell lines (Figure 3.10B).

**A**


**B**

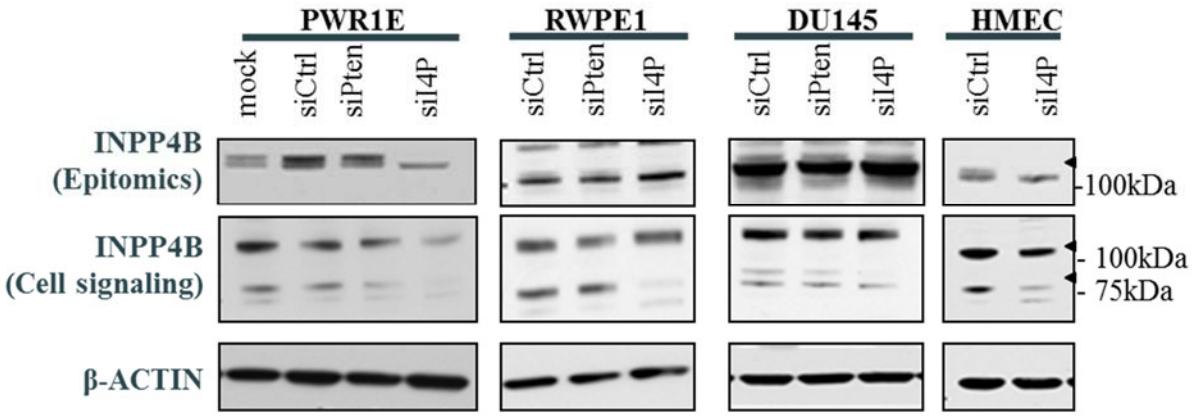


**Figure 3.10 Characterization of two commercially available antibodies against INPP4B**

(A) Diagram representing the structure of INPP4B, which contains an N-terminus C2 domain and a C-terminus phosphatase domain in Exon 26. Chevron arrows indicate the relative position of the epitope recognized by the respective antibodies. Red arrow indicates where siRNA against INPP4B targets. (B) Western blot analysis of lysates from siRNA mediated knock-down of

**Figure 3.10 (continued)**

INPP4B in PWR1E, RWPE1, DU145 and HMEC cell lines. Arrowhead indicates specific bands of INPP4B protein.

Interestingly, during this process, we made a serendipitous discovery of a potential novel isoform of INPP4B in our cell lines. Compared to full length INPP4B at 105kDa, this isoform is a little larger than 75kDa in size. The shorter isoform can only be detected by Cell Signaling antibodies (#8450), which is raised against the C-terminus of human INPP4B, suggesting that this isoform most likely lacks the N-terminus C2 domain (Figure 3.11).


**Figure 3.11 Proposed structure of truncated INPP4B isoform**

Diagram representing the potential structure of the shorter INPP4B isoform which is ~75kDa. This isoform is proposed to lack the C2 lipid membrane binding domain, but still contain the phosphatase catalytic domain.

Indeed, upon examination of the protein sequence of INPP4B, it is predicted that removal of the C2 domain results in an isoform that is approximately 85kDa in size. A potential alternative start codon close to the end of the C2 domain would result in a transcript encoding for an isoform that is approximately 84kDa in size. However, alignment and analysis of known *INPP4B* transcripts

on Ensembl suggested that such a transcript does not exist, indicating that this protein isoform could possibly be formed via protease mediated degradation. Future characterization of this shorter INPP4B isoform, its expression and localization pattern and the specific role it might play in cancer would undoubtedly yield further insights into the functions of INPP4B.

### 3.2.6 Knockdown of *INPP4B* in prostate cell lines increased metastatic potential

To study the effects of INPP4B loss in cancer assays, I generated prostate cell lines (PC3 and PWR1E) with a stable knockdown of *INPP4B* (Figure 3.12A, 3.12B and 3.13A). These three shRNA constructs against *INPP4B* were obtained from both Open Biosystems (sh21 and sh22) and Dr. Alex Toker (sh#2). Importantly, as seen with the knockdowns of *INPP4B* in both PWR1E and PC3, both sh21 and sh22 target both 105kDa and 75kDa isoforms of INPPB, but sh#2 seems to predominantly target the 105kDa isoform (Figure 3.12B, 3.12C and 3.13B). This was true in both prostate and thyroid cell lines. Because of the unspecific bands detected by the INPP4B antibodies, especially in the PC3 cell line, we further characterized the knockdown through immunoprecipitation of INPP4B, followed by a western blot, and this confirmed that both the 105kDa and 75kDa bands are decreased by sh21 and sh22 (Figure 3.12C and 3.13B). In addition, it also corroborated the specificity of the antibodies. For subsequent assays, we used only cell lines with *INPP4B* knocked down using sh21 and sh22. In addition, cell lines derived from infecting the respective parental lines with scrambled shRNA were used as negative controls.

To look at the effect of INPP4B loss on AKT signaling, I performed a serum starvation-restimulation assay with the PC3 cells. Upon serum re-stimulation for 5 minutes, we see increased AKT activation (monitored through an increase in phosphorylation of Ser473 and

**Figure 3.12 Validation of *INPP4B* knockdown in PWR1E cells**

(A) RT-qPCR analysis of *INPP4B* upon shRNA-mediated knockdown. (B) Western blot analysis of INPP4B levels in PWR1E cells after shRNA-mediated knockdown. Arrowhead indicates specific band of INPP4B protein. (C) Western blot analysis of INPP4B levels in PWR1E cells after shRNA-mediated knockdown. Lysates were obtained via immunoprecipitation with anti-INPP4B from Cell Signaling Technologies (#8450), followed by reciprocal western blotting with anti-INPP4B from Epitomics (EPR3108Y) and Cell Signaling Technologies (#8450).

**Figure 3.12 (continued)**

**A**

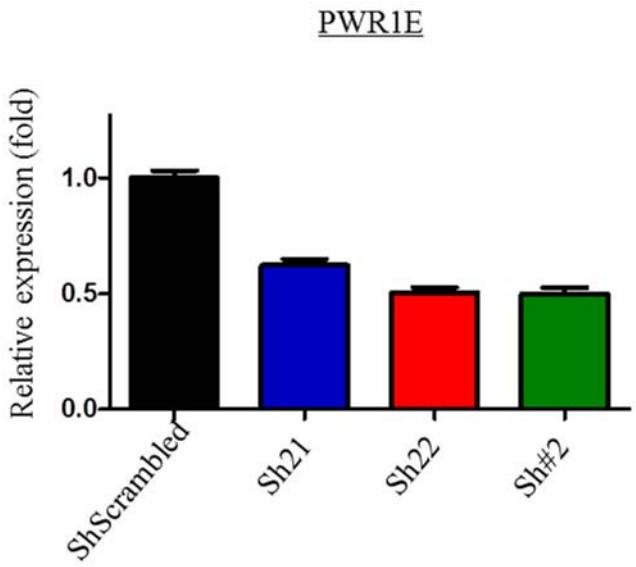


**B**

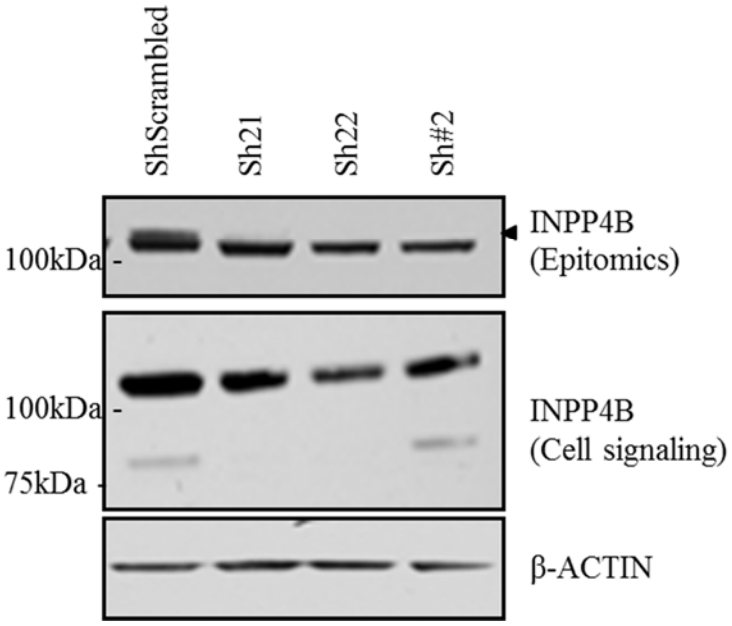

**Figure 3.12 (continued)**

**C**

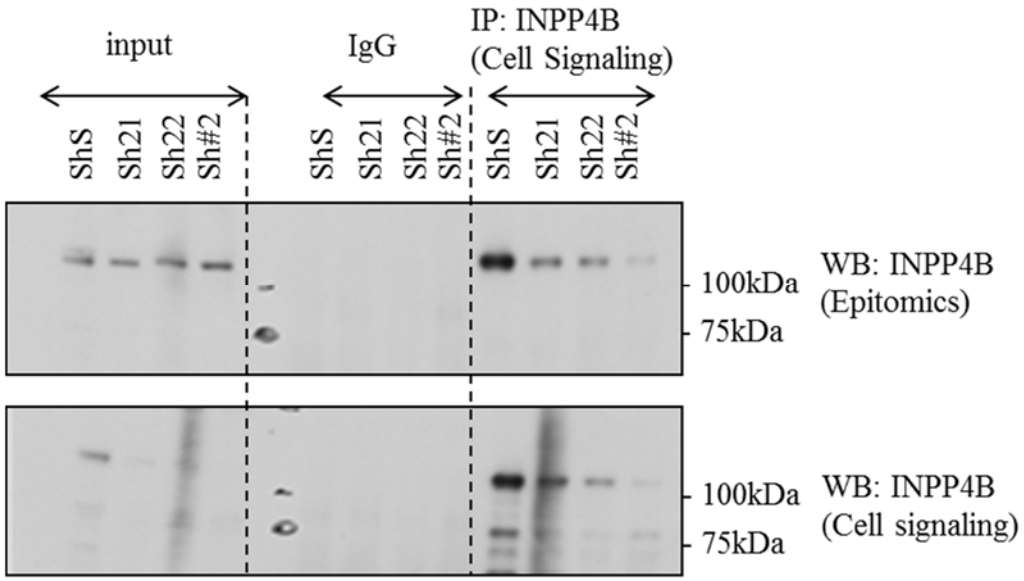

**Figure 3.13 Validation of *INPP4B* knockdown in PC3 cells**

(A) RT-qPCR analysis of *INPP4B* upon shRNA-mediated knockdown. (B) Western blot analysis of INPP4B levels in PC3 cells after shRNA-mediated knockdown. Lysates were obtained via immunoprecipitation with anti-INPP4B from Cell Signaling Technologies (#8450), followed by reciprocal western blotting with anti-INPP4B from Epitomics (EPR3108Y) and Cell Signaling Technologies (#8450).

**Figure 3.13 (continued)**

**A**

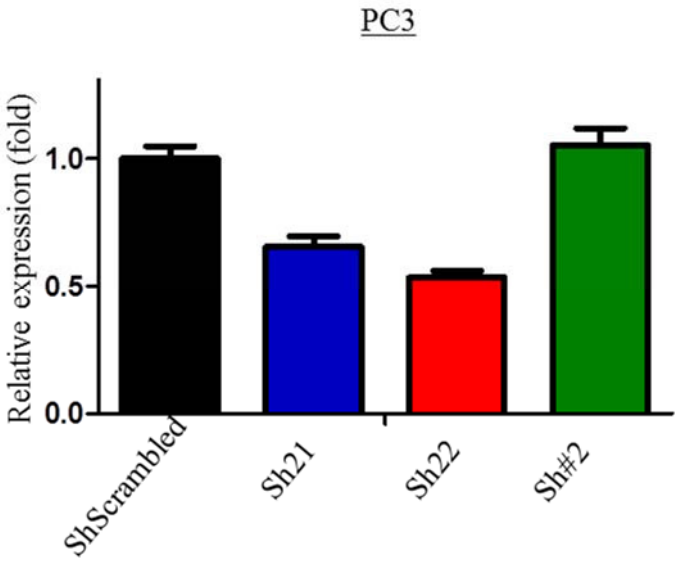


**B**

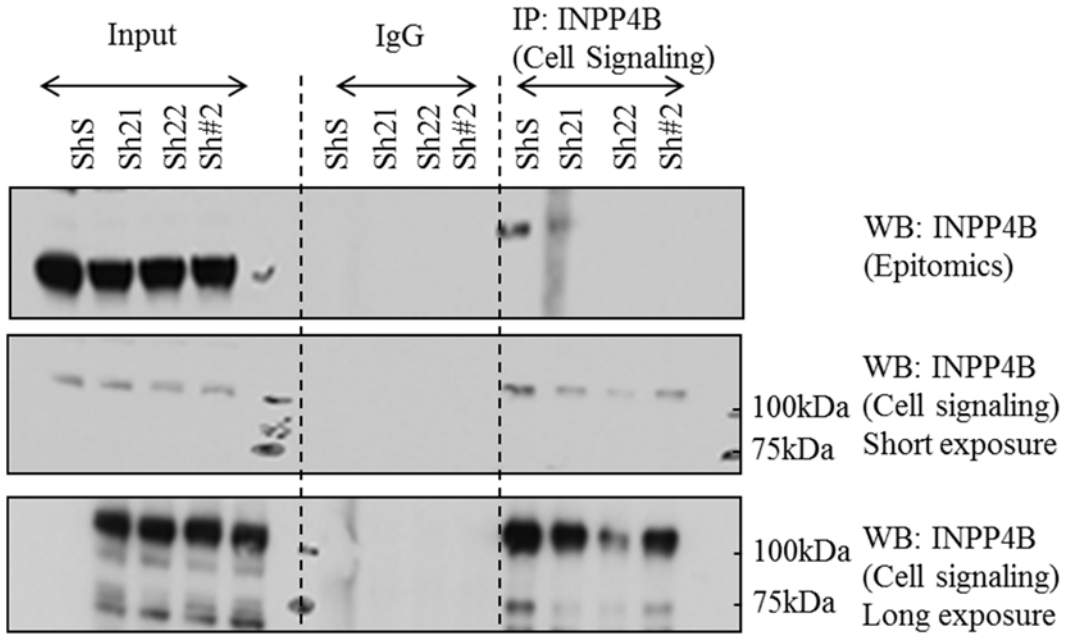

Thr308) for both sh21 and sh22 cells in PC3 cells, when compared to PC3-shScrambled (Figure 3.14A).

We next conducted cell proliferation assays on PWR1E and PC3 cell lines. We found that knockdown of *INPP4B* did not confer a growth advantage for prostate cell lines under full serum growth conditions (Figure 3.14B), in keeping with our observations in the thyroid cell lines (Figure 2.5C).

To find out if INPP4B loss in conjunction with PTEN loss would contribute to a more aggressive prostate cancer phenotype, we performed *in vitro* metastasis assays with PC3 cells, which are PTEN null. We found that knockdown of *INPP4B* in PC3 cells resulted in increased migration and invasion of PC3 cells (Figure 3.15A-B).

To further explore the functional effect of INPP4B loss, a subcutaneous xenograft assay using PC3-sh21 and PC3-sh22 was performed using NCr nude mice. The procedure is described in the "*Methods*" section. In line with our findings that INPP4B loss did not provide a proliferative advantage, we did not observe a significant difference in xenograft volume and weight between PC3-shScrambled and PC3-sh22 xenografts (Figure 3.16A-B). PC3-sh21 cells appeared to proliferate at a rate slower than both PC3-shScrambled and PC3-sh22 cells (Figure 3.16A-B). This could be due to the instability of sh21 knockdown *in vivo*. It could also be due to specific and/or nonspecific off-target effects of sh21, triggering an interferon response (21), affecting the general expression levels and efficiency of sh21 *in vivo*. With the frozen xenograft tumors, we are going to perform rt-qPCR and a western blot to look at INPP4B levels to verify the stability of the knockdown.

Strikingly, however, histopathological analyses revealed the occurrence of distant metastases of xenograft cells to the lungs in 2 of 5 mice injected with PC3-sh22 cells (Figure 3.16C). To

**Figure 3.14 Knockdown of *INPP4B* in prostate cell lines leads to increased AKT activation, but did not provide an advantage for proliferation**

(A) Western blot analysis of phosphorylated AKT (Thr308 and Ser473) in lysates derived from serum restimulation of PC3 cells infected with either a non-targeting shRNA or an shRNA that targets *INPP4B* (sh21, sh22 and sh#2). Cells were stimulated with serum for 5 minutes. (B) Proliferation of PWR1E and PC3 cell lines infected with either a non-targeting shRNA or a shRNA that targets *INPP4B* (sh21 and sh22). Cells were cultures in complete media (10% serum), stained with crystal violet, and lysed. Absorbance was measured at OD595nm.

**Figure 3.14 (continued)**

**A**

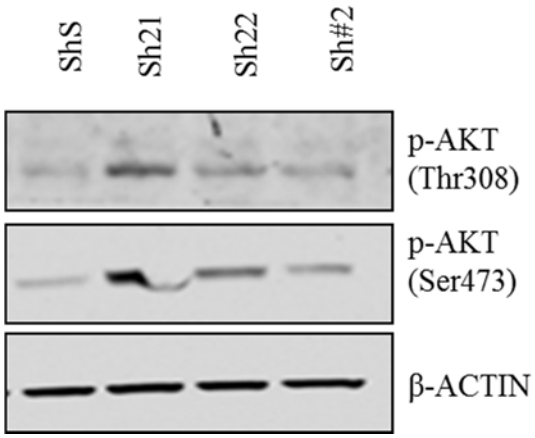


**B**

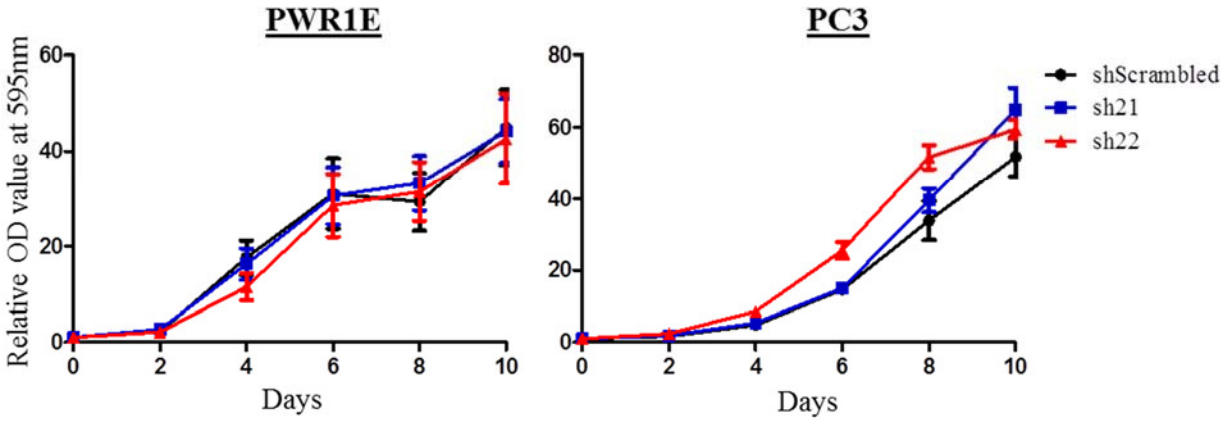

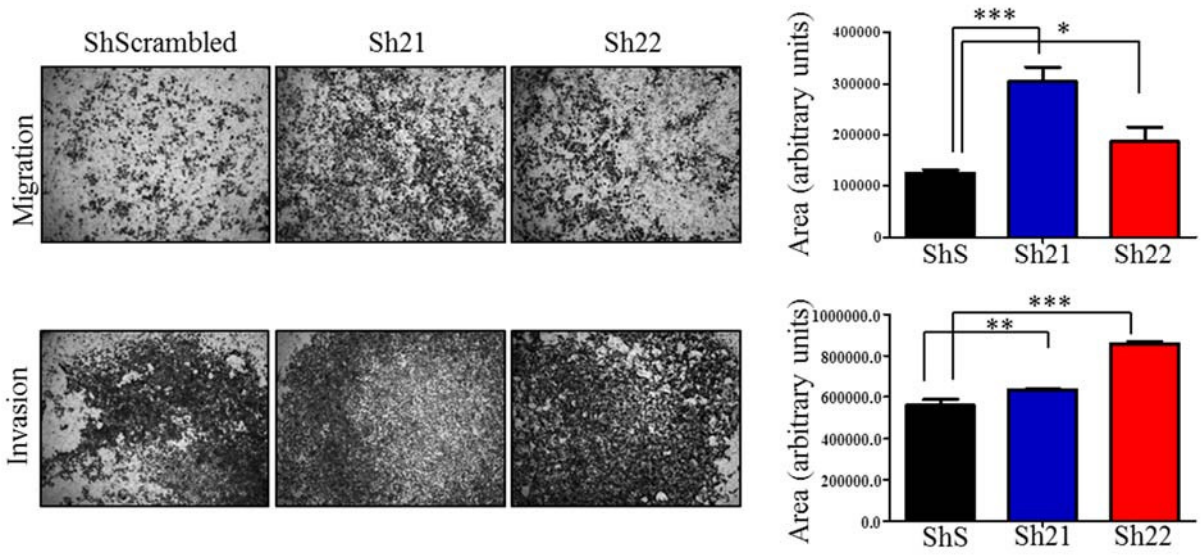


**Figure 3.15 Knockdown of *INPP4B* in PC3 cells provided an advantage for migration and invasion**

(A-B) Transwell migration and invasion assays using PC3 cells infected with either a non-targeting shRNA or an shRNA that targets *INPP4B* (sh21 and sh22). The chemoattractant used was serum. Cells were fixed and stained with crystal violet, and then photographed (A) and the total area occupied by the cells was determined using *ImageJ* (B).

confirm the human origin of the metastatic deposits, parallel sections to H&E-stained lung sections in which metastases were observed were immunostained for a panel of markers specific to human PC3 cells. These metastases were strongly positive for pan cytokeratin and human promyelocytic leukemia protein (PML) (stained with human-specific antibody), confirming the human origin of the metastases (Figure 3.16C). In addition, these lesions stained negative for thyroid transcription factor 1 (TTF-1), indicating that they did not originate from a lung

adenocarcinoma (Figure 3.16C). Strong AKT activation was also observed by immunohistochemistry in the lung metastases (Figure 3.16C). We are in the process of repeating the xenograft assay to ensure the reproducibility of the results. Taken together, these results serve as a preliminary indication of the cooperativity between INPP4B and PTEN loss in increasing the metastatic potential of prostate cancer cells.

**Figure 3.16 Knockdown of *INPP4B* in PC3 cells provided an advantage for distant metastasis**

(A) Increase in tumor volume of subcutaneous tumors arising from the xenograft of PC3 cells infected with either a non-targeting shRNA or an shRNA that targets *INPP4B* (sh21 and sh22). (B) Dot plot representing the final weight and volume of the tumors arising from the xenograft of PC3 cells infected with either a non-targeting shRNA or an shRNA that targets *INPP4B* (sh21 and sh22). (C) H&E, pan-cytokeratin, human PML, p-AKT and TTF-1 staining of lung metastases arising from PC3 cells infected with a shRNA that targets *INPP4B* (sh22). Scale bar represents 50μm.

**Figure 3.16 (continued)**

**A**

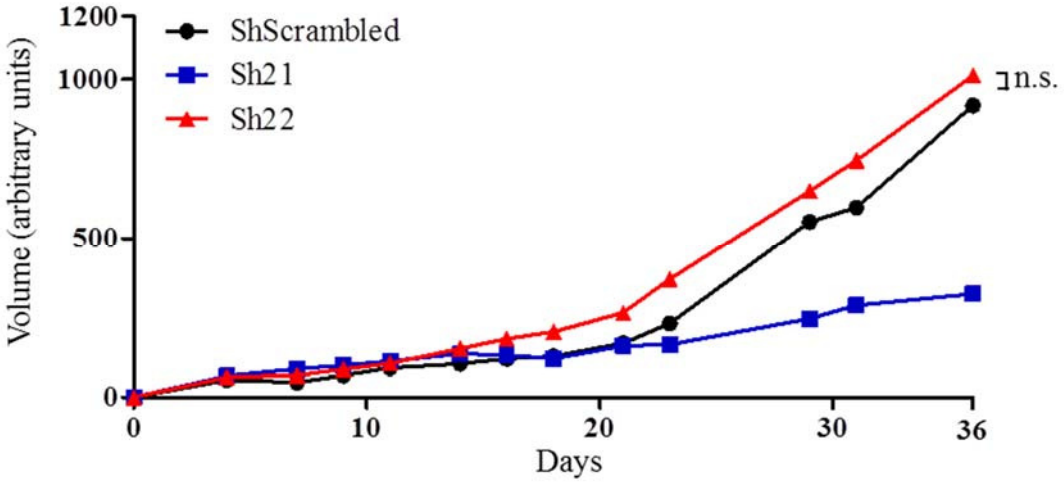


**B**

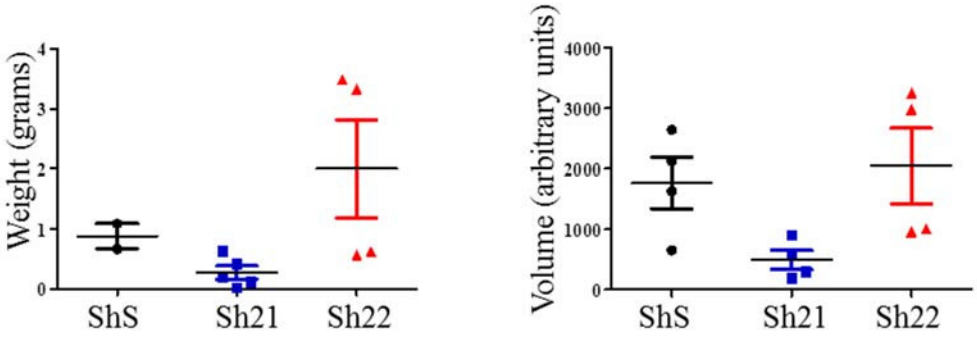


**C**

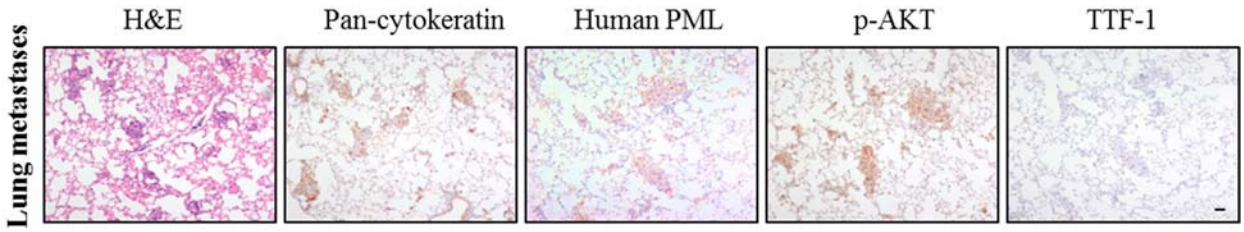

### 3.2.7 Discussion

The results described in this chapter provide further support for the tumor suppressive role of INPP4B in prostate carcinogenesis. Through our mouse model, we show that partial loss of *Inpp4b* in a *Pten* heterozygous background results in prostate cancer progression, particularly in the ventral and anterior lobes of the prostate. The evidence that INPP4B is a relevant tumor suppressor in CaP is further supported through the observation that *INPP4B* is downregulated in metastatic human CaP, and that its loss favors metastatic dissemination of PC3 cells in subcutaneous xenografts.

Our findings reinforce the importance of PI3K-AKT activation in CaP oncogenesis. Genomic profiling of human CaP samples have revealed that the PI3K signaling pathway is activated in nearly half of all primary CaP cases and all of metastatic CaP cases (2). Importantly, *PTEN* is lost or downregulated in close to 50% of all metastatic cases (2), in line with previous reports that show *PTEN* mutations or loss of expression in human CaP (22). Interestingly, the authors also report a downregulation of *INPP4B* in 47% of the metastatic CaP cases (2), although the co-occurrence of these lesions has not been described. While we speculate that the loss of function of the second allele of *Inpp4b* in $Pten^{+/-}Inpp4b^{+/-}$ mice could potentially result in the progression of early CaP, the early mortality that occurred in the $Pten^{+/-}Inpp4b^{-/-}$ mice precluded analyses of CaP in older mice. One approach to circumvent this would be to use conditional knockout mouse models, which would allow us to study the effect of complete loss of *Pten* and *Inpp4b* on CaP progression. While it was initially thought that loss of the second allele of *Pten* potentiates the progression of HGPIN lesions into CaP, prostate tumors in the $Pten^{pc-/-}$ mice despite being high-grade and highly proliferative lesions do not metastasize (12). This is due to the activation of the p53-dependent cellular senescence pathway upon complete Pten

inactivation, also known as Pten-loss-induced cellular senescence (PICS), thereby restricting tumorigenesis (13). Further, concomitant loss of both PTEN and INPP4B induces cellular senescence in breast cancer cell lines (20). Thus, while we are currently analyzing *Pten*$^{pc-/-}$ *Inpp4b*$^{pc-/-}$ mice for CaP progression, interpretation of the data might be confounded by PICS. Thus, a potentially more insightful model would be a *Pten*$^{pc-/-}$*p53*$^{pc-/-}$*Inpp4b*$^{pc-/-}$ mouse model, where the senescence response triggered in *Pten*$^{pc-/-}$ is bypassed with the loss of *Trp53*.

Despite Akt activation in *Pten* heterozygous mice, this only initiates PIN, some of which progress to HGPIN, but not invasive or metastatic adenocarcinoma (7,9). Furthermore, prostate neoplasia is rarely detected in the anterior and ventral prostates of *Pten*$^{+/-}$ mice. Thus, our observation of invasive prostate adenocarcinoma in the ventral prostates and cystic lesions in the anterior prostates of the *Pten*$^{+/-}$*Inpp4b*$^{+/-}$ mice suggests that the tumor suppressive function of Inpp4b in the mouse prostate is distinct from Pten. The specific lobe of the mouse prostate in which the neoplastic lesion occurs has traditionally thought to be relevant in CaP modeling, since human and mouse prostates have different anatomy and histology (23). While there is no known analogous structure to the ventral prostate lobe of mice, the dorsolateral prostate lobe is believed to correspond to the peripheral zone of the human prostate, from which approximately 80% of CaP arise (9,24). Nonetheless, leading CaP experts agree that it is premature to conclude that lesions in any given lobe are more representative of human disease (23).

In Chapter 2, we have demonstrated that loss of INPP4B specifically increases activation of AKT2 in thyroid tissue and cell lines. The inhibition of Akt2 activation by Inpp4b could well be tissue specific, and particularly relevant in the thyroid because 1) knockout of Akt2 specifically rescued thyroid, but not prostate carcinogenesis in *Pten*$^{+/-}$ mice (25) 2) the Akt1:Akt2 ratio in thyroid tissue is 0.5 but this ratio is 1.65 in prostate tissue, suggesting a dependence on Akt2

signaling in the thyroid glands but not the prostate (25). In the case of the prostate, a deficiency for Akt1 but not Akt2 was sufficient to inhibit the development of PIN in *Pten* heterozygous mice, suggesting a role of Akt1 in the initiation of CaP (13). However, it has also been shown that the specific knockdown of AKT2 but not AKT1 results in the regression of *PTEN* null prostate xenografts, suggesting that AKT2 signaling is essential in tumor maintenance in a PTEN deficient context (26). Furthermore, inactivation of Phlpp1, which specifically inactivates Akt2 and Akt3 (27), triggered HGPIN at complete penetrance by 9 months of age (28). *Phlpp1* loss in $Pten^{+/-}$ mice accelerated CaP progression, resulting in invasive adenocarcinoma of the prostate at complete penetrance, suggesting that *Phlpp1* loss is synergistic with *Pten* heterozygosity (28). Significantly, *PHLPP1* and *PTEN* codeletion was found to be restricted to metastatic human CaP, but not primary CaP, potentially implicating PHLPP1 in metastatic progression of CaP (28). Taken together, these suggest that while Akt1 appears to be important for CaP initiation, there is synergy between Akt2 activation and Pten deficiency in CaP maintenance and progression, although the role of Akt3 cannot be completely dismissed.

In this thesis, I describe the discovery of a novel isoform of INPP4B, which has also been recently described (29). While the biological significance of this isoform remains unclear, we have systems that can potentially be used to study the effect of this isoform in cell lines. Because it lacks the C2 domain, this isoform is most likely not membrane-localized. Whether this represents a loss of the classical function of INPP4B, or a gain of a novel function, remains to be characterized. The mechanism through which this isoform is formed would also yield further insight into INPP4B regulation. Because a transcript corresponding to this isoform has not yet been isolated, and since INPP4A is known to be degraded via calpain proteases during allergic airway inflammation (30), we hypothesize that this isoform is likely formed through protease

mediated cleavage of the full length protein. It would be especially interesting to uncover a particular correlation between the abundance of this isoform, and a particular protease, and the association with cancer progression.

A recent characterization of the catalytic domain of INPP4B revealed that it possesses protein tyrosine phosphatase activity and that the lipid and protein phosphatase activities are also modulated by other key residues in the catalytic motif (31). While we are confident of Inpp4b loss of function in *Inpp4b*$^{-/-}$ mice, we cannot neglect a potential contribution of the protein phosphatase function in modulating Inpp4b's tumor suppressive function.

Strikingly, we note that the loss of INPP4B in PTEN null PC3 cells appears to favor distant metastasis of subcutaneous xenografts to the lungs. While this data is preliminary and still needs to be repeated, it provides an initial confirmation of the role of INPP4B in suppressing metastasis. Although PC3 cells were established from the bone metastasis of grade IV CaP, distant metastases have never been observed with subcutaneous xenografts in NCr nude or Nod/Scid mice (32,33). Thus, PC3-shINPP4B xenograft models could represent a promising model for testing of therapies and understanding the pathogenesis of CaP.

To conclude, this chapter provides preliminary evidence supporting a tumor suppressive role of INPP4B in CaP. We show *in vivo* that partial loss of Inpp4b can cooperate with *Pten* haploinsufficiency to promote prostate tumorigenesis. Notably, high-grade prostatic intraepithelial neoplasia (HG-PIN) lesions in the ventral prostate of *Pten*$^{+/-}$ mice were transformed into invasive carcinoma in *Pten*$^{+/-}$*Inpp4b*$^{+/-}$ mice. There was also extensive cystic remodeling and invasion in the anterior prostates of *Pten*$^{+/-}$*Inpp4b*$^{+/-}$ mice, a phenotype not observed in the prostates of age-matched *Pten*$^{+/-}$ mice. *In vitro*, we found that knockdown of

INPP4B in PTEN deficient PC3 cells increased their migratory and invasive properties. Importantly, we demonstrate that INPP4B loss in PC3 cells also promotes distant metastasis in xenograft assays. In summary, these data show that INPP4B cooperates with PTEN in suppressing prostate cancer progression and metastasis, providing further support for its role as a tumor suppressor.

### 3.3 Concluding remarks and future directions

The work in my thesis has allowed us to reach important conclusions regarding the molecular mechanisms underlying the tumor suppressive function of INPP4B, and its role in tumorigenesis *in vivo*. First, we have provided strong evidence that INPP4B is not epistatic to PTEN, and that Inpp4b loss can cooperate with *Pten* haploinsufficiency in promoting FTC progression and metastasis. We provide preliminary evidence that the same could also be true for CaP. Second, we show that in the thyroid, INPP4B can regulate AKT signaling in an isoform-specific fashion at the endosomes.

These findings present many exciting avenues for future study. More work will be necessary to determine if the isoform-specific regulation of AKT by INPP4B can be generalized to other tissues, in particular the prostate, where several lines of evidence point to the importance of the synergy between AKT2 signaling and PTEN deficiency for CaP maintenance and progression. While our data suggests a role for AKT2 in thyroid cancer metastasis, more experiments need to be done to uncover the specific genes and proteins that are mediating AKT2's role in metastasis. In addition, it is important to continue our efforts in optimizing the detection of INPP4B via immunohistochemistry in human FTC samples, which would allow us to determine the clinical relevance of our findings.

*In vivo* modeling of cancer progression is important for the understanding of the mechanisms of cancer pathogenesis, and can yield insight into the mechanisms of metastasis, which are still poorly understood. It is my hope that as we dissect these pathways of tumor suppression, we will one day be able to better diagnose and develop therapies to treat metastatic cancer.

## 3.4 Experimental Methods

### Mice and histopathological analyses

*Inpp4b* knockout mice were generated by Sasaki and colleagues in the C57BL/6J background, as described in Chapter 2 (Figure 2.1B). *Pten*$^{pc-/-}$ mice used in this study are described in (12). Histopathological analyses were performed on the prostates obtained from cohorts of male mice from 6-15 months of age. Mouse tissues were fixed in 4% paraformaldehyde and embedded in paraffin. They were then sectioned and stained with hematoxylin and eosin (H&E) for pathological analyses. The use of these mice and procedures performed were in accordance to NIH-approved guideline, and the Institutional Animal Care and Use Committee (IACUC) ate Beth Israel Deaconess Medical Center approved the studies.

### Studies with Primary cells

Mouse embryonic fibroblasts (MEFs) were isolated at day E13.5, immortalized with SV40 large T antigen, and maintained in DMEM supplemented with 10% fetal bovine serum, 2mM glutamine, 100 U/ml penicillin and streptomycin (Invitrogen).

### Cell lines

All cells were maintained in DMEM, KSFM or MEGM (Cambrex) supplemented with 10% fetal bovine serum, 2 mM glutamine, 100 U/ml penicillin and streptomycin (Invitrogen). PWR1E, RWPE1, DU145, and PC3 cells were purchased from ATCC. HMEC cells were a kind gift from the Lewis Cantley (Weill-Cornell) Cell lines were tested for specific markers by Western blot and qRT-PCR in our laboratory, routinely tested for *Mycoplasma* (MycoAlert; Lonza), but not further authenticated.

### Western blotting and immunohistochemistry

Cells and tissues were lysed with RIPA buffer (50mM Tris [pH8], 150mM NaCl, 0.1% SDS, 0.5% sodium deoxycholate, 1% NP40, 1mM EDTA and protease and phosphatase inhibitor cocktail [Roche]). For western blotting, the following antibodies were used: anti-AKT (9272), anti-Phospho-AKT (pSer473, 9271; pThr308, 9275), anti-PTEN (9559), anti-INPP4B(8450) were from Cell Signaling Technology. Anti-INPP4B (81269/EPR3108Y) was from Epitomics. Anti-β-actin (A3853) was from Sigma. For immunohistochemistry, anti-phospho-Akt (pSer473, 4060) was from Cell Signaling Technology, anti-TTF1 (3575) and anti-smooth muscle actin (M0851) is from DAKO, Ki67 (9106) and pan-cytokeratin (MS343P) are from Thermo Scientific Lab Vision, anti-human PML (A301-167) is from Bethyl Laboratories.

**RNA isolation and RT-qPCR**

Total RNA was purified from cell lines and tissues using the PureLink RNA Mini Kit (Invitrogen). For qPCR analysis, 2ug of total RNA was reverse transcribed into cDNA using the High Capacity cDNA Reverse Transcription Kit (Applied Biosystems). SYBR-Green qPCR analysis was then performed using Applied Biosystems StepOnePlus in accordance to the manufacturer's protocol. Each target was run in triplicate, and expression levels were normalized to mouse hypoxanthine-guanine phosphoribosyltransferase (*HPRT*) or human porphobilinogen (PBGD).

**Semi-quantitative PCR for *Inpp4b***

The following primer sequences were used:

Exons 1 - 2

Forward: GCCCTAAAACCAGCGAAACA; Reverse: CCACCTCACAACGGACCTAT

Exons 5 – 7

Forward: TGTGGAGGGAACAAAAGACC; Reverse: CAGCAGCTCCCCAACTTTAA

Exons 12 – 13

Forward: ACAGAGAGAAGGAACACCGG; Reverse: CAGAGGTTAGCAGCAGGTCT

Exons 19-23

Forward: GGGAGACGGGAACACTATGT; Reverse: AAGTGCCTTCTGGAGGTCTG

**Genotyping**

The following genotyping primers were used:

Inpp4b del1: GTTTACATTTGACAGGGTGGTTGG

Inpp4b del2: TGCTGTCGCCGAAGAAGTTA

Inpp4b del3: CCTGCCATGGGTAGATTTCT

Pgen-1: TGGGAAGAACCTAGCTTGGAGG

Pgen-3: ACTCTACCAGCCCAAGGCCCGG

3193: CGAGACTAGTGAGACGTGCTACTTCC

**Growth proliferation assay**

Cells were plated at a density of $2.5x10^4$ cells/well in 12-well plates and each sample was plated in triplicate. Plates were collected on day 0, day 2, day 4 and day 6. The wells were washed with PBS and cells were fixed with 4% paraformaldehyde (Santa Cruz Biotechnology). Wells were stained with 0.1% Crystal Violet solution, washed and dried. The absorbed stained was then solubilized with 10% acetic acid, and the absorbance was measured at 595nm.

**Transwell migration and invasion assay**

Migration transwell and Matrigel Invasion Chambers were purchased from BD Biosciences. Cells were seeded in triplicate on the top of the transwell, and allowed to migrate and/or invade for 20 hours through 8 μm pores towards 10% FBS DMEM in the bottom chamber. A cotton swab was used to clean the seeding section of the membrane, and the bottom surface was stained with 0.1% Crystal Violet solution, washed and imaged. Cells were then counted using *ImageJ*.

**Xenograft assay**

Six-week-old male NCr Nu/Nu immunodeficient mice were purchased from Jackson Laboratory. Mice were anaesthesized with isoflurane, after which PC3 cells ($2 \times 10^6$) were injected into the subcutaneous region of the flank in 100 μl growth medium/matrigel (BD Biosciences) (n=5 for each stable cell lines). Tumor growth was followed for up to 36 days, but mice were euthanized and analyzed at Day 46.

**Statistical analysis**

For quantitative data, data sets were generally analyzed using the unpaired, two-tailed Student's *t* tests (GraphPad Prism, GraphPad Software). $p<0.05$ was considered significant.

## 3.5 References


1. Nelson W, De Marzon A, Isaacs W. Prostate Cancer. N Engl J Med. 2003;349(4):366–81.

2. Taylor BS, Schultz N, Hieronymus H, Gopalan A, Xiao Y, Carver BS, et al. Integrative genomic profiling of human prostate cancer. Cancer Cell. 2010;18(1):11–22.

3. Mcmenamin E, Soung P, Perera S, Kaplan I, Loda M, Sellers WR. Loss of PTEN Expression in Paraffin-embedded Primary Prostate Cancer Correlates with High Gleason Score and Advanced Stage. Cancer Res. 1999;59(43):4291–6.

4. Greenberg NM, DeMayo F, Finegold MJ, Medina D, Tilley WD, Aspinall JO, et al. Prostate cancer in a transgenic mouse. Proc Natl Acad Sci. 1995;92(8):3439–43.

5. Gingrich JR, Barrios RJ, Morton R a, Boyce BF, DeMayo FJ, Finegold MJ, et al. Metastatic prostate cancer in a transgenic mouse. Cancer Res. 1996;56(18):4096–102.

6. Parisotto M, Metzger D. Genetically engineered mouse models of prostate cancer. Mol Oncol. 2013;7(2):190–205.

7. Di Cristofano a, Pesce B, Cordon-Cardo C, Pandolfi PP. Pten is essential for embryonic development and tumour suppression. Nat Genet. 1998 Aug;19(4):348–55.

8. Chen M, Xu P, Peng X, Chen WS, Guzman G, Yang X, et al. The deficiency of Akt1 is sufficient to suppress tumor development in Pten + / − mice. Genes Dev. 2006;20(312):1569–74.

9. Cristofano A Di, Acetis M De, Koff A, Cordon-cardo C, Pandolfi PP. Pten and p27 KIP1 cooperate in prostate cancer tumor suppression in the mouse. Nat Genet. 2001;27:222–4.

10. Abate-shen C, Banach-petrosky WA, Sun X, Economides KD, Desai N, Gregg JP, et al. Nkx3.1 ; Pten Mutant Mice Develop Invasive Prostate Adenocarcinoma and Lymph Node Metastases. Cancer Res. 2003;63:3886–90.

11. Wu X, Wu J, Huang J, Powell WC, Zhang J, Matusik RJ, et al. Generation of a prostate epithelial cell-specific Cre transgenic mouse model for tissue-specific gene ablation. Mech Dev. 2011;101(2001):61–9.

12. Trotman LC, Niki M, Dotan Z a, Koutcher J a, Di Cristofano A, Xiao A, et al. Pten dose dictates cancer progression in the prostate. PLoS Biol. 2003;1(3):E59.

13. Chen Z, Trotman LC, Shaffer D, Lin H-K, Dotan Z a, Niki M, et al. Crucial role of p53-dependent cellular senescence in suppression of Pten-deficient tumorigenesis. Nature. 2005;436:725–30.

14. Wang G, Lunardi A, Zhang J, Chen Z, Ala U, Webster K a, et al. Zbtb7a suppresses prostate cancer through repression of a Sox9-dependent pathway for cellular senescence bypass and tumor invasion. Nat Genet. 2013;45(7):739–46.

15. Ding Z, Wu C-J, Chu GC, Xiao Y, Ho D, Zhang J, et al. SMAD4-dependent barrier constrains prostate cancer growth and metastatic progression. Nature. 2011;470(7333):269–73.

16. Ding Z, Wu C-J, Jaskelioff M, Ivanova E, Kost-Alimova M, Protopopov A, et al. Telomerase reactivation following telomere dysfunction yields murine prostate tumors with bone metastases. Cell. 2012;148(5):896–907.

17. Lapointe J, Li C, Higgins JP, van de Rijn M, Bair E, Montgomery K, et al. Gene expression profiling identifies clinically relevant subtypes of prostate cancer. Proc Natl Acad Sci U S A. 2004;101(3):811–6.

18. Vanaja DK, Ballman K V, Morlan BW, Cheville JC, Neumann RM, Lieber MM, et al. PDLIM4 repression by hypermethylation as a potential biomarker for prostate cancer. Clin Cancer Res. 2006;12(4):1128–36.

19. Varambally S, Yu J, Laxman B, Rhodes DR, Mehra R, Tomlins S a, et al. Integrative genomic and proteomic analysis of prostate cancer reveals signatures of metastatic progression. Cancer Cell. 2005;8(5):393–406.

20. Gewinner C, Wang ZC, Richardson A, Teruya-Feldstein J, Etemadmoghadam D, Bowtell D, et al. Evidence that inositol polyphosphate 4-phosphatase type II is a tumor suppressor that inhibits PI3K signaling. Cancer Cell. 2009;16(2):115–25.

21. Rao DD, Vorhies JS, Senzer N, Nemunaitis J. siRNA vs. shRNA: similarities and differences. Adv Drug Deliv Rev. 2009;61(9):746–59.

22. Pourmand G, Ziaee A, Abedi AR, Mehrsai A, Alavi HA, Ahmadi A, et al. Role of PTEN Gene in Progression of Prostate Cancer. Urol J. 2007;4(2):95–100.

23. Ittmann M, Huang J, Radaelli E, Martin P, Signoretti S, Sullivan R, et al. Animal models of human prostate cancer: the consensus report of the New York meeting of the Mouse Models of Human Cancers Consortium Prostate Pathology Committee. Cancer Res. 2013;73(9):2718–36.

24. Berquin IM, Min Y, Wu R, Wu H, Chen YQ. Expression signature of the mouse prostate. J Biol Chem. 2005;280(43):36442–51.

25. Xu P-Z, Chen M-L, Jeon S-M, Peng X, Hay N. The effect Akt2 deletion on tumor development in Pten(+/-) mice. Oncogene. 2012;31(4):518–26.

26. Chin YR, Yuan X, Balk SP, Toker A. PTEN-deficient tumors depend on AKT2 for maintenance and survival. Cancer Discov. 2014;4(8):942–55.

27. Brognard J, Sierecki E, Gao T, Newton AC. PHLPP and a second isoform, PHLPP2, differentially attenuate the amplitude of Akt signaling by regulating distinct Akt isoforms. Mol Cell. 2007;25(6):917–31.

28. Chen M, Pratt CP, Zeeman ME, Schultz N, Taylor BS, O'Neill A, et al. Identification of PHLPP1 as a tumor suppressor reveals the role of feedback activation in PTEN-mutant prostate cancer progression. Cancer Cell. 2011;20(2):173–86.

29. Perez-Lorenzo R, Gill KZ, Shen C-H, Zhao FX, Zheng B, Schulze H-J, et al. A tumor suppressor function for the lipid phosphatase INPP4B in melanocytic neoplasms. J Invest Dermatol. 2014;134(5):1359–68.

30. Aich J, Mabalirajan U, Ahmad T, Agrawal A, Ghosh B. Loss-of-function of inositol polyphosphate-4-phosphatase reversibly increases the severity of allergic airway inflammation. Nat Commun. 2012;3:877.

31. Lopez SM, Hodgson MC, Packianathan C, Bingol-Ozakpinar O, Uras F, Rosen BP, et al. Determinants of the tumor suppressor INPP4B protein and lipid phosphatase activities. Biochem Biophys Res Commun. 2013;440(2):277–82.

32. Wu X, Gong S, Roy-Burman P, Lee P, Culig Z. Current mouse and cell models in prostate cancer research. Endocr Relat Cancer. 2013;20:R155–70.

33. Bastide C, Bagnis C, Mannoni P, Hassoun J, Bladou F. A Nod Scid mouse model to study human prostate cancer. Prostate Cancer Prostatic Dis. 2002;5(4):311–5.

# APPENDIX

## (Supplementary information)

**Chapter 2 Supplementary information:**

**Supplementary Figure S2.1. Generation of *Pten*$^{+/-}$*Inpp4b*$^{+/-}$ and *Pten*$^{+/-}$*Inpp4b*$^{-/-}$ mice. A.** The breeding scheme was depicted between *Pten*$^{+/-}$*Inpp4b*$^{+/-}$ mice and *Inpp4b*$^{+/-}$ mice to establish a study cohort of *Pten*$^{+/-}$, *Pten*$^{+/-}$*Inpp4b*$^{+/-}$ and *Pten*$^{+/-}$*Inpp4b*$^{-/-}$ mice. **B.** H&E staining of thyroid tumor and lung metastases from *Pten*$^{+/-}$*Inpp4b*$^{+/-}$ mice; Scale bar, 100μm. Insets show thyroid cancer cells. **C.** Serum TSH levels for mice of the respective genotypes are as marked (n=3-5, age 3-5 months).

**Supplementary Figure S2.1 (continued)**

**A**

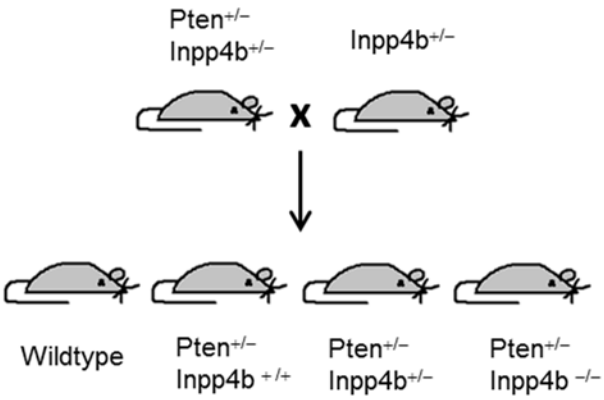


**B**

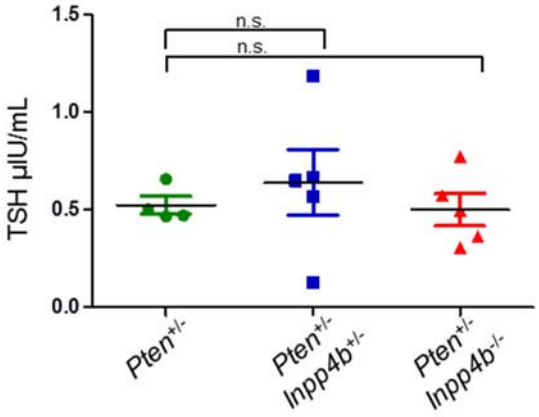

**Supplementary Figure S2.1 (continued)**

**C**

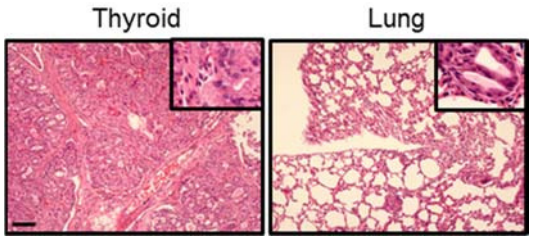

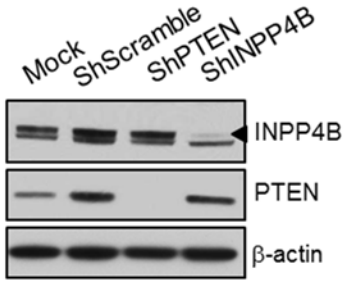


**Supplementary Figure S2.2. Validation of INPP4B antibody.** The specificity of the bands detected by the INPP4B antibody (Epitomics) was determined by western blotting analysis via shRNA mediated knock-down of INPP4B in PWR1E cells. The arrowhead indicates the specific band of INPP4B protein.

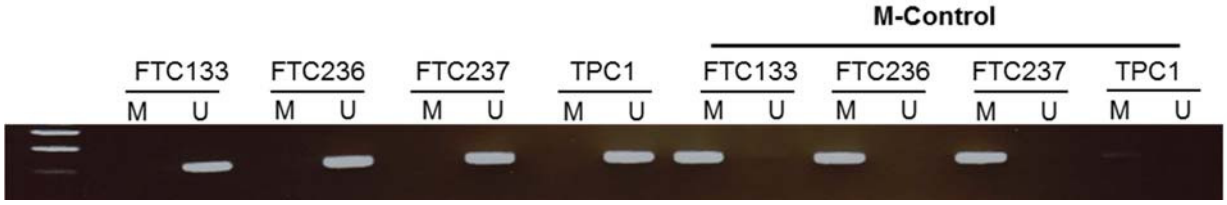


**Supplementary Figure S2.3. INPP4B's promoter is not directly methylated.** Methylation specific PCR (MSP) of thyroid cancer cell lines. For M-control (positive control for M-primers), cells were treated with M. SssI then subjected to bisulfite treatment and MSP. M: methylated alleles; U: unmethylated alleles.

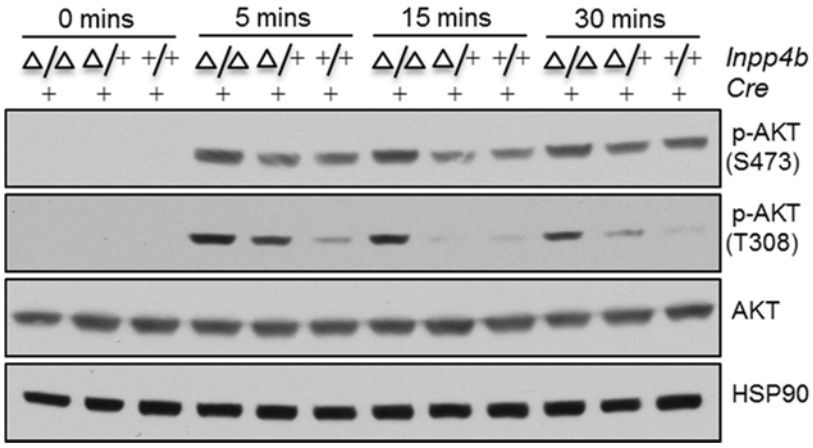


**Supplementary Figure S2.4. Loss of Inpp4b in MEFs lead to increased Akt activation.**

Western blot analysis of lysates from immortalized and *Cre* mediated Inpp4b inactivation of WT, $Inpp4b^{flox/+}$, $Inpp4b^{flox/flox}$ MEFs.

**A**

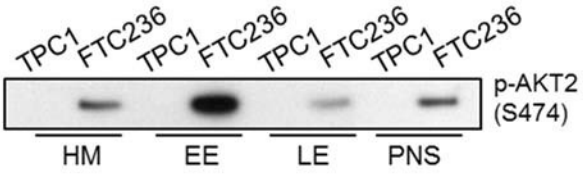


**B**

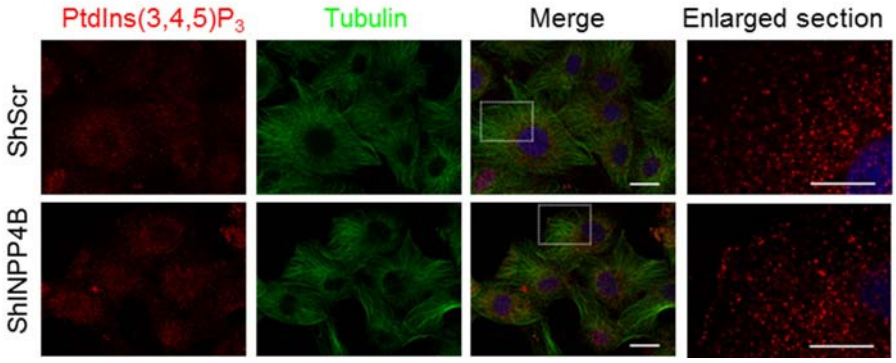


**Supplementary Figure S2.5. Loss of INPP4B results in increased AKT2 activation. A.** Western blot analysis of phosphorylated Akt2 in different cell fractions derived from TPC1 and FTC236 cells. B. Immunofluorescence of PI(3,4,5)$P_3$ and tubulin in TPC1 cells infected with either a non-targeting shRNA or a shRNA that targets INPP4B. Scale bars, 20 μm.

**Supplementary Figure S2.6. PI3K-C2α regulates AKT2 signaling. A.** Western blot analysis of PI3K-C2α in total lysate from different thyroid cancer cells. B. Western blot analysis of phosphorylated-AKT1 and phosphorylated- AKT2 in total cell lysates of FTC236 cells. Arrow indicates specific band (see also Methods). C. Proliferation of TPC1, 8505C and FTC236 cells transfected with either a non-targeting siRNA or a siRNA which targets PI3K-C2α.

**Supplementary Figure S2.6 (continued)**

**A**

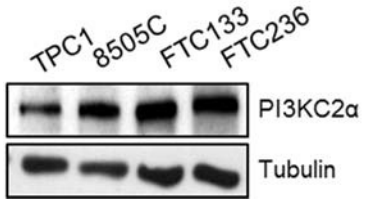


**B**

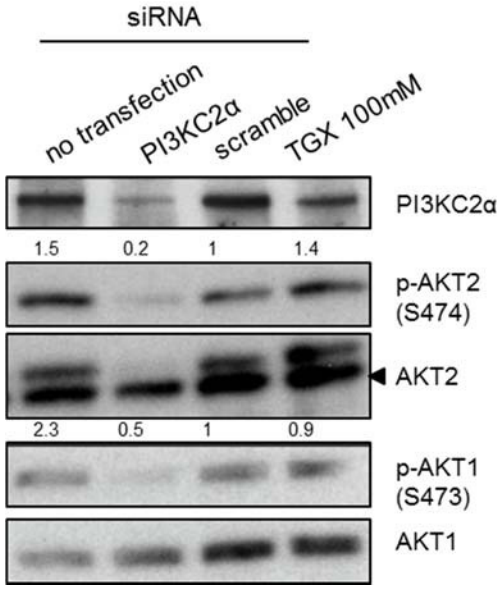

**Supplementary Figure S2.6 (continued)**

**C**

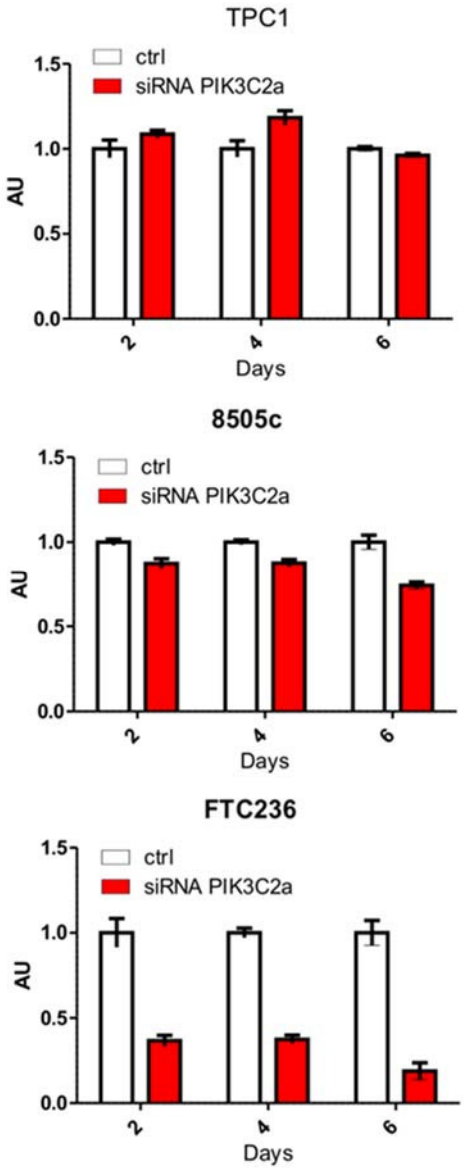

**Supplementary Figure S2.7. INPP4B loss does not produce any morphological or cytoskeletal differences. A.** Proliferation of TPC1 cell line infected with either a non-targeting shRNA or a shRNA that targets INPP4B. Cells were cultured in media containing 5% and 1% serum, stained with crystal violet, and lysed. Absorbance was measured at OD595nm. **B-C.** Phase contrast (left panel) and immunofluorescence for tubulin (middle panel).

**Supplementary Figure S2.7 (continued)**

**A**

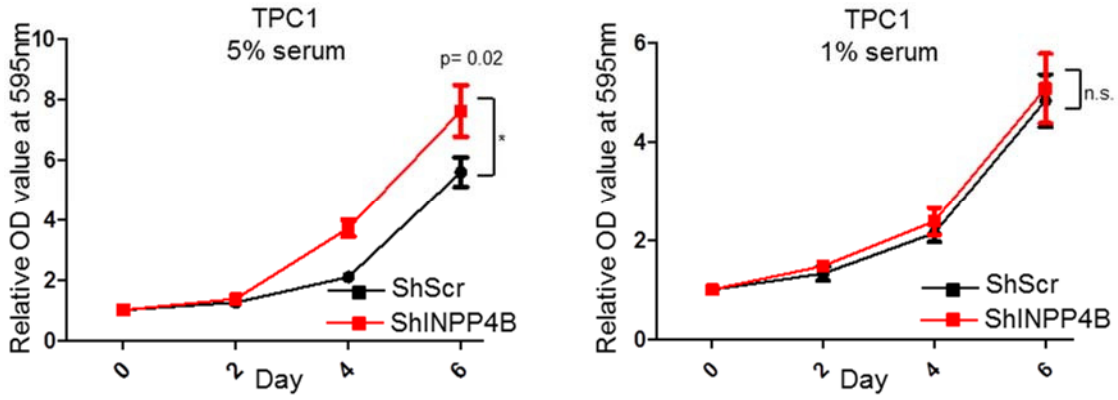


**B**

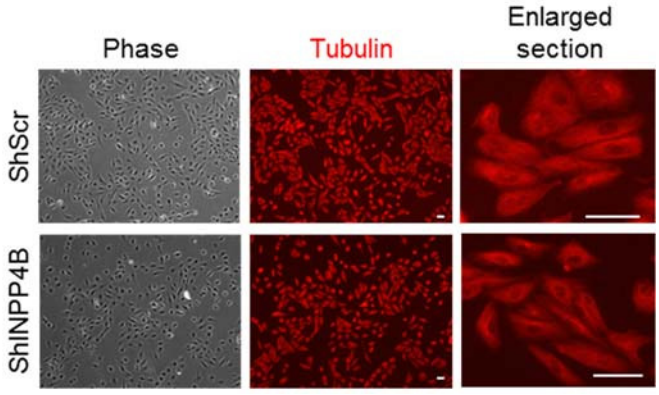

**Supplementary Figure S2.7 (continued)**

**C**